MODELING FOR VOLTAGE SOURCE CONVERTER CONTROLLED POWER TRANSFER FOR HVDC APPLICATIONS

SEUMSAK DOUANGSYLA

A THESIS SUBMITTED IN PARTIAL FULFILLMENT

OF THE REQUIREMENT FOR THE DEGREE OF

MASTER OF ENGINEERING IN ELECTRICAL ENGINEERING

SCHOOL OF GRADUATE STUDIES

KING MONGKUT'S INSTITUTE OF TECHNOLOGY LADKRABANG

2005

ISBN 974 -15 -1530 -8

หัวข้อวิทยานิพนธ์	**แบบจำลองคอนเวอร์เตอร์ชนิดแหล่งจ่ายแรงดันที่ใช้ควบคุมการส่งถ่ายพลังงานสำหรับการประยุกต์ใช้ในแหล่งจ่ายกระแสตรงแรงดันสูง**
ชื่อนักศึกษา	นายเสริมศักดิ์ ดวงศิลา
รหัสประจำตัว	46060341
ปริญญา	วิศวกรรมศาสตรมหาบัณฑิต
สาขาวิชา	วิศวกรรมไฟฟ้า
พ.ศ.	2548
อาจารย์ผู้ควบคุมวิทยานิพนธ์	รศ. ดร. วิจิตร กิณเรศ
อาจารย์ผู้ควบคุมวิทยานิพนธ์ร่วม	ศ.ดร. มาซาอากิ คันโดะ ผศ.ดร.สุพัฒน์ กิจติรัตน์สัจจา

บทคัดย่อ

วิทยานิพนธ์นี้ได้จัดการเกี่ยวกับการจำลองคอนเวอร์เตอร์ชนิดแหล่งจ่ายแรงดันที่ใช้ในการควบคุมการส่งถ่ายพลังงานสำหรับการประยุกต์ใช้ในแหล่งจ่ายไฟฟ้ากระแสตรงแรงดันสูง วงจรจำลองการทำงานของคอนเวอร์เตอร์ชนิดแหล่งจ่ายแรงดันภายใต้การเชื่อมโยงกับดีซีลิงค์ โดยใช้เทคนิคการควบคุมพีดับบลิวเอ็มเป็นสัญญาณในการสวิตช์ของไอจีบีที การกำหนดค่าตัวแปรที่ใช้ในการควบคุมจะอาศัยสมการทางคณิตศาสตร์และยังได้มีการนำเสนอเทคนิคพีดับบลิวเอ็มแบบเวกเตอร์คอนโทรล วิทยานิพนธ์นี้ได้สำรวจคอนเวอร์เตอร์พีดับบลิวเอ็มชนิดจ่ายแรงดันต่อเข้ากับโครงข่ายเอซีโดยใช้เทคนิคเวกเตอร์คอนโทรล การสร้างรูปแบบพีดับบลิวเอ็มได้ใช้ชนิดมีคลื่นพาหะ สัญญาณพีดับบลิวเอ็มได้จากการสังเคราะห์คลื่นพาหะ แรงดันและกระแสไฟฟ้าสลับ 3 เฟสจะถูกเปลี่ยนแปลงเป็นไปตามรูปแบบของการวิเคราะห์ในแกนดีคิวซึ่งหมุนไปตามความถี่เชิงมุมของแหล่งจ่ายซึ่งเป็นไปได้ที่จะควบคุมการไหลกำลังไฟฟ้าแอคทีฟและรีแอคทีฟให้ออกจากกันอิสระและมีความจำเป็นที่จะต้องพัฒนาแบบจำลองคณิตศาสตร์ของคอนเวอร์เตอร์จ่ายแรงดันเพื่อที่จะควบคุมตัวแปร การออกแบบและสมรรถนะของตัวควบคุมก็ถูกสำรวจด้วย ความถูกต้องของแบบจำลองที่นำเสนอและวิธีการควบคุมถูกตรวจสอบโดยการจำลองทางดิจิตอลโดยใช้โปรแกรมซิมูลิงค์/แมทแลป

Thesis Title	Modeling for Voltage Source Converter Controlled Power Transfer for HVDC Applications
Student	Mr. Seumsak Douangsyla
Student ID.	46060341
Degree	Master of Engineering
Programme	Electrical Engineering
Year	2005
Thesis Advisor	Assoc. Prof. Dr. Vijit Kinnares
Co-Thesis Advisor	Prof. Dr. Masaaki Kando
	Asst. Prof. Dr. Supat Kittiratsatcha

ABSTRACT

The thesis deals with modeling for voltage source converter controlled power transfer for HVDC applications. A model of a VSC based dc link using PWM control strategy and IGBT switched mode converters is described. The control variables based on mathematical model are determined and vector control strategy is proposed. This thesis investigates the PWM Voltage Source Converter connected to an AC network with vector control strategy. PWM pattern generation is based on a carrier technique. The instantaneous three-phase voltages and currents are transformed to a two-axis (d-q) reference frame system which rotates at the supply angular frequency (ω_e). Thus it is possible to have decoupled control of the active (P) and reactive (Q) power flow and it is necessary to develop a mathematical model for VSC to determine controlling variables. The design and the performance of controllers are also investigated. The validity of proposed model and control strategy has been verified by digital simulation using SIMULINK / MATLAB.

ACKNOWLEDGEMENT

This work is carried out at the Department of Electrical Engineering, Faculty of Engineering, King Mongkut's Institute of Technology Ladkrabang (KMITL).

First, I would like to express my deepest gratitude to Assoc. Prof. Dr. Vijit Kinnares, my supervisor and examiner, for giving me the opportunity to explore the interesting field of power engineering, and for his encouragement and guidance during the research. I would like to thank Prof. Masaaki Kando from Department of Electrical and Electronic, Tokai University, Japan, my co-supervisor, for his encouragement.

I would like to thank Asst. Prof. Dr. Supat Kittiratsatcha from Department of Electrical Engineering, KMITL, Thailand, my co-supervisor, for his encouragement.

I would like to thank all my KMITL's teachers for giving me very useful knowledge and experience.

The financial support is provided by JICA. This is gratefully acknowledged.

I would like also to thank my Thai friends and colleagues at the Department of Electrical Engineering for making such a productive working environment, for their encouragement and very useful comments.

Finally, I would like to thank King Mongkut's Institute of Technology Ladkrabang (KMITL) and AUN/SEED-Net for giving me an opportunity to upgrade my knowledge.

Table of Contents

Table of Contents (Cont.)

Table of Contents (Cont.)

Table of Contents (Cont.)

List of Illustration or Figures

List of Illustration or Figures (Cont.)

List of Illustration or Figures (Cont.)

List of Illustration or Figures (Cont.)

List of Illustration or Figures (Cont.)

Chapter 1

Introduction

1.1 Background

Industrial power systems are characterized by high concentration of load and high costs associated with equipment mal-operation. Many industrial loads cause disturbances in the system like equipment starting dips and transients, harmonic distortion and flicker. Industrial loads are also very sensitive to voltage dips and other disturbances originating from the grid. So electric power systems are faced with the challenge of providing high-quality power to industrial loads and at the same time limiting the disturbances originating in the industrial systems.

Power-electronics solutions have been suggested to solve specific power quality and other problems in industrial distribution systems. An uninterruptible power supply (UPS) can provide 'ride-through' capability against voltage interruptions and dips for small loads [1]. Dynamic voltage restorer (DVR) can alleviate a range of dynamic power quality problems such as voltage dips and swells for large loads (up to a few MVA)[2]. STATCOM has the ability to either generate or absorb reactive power at a faster rate than classical solutions allowing for the mitigation of flicker and alleviation of stability problems [3]. Several options are explained in the literature [4][5][6].

High Voltage Direct Current traditionally has been used to transfer large amounts of power over long distances. Sometimes also for control purposes [7][8][9]. But for traditional HVDC the reactive power cannot be controlled independently of the active power. Recent development in power systems is voltage source converters (VSC) based High Voltage Direct Current which is referred to as Voltage Source Converter-High Voltage Direct Current in the thesis. There is an additional degree of freedom which makes it possible to control the reactive power and the active power independently. Application of such dc links is expected to solve power-quality related problems in industrial power systems.

1.2 Objective of the study

The objective of this research is to develop a model for voltage source converter controlled power transfer for HVDC applications. A control scheme for a VSC-HVDC link connecting two

grids and isolated loads is studied. A vector control scheme is studied to investigate the behavior of VSC-HVDC during the disturbances. The power flow via DC-link is investigated.

1.3 Problem Statement

In this thesis, a model for voltage source converter controlled power transfer for HVDC applications is developed. The control variables based on mathematical model are determined and vector control strategy is introduced.

Under steady state conditions, the 3-phase quantities when expressed in the synchronously rotating frame become dc quantities. If one of the axes, (usually) the d-axis, arbitrarily aligned with supply voltage vector, then the d and q axis supply current components automatically represent the active (P) and the reactive (Q) power flow respectively. Thus, it is possible to have decoupled control of the active and reactive power flow.

The DC-link voltage controller sets the active power demand whereas the reactive power demand can be set by an outer reactive power controller or by the required displacement angle between the phase current and voltages.

Therefore, the main advantages of the vector control technique are the direct control of the active and reactive power flow in the converter during transient, steady state and the fast dynamics of the current control loops.

Additionally, the current controllers deal with dc quantities, which using PI controllers, ensure zero current error in steady state. These are the main reasons for selecting the control strategy for the implementation of the VSC.

1.4 Proposed Solution

A model of the voltage source converter controlled power transfer for HVDC applications is developed by using the *d-q* transformation, It means the instantaneous 3-phase voltages and currents are transformed to a 2-axis (d-q) reference frame system [10] which rotates at the supply angular frequency (ω_e). Thus it is possible to have decoupled control of the active (P) and reactive (Q) power flow. This thesis studied the voltage source converter connected to an active ac network with vector control strategy. PWM pattern generation is based on a carrier technique. The digital simulation was carried out to verify the feasibility of the proposed model.

1.5 Scope of the research work

This research work is concerned with modeling for PWM Voltage source converter controlled power transfer for HVDC applications, the system was simulated and the control system was implemented using the vector control technique. Simulation results presented by using Simulink Matlab. The study was focused on power transfer and performance of the VSC-HVDC at steady state, load changes and disturbances in supplying network and supplying the passive loads.

1.6 Outline of the thesis

Chapter 2 presents classic HVDC and VSC-HVDC. In this chapter the arrangements of HVDC systems, the basic of PWM techniques, the configurations, the advantages and the applications of classic HVDC systems and VSC-HVDC are described.

Chapter 3 emphasizes the design of model for Voltage source converter controlled power transfer for HVDC applications and control loops design. The simulation results were also explained.

Chapter 4 discusses some simulations about VSC between two grids. In this chapter, the simulation results of four study cases were given and explained.

Chapter 5, the conclusions of the work and some suggestions for the future are pointed out in this chapter.

Chapter 2

Classic HVDC and VSC-HVDC

2.1 Introduction

The HVDC technology is a high power electronics technology used in electric power systems. It is an efficient and flexible method to transmit large amounts of electrical power over long distances by overhead transmission lines or underground/submarine cables. It is also used to interconnect separate power systems, where traditional alternating current (ac) connections can not be used. HVDC is used at many places all around the world. Until recently HVDC based on thyristors, which is called traditional HVDC or classic HVDC, was used for conversion from ac to dc and vice versa.

Recently a new type of HVDC has become available. It makes use of more advanced semiconductor technology instead of thyristors for power conversion between ac and dc. The semiconductors used are IGBTs (Insulated Gate Bipolar Transistors), the converters are VSCs (Voltage Source Converters) and they operate with medium switching frequency (1-2 kHz) utilizing PWM (Pulse Width Modulation). The technology is commercially available as HVDC light [11] or HVDC plus [12]. In this thesis we will refer to the new technology as VSC-HVDC (VSC based HVDC), where VSC stands for voltage source converter. VSC-HVDC is currently available for small to medium scale power transmission applications [13][14][15]. The technology is claimed to extend the economic power range of dc transmission down to just a few megawatts. One of the reasons for this is the development of a new type of cable for dc power transmission.

In this chapter, a brief overview of Pulse Width Modulation (PWM), a classic HVDC and its applications will be given. Next, the differences between VSC-HVDC and classic HVDC will be discussed followed by possible applications of VSC-HVDC.

2.2 Pulse Width Modulation (PWM).

There are many forms of modulation used for communicating information. The explanations of each form are shown in Figure 2.1-Figure 2.8. When a high frequency signal has an amplitude

varied in response to a lower frequency signal we have AM (Amplitude Modulation). When the signal frequency is varied in response to the modulating signal we have FM (Frequency Modulation). These signals are used for radio modulation because the high frequency carrier signal is needed for efficient radiation of the signal. When communication by pulses was introduced, the amplitude, frequency and pulse width become possible modulation options. In many power electronic converters where the output voltage can be one of two values the only option is modulation of average conduction time. Figure 2.1 shows unmodulated, sine modulated pulses.

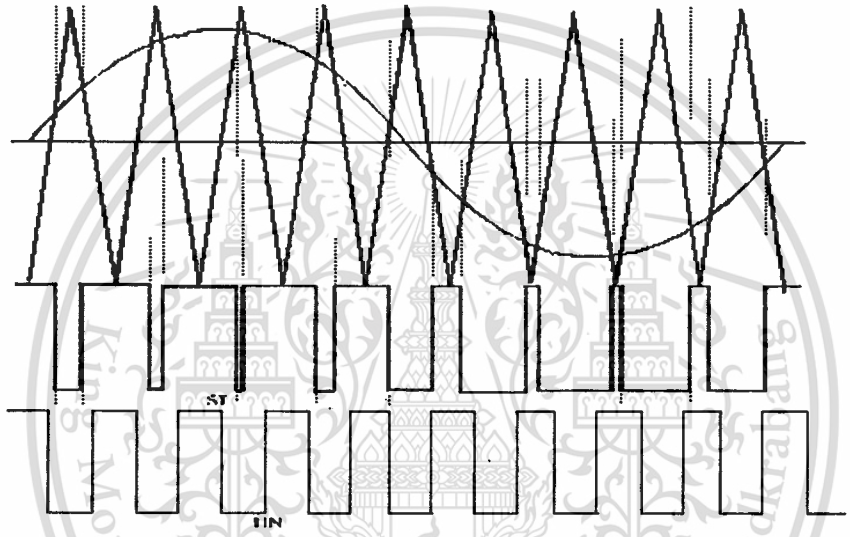

Figure 2.1 Unmodulated , sine modulated pulses

2.2.1 Linear Modulation

The simplest modulation to interpret is where the average ON time of the pulses varies proportionally with the modulating signal. The advantage of linear processing for this application lies in the ease of de-modulation. The modulating signal can be recovered from the PWM by low pass filtering. For a single low frequency sine wave as modulating signal modulating the width of a fixed frequency (f_s) pulse train the spectra is as shown in Figure 2.2. Clearly a low pass filter can extract the modulating component f_m.

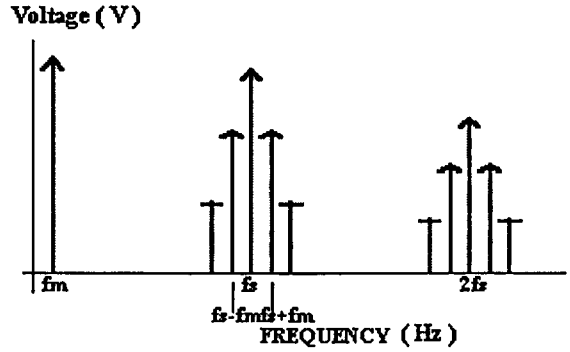

Figure 2.2 Spectra of PWM

2.2.2 Sampling Pulse Width Modulation

The simplest analog form of generating fixed frequency PWM is by comparison with a linear slope waveform such as a triangular (carrier). As seen in Figure 2.3, the output signal goes high when the sine wave (reference) is higher than the triangle. This is implemented using a comparator whose output voltage goes to logic HIGH when the input is greater than the other. This strategy is called PWM natural sampling (NS).

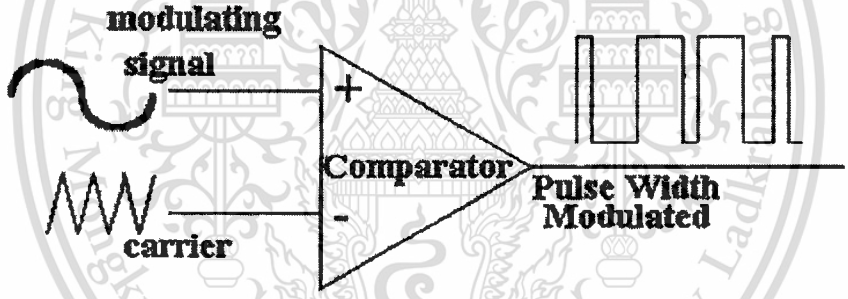

Figure 2.3 Natural Sinusoidal PWM

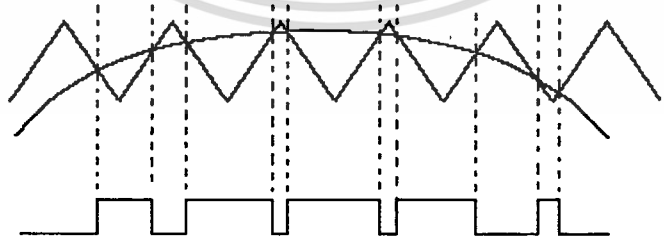

Figure 2.4 Waveform for converter switching

The triangular signal is the carrier or switching frequency of the converter. The modulation generator produces a sine wave signal that determines the width of pulses, and therefore the single-phase waveform for converter as shown in Figure 2.3 and Figure 2.4.

Similar to the single-phase waveform, the three-phase PWM waveforms and harmonic spectrum is shown in Figure 2.5 [16], Figure 2.6 shows the PWM line-to-neutral waveform and line current (load current).

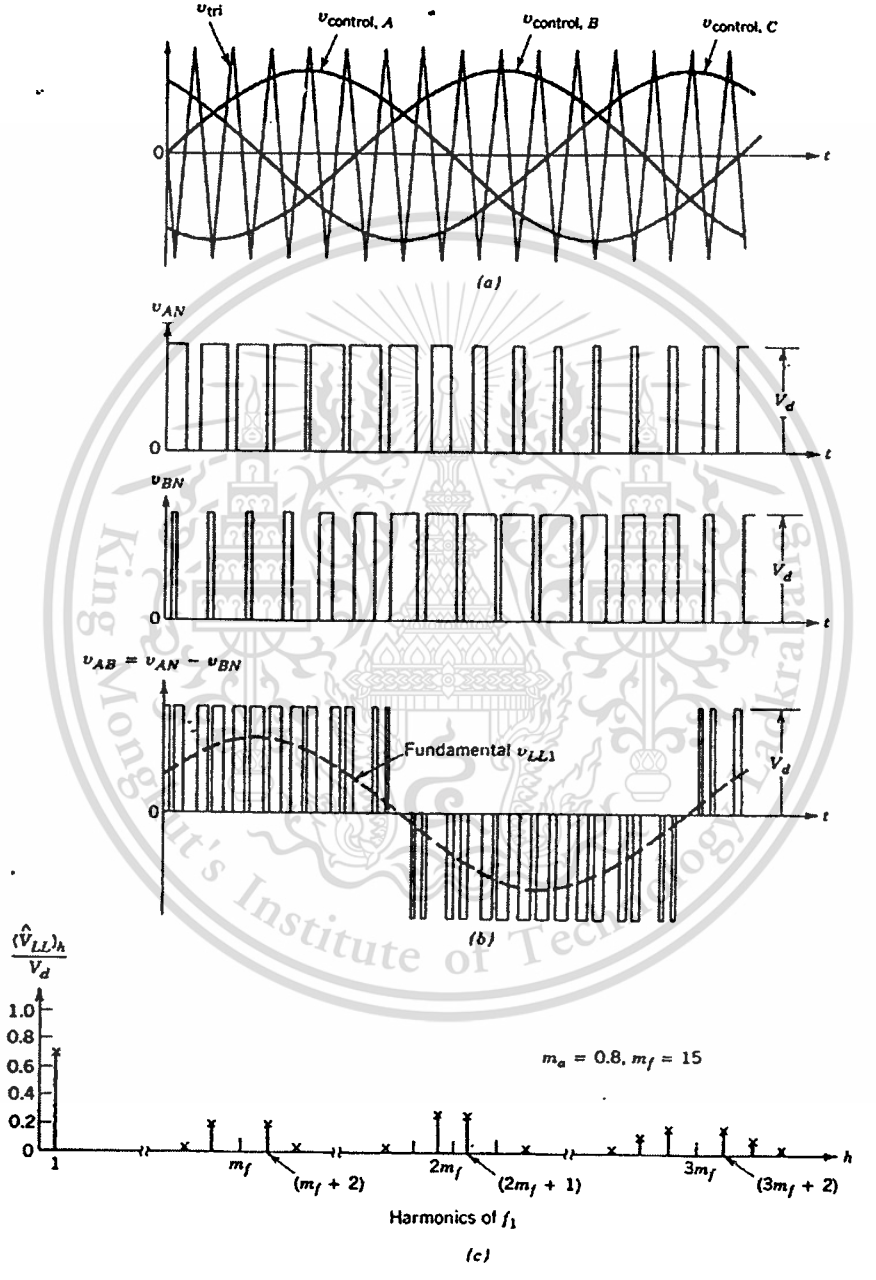

Figure 2.5 Three-phase PWM waveforms and harmonic spectrum

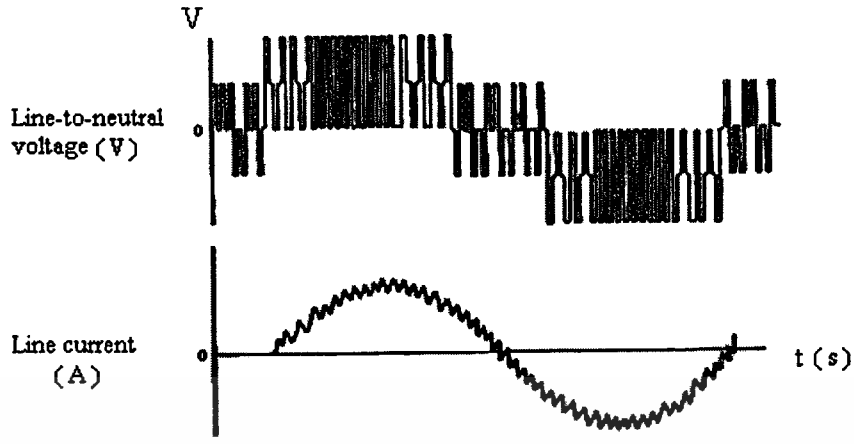

Figure 2.6 PWM line-to-neutral waveform and line current (load current)

2.2.3 Regular Sampled PWM

The scheme illustrated above generates a switching edge at the instant of crossing of the sinusoidal wave and the triangle. This is an easy scheme to implement using analog electronics but sufferring the imprecision and drift of all analog computation as well as having difficulties of generating multiple edges when the signal has even a small added noise. Many modulators are now implemented digitally but there is difficulty is computing the precise intercept of the modulating wave and the carrier. Regular sampled PWM makes the width of the pulse proportional to the value of the modulating signal at the beginning of the carrier period. In Figure 2.7 the intercept of the sample values with the triangle determine the edges of the Pulses

There are many ways to generate a Pulse Width Modulated signal other than fixed frequency sine triangular. For three phase systems the modulation of a Voltage Source Inverter can generate a PWM signal for each phase leg by comparison of the desired output voltage waveform for each phase with the same carrier. One alternative which is easier to implement in a computer and gives a larger modulation depth is using space vector modulation.

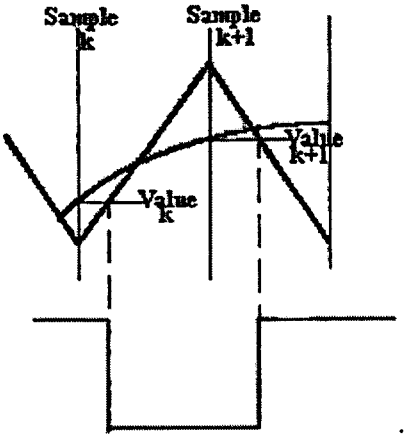

Figure2.7 Regular Sampled PWM

2.2.4 Modulation depth

For a single phase inverter modulated by a sine-sawtooth comparison, if we compare a sine wave of magnitude from -2 to +2 with a triangle from -1 to +1 the linear relation between the input signal and the average output signal will be lost. Once the sine wave reaches the peak of the triangle the pulses will be of maximum width and the modulation will then saturate. The Modulation depth is the ratio of the current signal to the case when saturation is just starting. Thus sine wave of peak 1.2 compared with a triangle with peak 2.0 will have a modulation depth of $m = 0.6$ as shown in Figure 2.8.

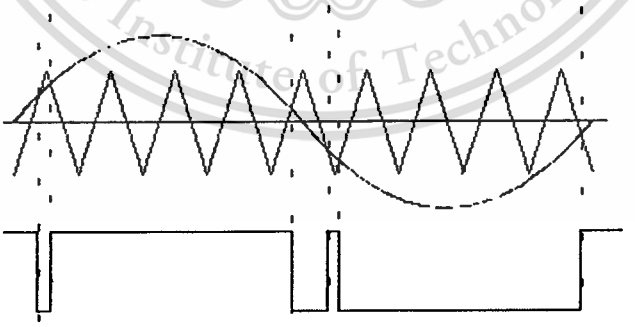

Figure 2.8 Saturated Pulse Width Modulation

2.3 Arrangements of HVDC systems

HVDC converter bridges and lines or cables can be arranged into a number of configurations for effective utilization. Converter bridges may be arranged either monopolar or bipolar as shown in Figure 2.9 and are described as follows:

2.3.1 Monopolar HVDC system

In monopolar links, two converters are used which are separated by a single pole line and a positive or a negative dc voltage is used. From Figure 2.9(a), there is only one insulated transmission conductor installed and the ground is used for the return current. For instance, the Konti-Skan (1965) project and Sardinia-Italy(mainland)(1967) project use monopolar links[8]. Instead of using the ground as a return path, a metallic return conductor may be used.

(a) Monopolar HVDC with earth return. (b) Bipolar HVDC

Figure 2.9 Monopolar and bipolar connection of HVDC converter bridges.

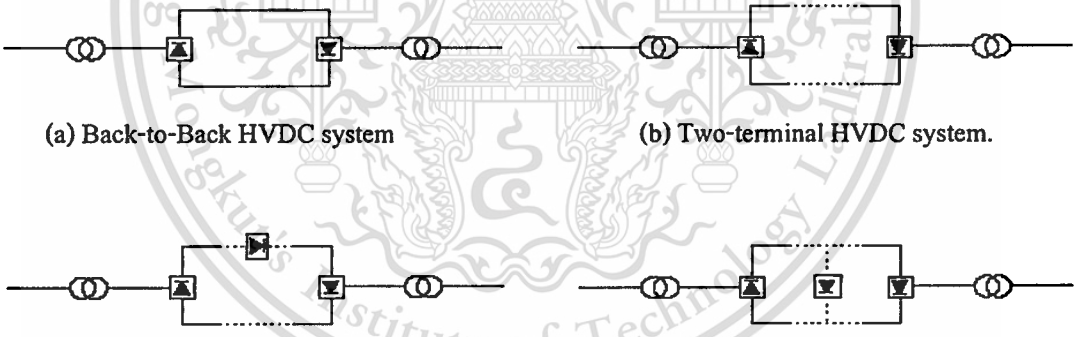

(a) Back-to-Back HVDC system (b) Two-terminal HVDC system.

(c) Series multi-terminal HVDC system (d) Parallel multi-terminal HVDC system

Figure 2.10 Various arrangements of HVDC systems.

2.3.2 Bipolar HVDC system

This is the most commonly used configuration of HVDC power transmission systems[8]. The bipolar circuit link, shown in Figure 2.9(b), has two insulated conductors used as plus and minus poles. The two poles can be used independently if both neutrals are grounded. It increases power transfer capacity. Under normal operation, the currents flowing in each pole are equal, and

there is no ground current. In case of failure of one pole power transmission can continue on the other pole, so its reliability is high. Most overhead line HVDC transmission systems are bipolar [8].

The selection of configurations of HVDC system depends on the function and location of the converter stations. Various schemes and configurations of HVDC systems are shown in simplified form in Figure 2.10[9]:

2.3.2.1 Back-to-back HVDC system

In this case the two converter stations are located at the same site and no transmission line or cable is required between the converter bridges. The connection may be monopolar or bipolar. A block diagram of a back-to-back system is shown in Figure 2.10(a). The two ac systems interconnected may have the same or different nominal frequency, i.e. 50Hz and 60Hz (The back-to-back link can be used to transmit power between two neighboring non-synchronous systems). Examples of such system can be found in Japan and South America [17]. The dc voltage in this case is quite low (i.e. 50kV -150kV) and the converter does not have to be optimized with respect to the dc bus voltage and the associated distance to reduce costs, etc.

2.3.2.2 Transmission between two substations (Long distance HVDC)

When it is economical to transfer electric power through dc transmission from one geographical location to another, a two-terminal or point-to-point HVDC transmission shown in Figure 2.10(b) is used. In other words, dc power from a dc rectifier terminal is transported to the other terminal operating as an inverter.

This is typical of most HVDC transmission systems. The link may connect two non-synchronous systems (e.g. between Sweden and Denmark) or connect two substations within one interconnected system (e.g. between Sweden and Finland, or the Three-gorges to Shanghai link in China).

2.3.3 Multi-terminal HVDC transmission system

When three or more HVDC substations are geographically separated with interconnecting transmission lines or cables, the HVDC transmission system is multiterminal. If all substations are connected to the same voltage then the system is parallel multi-terminal dc shown in Figure 2.10(d). If one or more converter bridges are added in series in one or both poles, then the system is series multi-terminal dc shown in Figure 2.10(c). A combination of parallel and series connections of converter bridges is a hybrid multi-terminal system. Multi-terminal dc systems are

more difficult to justify economically because of the cost of the additional substations. Examples of multi-terminal HVDC were implemented in the connection Sardinia-Corsica-Italy(SACOI), the Pacific Inter tie in the US and the connection Hydro Quebec-New England Hydro from Canada to the US[18].

2.3.4 Operating modes

In case of an outage of one pole or one line, there are several operating modes possible, that allow an operation of the workable system parts. If overload capabilities are used, half of the converter equipment is out of order, but less than half of the power rating is lost. Figure 2.11 shows the normal bipole operation. In case of fault in one of DC line for monopolar, ground return scheme is shown in Figure 2.12. But Figure 2.13, Figure 2.14 show monopolar, metallic return and monopolar, metallic return with two DC line parallel respectively in case of one converter pole fault.

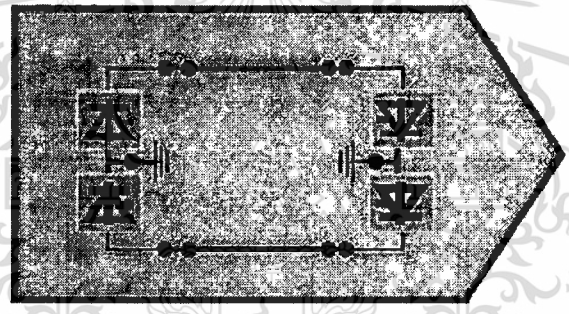

Figure 2.11 Normal bipole operation

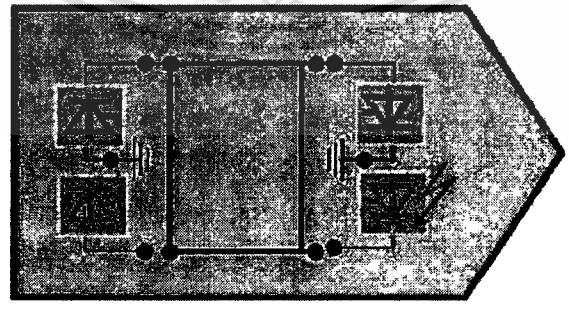

Figure 2.12 Monopolar, ground return (in Case of fault in one DC line)

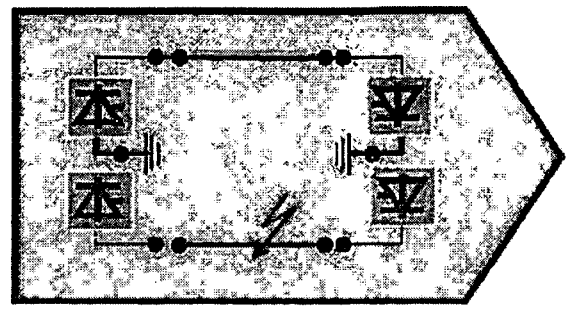

Figure 2.13 Monopolar, metallic return (in case of one converter pole fault)

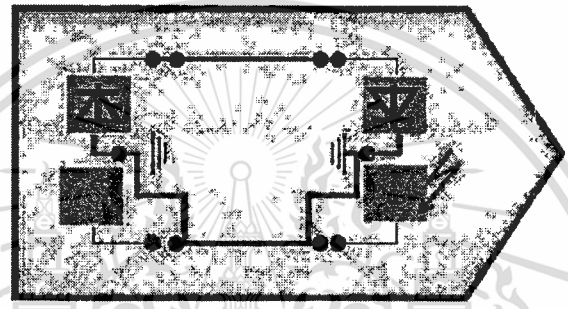

Figure 2.14 Monoplar, ground return, two DC lines parallel (in case of one converter pole fault)

2.3.5 Twelve-pulse line-frequency converters

It is important to reduce the current harmonics generated on the ac side and the voltage ripple produced on the dc side of the converter. This is accomplished by mean of a twelve-pulse converter operation, requires two 6-pulse converters connected through a Y-Y and a Δ-Y transformer, as is shown in Figure 2.15. The two 6-pulse converters are connected in series on a dc side and in parallel on the ac side. The series connection of two 6-pulse converters on the dc side is important to meet the high voltage requirement of an HVDC system.

In Figure 2.15, V_{as1n1} leads V_{as2n2} by 30°. The voltage and current waveforms can be drawn by assuming the current I_d on the dc side of the converter to be a pure dc in the presence of the large smoothing inductor L_d shown in Figure 2.15. Initially, for simplicity, we will assume that the per-phase ac side commutating inductance L_s is negligible, thus resulting rectangular current pulses. In practice, however, substantial commutating inductances are present as a result of the transformer leakage inductances.

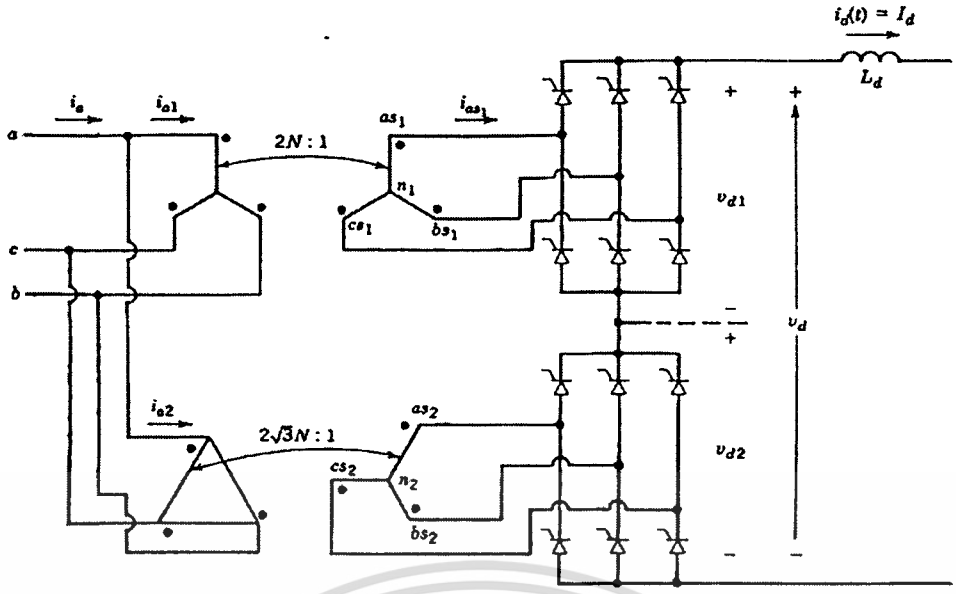

Figure 2.15 Twelve-pulse converter arrangement

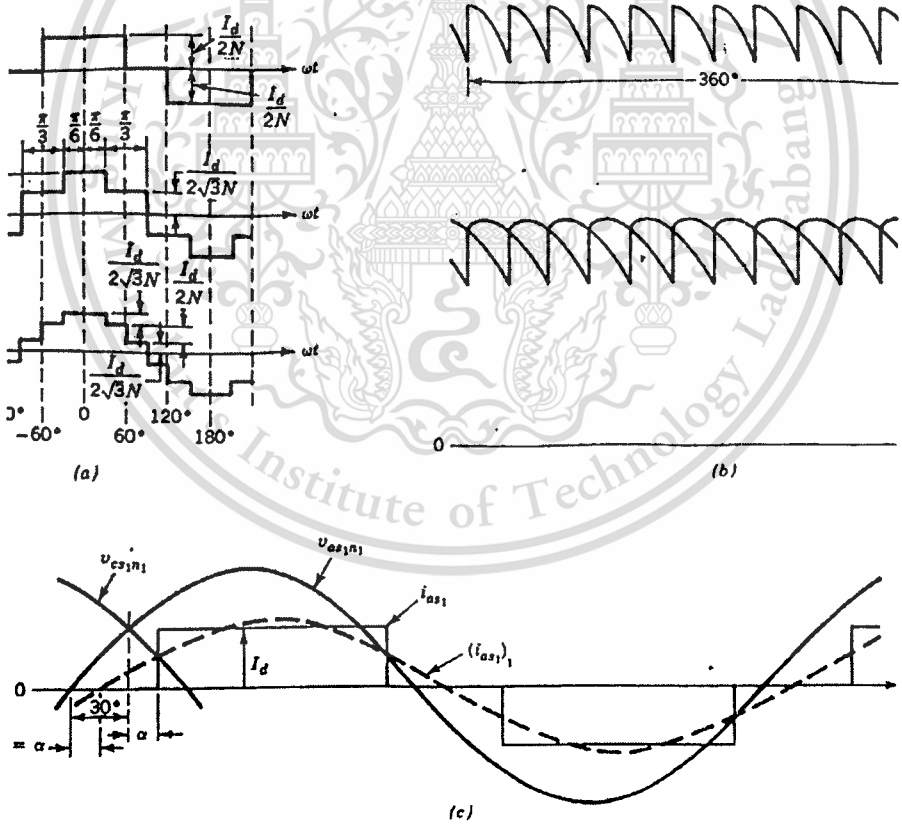

Figure 2.16 Idealized waveforms assuming $L_S = 0$

With the forgoing assumptions of $L_S = 0$ and $I_d(t) \approx I_d$ and recognizing that V_{as1n1} leads V_{as2n2} by 30°, we can draw the current waveforms as in Figure 2.16a.

Each 6-pulse converter operate at the same delay angle α. The waveform of the total per-phase current $i_a = i_{a1} + i_{a2}$ clearly shows that it contains fewer harmonics than either i_{a1} or i_{a2} drawn by the 6-pulse converters. In terms of their Fourier components.

$$i_{a1} = \frac{2\sqrt{3}}{2N\pi} I_d (\cos\theta - \frac{1}{5}\cos 5\theta + \frac{1}{7}\cos 7\theta - \frac{1}{11}\cos 11\theta + \frac{1}{13}\cos 13\theta ...) \qquad (2.1)$$

$$i_{a2} = \frac{2\sqrt{3}}{2N\pi} I_d (\cos\theta + \frac{1}{5}\cos 5\theta - \frac{1}{7}\cos 7\theta - \frac{1}{11}\cos 11\theta + \frac{1}{13}\cos 13\theta ...) \qquad (2.2)$$

where $\theta = \omega t$ and transformer turns ratio N is indicated in Figure 2.13. Therefore, the combined current drawn is

$$i_a = i_{a1} + i_{a2} = \frac{2\sqrt{3}}{N\pi} I_d (\cos\theta - \frac{1}{11}\cos 11\theta + \frac{1}{13}\cos 13\theta ...) \qquad (2.3)$$

This Fourier analysis shows that the combined line current has harmonics at the order resulting in a 12-pulse operation, as compared with a 6-pulse operation where the ac current harmonics are of the order $6k \pm 1$ (where k is integer).

$$h = 12k \pm 1 \qquad (2.4)$$

where k is an integer

The harmonic current amplitude in (2.3) for a 12-pulse converter are inversely proportional to their harmonic order and the lowest order harmonics are the eleventh and the thirteenth. The current on the ac side for the two 6-pulse converters add, confirming that the two converters are effectively in parallel on the ac side.

On the dc side, the voltage waveform V_{d1} and V_{d2} for the two 6-pulse converters are shown in Figure 2.16b. These two voltage forms are shifted by 30° with respect to each other. Since the two 6-pulse converters are connected in series on the dc side, the total dc voltage $V_d = V_{d1} + V_{d2}$

has 12 ripple pulses per fundamental-frequency ac cycle. This results in the voltage harmonics of the order h in V_d, where

$$h = 12k \tag{2.5}$$

where k is an integer

and the twelfth harmonic is the lowest order harmonic. Magnitude of the dc-side voltage harmonics vary significantly with the delay angle α.

In practice, L_S is substantial because of the leakage inductance of the transformers. The presence of L_S does not change the order of characteristic harmonics produced either on the ac side or on the dc side, provided that the two 6-pulse converters operate under identical conditions. However, the harmonic magnitudes depend significantly on L_S, delay angle α, and dc current I_d.

The average dc voltage can be written as

$$V_{d1} = V_{d2} = \frac{V_d}{2} = \frac{3\sqrt{2}}{\pi} V_{LL} \cos\alpha - \frac{3\omega L_s}{\pi} I_d \tag{2.6}$$

where V_{LL} is the line-to line rms voltage applied to each of the 6-pulse converters and L_S is the per-phase leakage inductance of each of the transformer, referred to their converter side.

2.3.5.1 Rectifier mode of operation

With the initial assumption that Ls = 0 in Figure 2.15, Figure 2.16c shows the phase-to-neutral voltage Vas1n1 and the current ias1 (corresponding to converter 1 in Figure 2.16) with $i_d(t) \approx I_d$ at a delay angle α. The fundamental-frequency current component$(ias1)_1$ shown by the dashed curve lags behind the phase voltageV_{as1n1} by the displacement power factor angle Φ_1, where

$$\phi_1 = \alpha \tag{2.7}$$

Therefore, the three-phase reactive power (lagging) required by the 6-pulse converter because of the fundamental-frequency reactive current components, which lag their respective phase voltage by 90°, equals

$$Q_1 = \sqrt{3} V_{LL} (I_{as1}) \sin\alpha \tag{2.8}$$

where V_{LL} is the line-to-line voltage on the ac side of the converter.

From the Fourier analysis of the ias1 in Figure 2.16c, the rms value of its fundamental-frequency component is

$$(I_{as1})_1 = \frac{\sqrt{6}}{\pi} I_d \approx 0.78 I_d \tag{2.9}$$

Therefore, from (equation 2.8 and 2.9)

$$Q_1 = \sqrt{3} V_{LL} (\frac{\sqrt{6}}{\pi} I_d) \sin\alpha = 1.35.78 I_d V_{LL} I_d \sin\alpha \tag{2.10}$$

The real power transfer through each of the 6-pulse converter can be calculated from (2.6) with L_s = 0 as

$$P_{d1} = V_{d1} I_d = 1.35 V_{LL} I_d \cos\alpha \tag{2.11}$$

For a desired power transfer P_{d1}, the reactive power demand Q_1 should be minimized as much as possible. Similarly, I_d should be kept as small as possible to minimize I^2R losses on the dc transmission line. To minimize Id and Q_1, noting that V_{LL} is essentially constant in (2.10,2.11), we should choose a small value for the delay α in the rectifier mode of operation. For practical reasons, the minimum value of α is chosen in a range of $10^\circ - 20^\circ$.

2.3.5.2 Inverter mode of operation

In the inverter mode, the dc voltage of the converter acts like a counter emf in a dc motor. Therefore, it is convenient to define the dc voltage polarity as shown in Figure 2.17a, so that the dc voltage is positive when written specifically for the inverter mode of operation. The extinction angle γ for the inverter was defined in terms of α and u as

$$\gamma = 180^\circ - (\alpha + u) \tag{2.12}$$

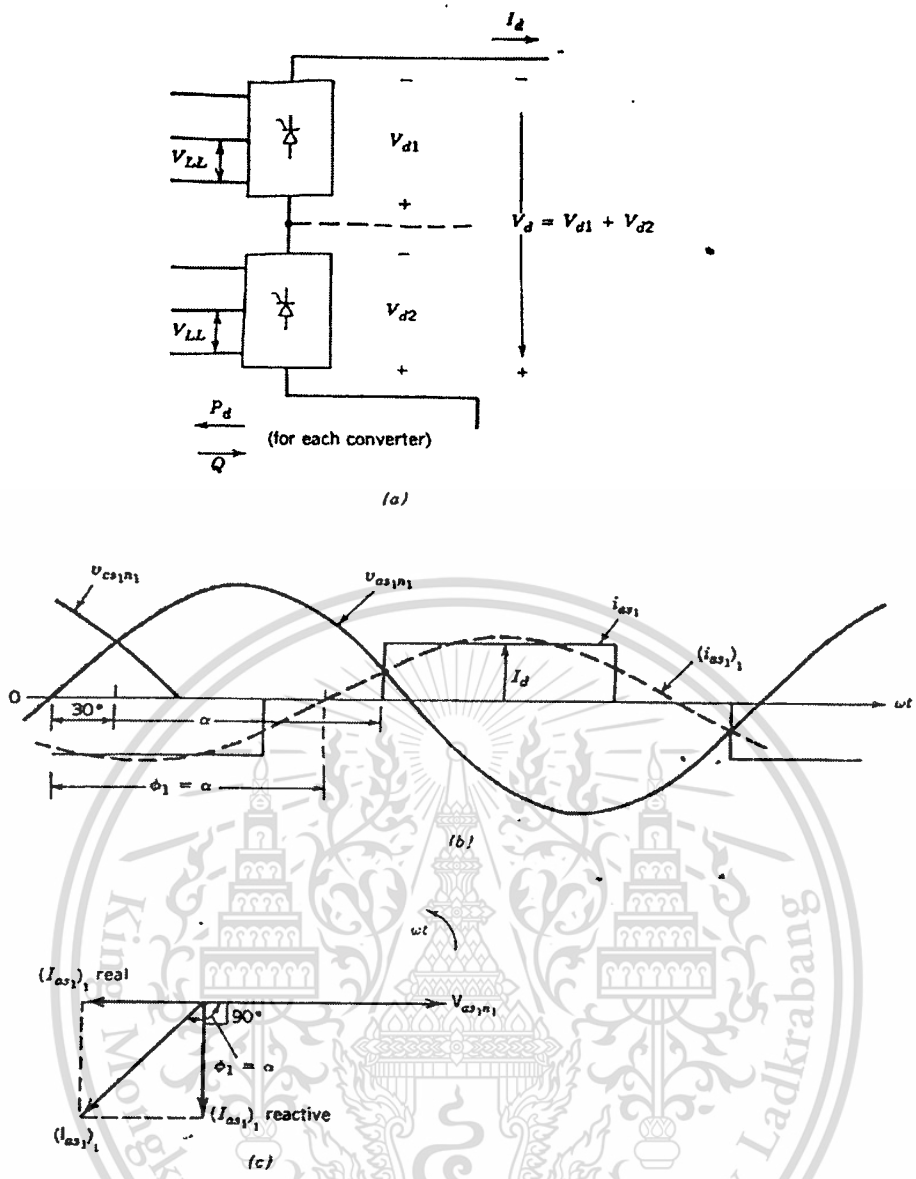

Figure 2.17 Inverter mode of operating (assuming $L_S = 0$)

where α is the delay angle and u is the commutation or the overlap angle. The inverter voltage in Figure 2.17 can be obtained as (see Problems 2.7)

$$V_{d1} = V_{d2} = \frac{V_d}{2} = 1.35V_{LL}\cos\gamma - \frac{3\omega L_S}{\pi} I_d \qquad (2.13)$$

Again with the assumption that $L_S = 0$ for simplicity, Figure 2. 17(b) shows the idealized waveform for V_{asln} and i_{as} at an $\alpha > 90^\circ$, corresponding to the inverter mode of operation. The fundamental-frequency component $(i_{as1})_1$ of the phase current is shown by the dashed curve. In the phasor diagram of Figure 2.17(c), the fundamental-frequency reactive current component lags behind the phase-to-neutral voltage, indicating that even in the inverter mode, where the direction of power flow through the converter has reversed, the converter requires reactive power (lagging) from the ac system.

With $L_S = 0$, $u = 0$ in (2.12) and $\gamma = 180^\circ - \alpha$. Therefore, the expressions for per-converter Q_1 and P_{d1} in (2.10, 2.11) can be obtained specifically for the inverter mode in terms of γ as

$$Q_1 = 1.35 V_{LL} I_d \sin\gamma \tag{2.14}$$

and

$$P_{d1} = 1.35 V_{LL} I_d \cos\gamma \tag{2.15}$$

where the directions of the reactive power (lagging) and the real power are as shown in Figure 2.17a. From equation 2.14 and 2.15), γ should be as small as possible for a given power transfer level to minimize I_2R losses in the transmission line due to Id and to minimize the reactive power demand of the converter. The minimum value that is allowed to attain is called the minimum extinction angle that is based on allowing sufficient turn-off time to the thyristors.

In a 12-pulse converter arrangement, the reactive power requirement is the sum of the reactive powers required by each of the two 6-pulse converters. The ac-side filter banks and the power factor correction capacitors partially provide the reactive power demand of the converters[16].

2.4 Classic HVDC systems

2.4.1 Configuration of classic HVDC systems

A classic HVDC system operating in bipolar mode, shown in Figure 2.18, consists of ac filters, shunt capacitor banks or other reactive-compensation equipment, converter transformers, converters, dc reactors, dc filters, and dc lines or cables [9].

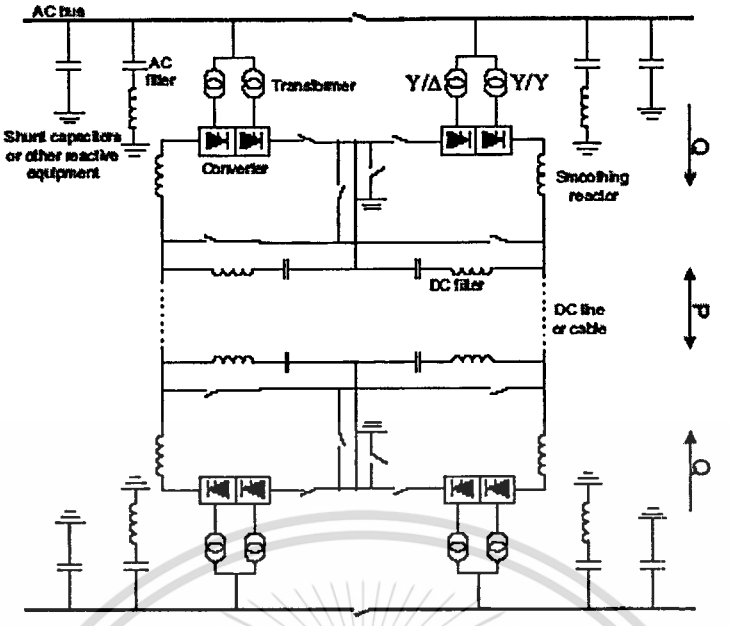

Figure 2.18 A basic configuration for a classic HVDC system.

2.4.1.1 Converters

The HVDC converters are an HVDC system's hearts. They perform the conversion from ac to dc (rectifier) at the sending end and from dc to ac (inverter) at the receiving end. HVDC converters are connected to the ac system by means of converter transformers. The classic HVDC converters are current source converters (CSCs). The dc current is kept constant. Magnitude and direction of power flow are controlled by changing magnitude and direction of the dc voltage[19].

The main components are the thyristor valves. The six pulse valve bridge of Figure 2.19 as the basic converter unit of classic HVDC is used equally well for rectification and inversion. The inductance is normally in the form of a transformer. A 12 pulse converter bridge can be built by connecting two six pulse bridges in series or parallel. Each single bridge consists of a certain amount of series connected thyristors with their auxiliary circuits. The bridges are then connected separately to the ac system by means of converter transformers, one of Y-Y winding structure and another Y-ϕ winding structure, as shown in Figure 2.18. In this way the 5th and 7th harmonic currents through the two transformers are in opposite phase. This significantly reduces the distortion in the ac system due to the HVDC converters [20][21].

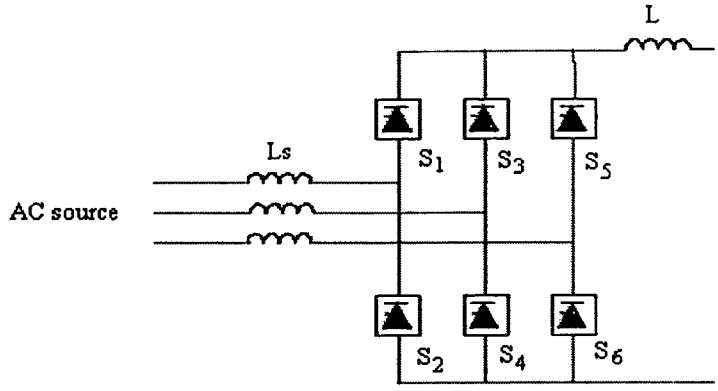

Figure 2.19 Configuration of the basic six pulse valve group.

2.4.1.2 Transformers

The transformers connect the ac network to the valve bridges, and adjust the ac voltage level on the rectifier terminals to a suitable level based on the dc voltage used for the transmission. The transformers can be of different design depending on the power to be transmitted, and possible transport requirements. The most common type is a single-phase-three-winding design. The windings on network side are connected in star. The windings on converter side are connected in star for one converter and in delta for the other converter. Three identical transformers are then needed per converter.

2.4.1.3 AC-side harmonic filters

The HVDC converters produce current harmonics on the ac side, these harmonics are prevented from entering into the connected ac network by ac filters. For example, on the ac side of a 12-pulse HVDC converter, current harmonics of the order of 11, 13, 23, 25 and higher are generated. Filters are installed in order to limit the amount of harmonics to a level allowed by the network. In the conversion process the converter consumes reactive power which is compensated in part by the filter banks and the rest by capacitor banks. In the case of the CCC (capacitor commutated converter) the reactive power is compensated by series capacitors installed in series between the converter valves and the converter transformer. The elimination of switched reactive power compensation equipment simplifies the ac switchyard and minimizes the number of circuit-breakers needed, which will reduce the area required for an HVDC station built with CCC [22] [23].

2.4.1.4 Dc filters

The HVDC converters produce ripple on the dc voltage. Voltage ripple in the frequency band between a few hundred hertz and a few kilohertz causes interference to telephone circuits near the dc line. Therefore, specially designed dc filters are used in order to reduce the ripple. Usually no dc filters are needed for pure cable transmission nor for Back-to-Back HVDC stations. However, it is necessary to install dc filters if an overhead line is used in part or all of the transmission system. The filters needed to take care of the harmonics generated on the dc end, are usually considerably smaller and less expensive than the filters on the ac side. Both passive and active dc filters can be used. In active filters power electronics is used to compensate the harmonic distortion. In modern installations active dc filters are used. Active filters are considered more flexible than passive filters, and become cheaper than passive filters for more complex tasks [24].

2.4.1.5 HVDC cables or overhead lines

HVDC cables are normally used for submarine transmission. No serious length limitation exists for HVDC cables. For a back to back HVDC system, no dc cable or overhead line is needed. For connections over land, overhead lines are typically used. However the tendency is to also move to cables for connections over land, due to environmental concerns.

2.4.1.6 Control of classic HVDC systems

The power transmitted over the HVDC link is controlled through the control system where one of the converters controls the dc voltage and the other converter controls the current through the dc circuit. The control system acts through firing angle adjustments of the valves and through tap changer adjustments on the converter transformers to obtain the desired combination of voltage and current. The control systems of the two stations of a bipolar HVDC system usually communicate with each other through a telecommunication link.

2.4.1.7 Protection of classic HVDC systems

DC converter stations form an integral part with the ac system, and their basic protection philosophy is thus greatly influenced by ac-system protection principles. However, the limitations of dc circuit breakers and the speed of controllability of HVDC converters influence some departure from the conventional protection philosophy. Furthermore, the series connection for converter equipment also presents some special problems not normally encountered in ac substations.

2.4.2 Advantages of classic HVDC systems

It is important to remark that an HVDC system not only transmits electrical power, but it also has a lot of value added which should have been necessary to solve by other means in the case of using conventional ac transmission. Some of these aspects are:

- No limits in transmitted distance. This is valid for both overhead lines and sea or underground cables.
- Very fast and accurate control of power flow, which implies stability improvements, not only for the HVDC link but also for the surrounding ac system.
- Magnitude and direction of power can be changed very quickly (bi-directionality).
- An HVDC link does not increase the short-circuit power in the connecting point. This means that it will not be necessary to change the circuit breakers in the existing network.
- HVDC can carry more power for a given size of conductor.
- The need for right-of-way is much smaller for HVDC than for an ac connection, for the same transmitted power. The environmental impact is therefore smaller with HVDC, and it is easier to obtain permission to build.
- Power can be transmitted between two ac-systems operating at different nominal frequencies or at the same frequency but without being synchronized.

2.4.3 Applications of classic HVDC systems

The first application for classic HVDC systems was to provide point to point electrical power interconnections between asynchronous ac power networks. There are other applications which can be met by HVDC converter transmission which include:

- Interconnections between asynchronous systems. Some continental electric power systems consisting of asynchronous networks such as the East, West, Texas and Quebec networks in North America make use of HVDC interconnections.
- Deliver energy from remote energy sources. Where generation has been developed at remote sites of available energy, HVDC transmission has been an economical means to bring the electricity to load centers. The main application has been the connection of remote hydro-stations to load centers.
- Import electric energy into congested load areas. In areas where new generation is impossible to bring into service to meet load growth or replace inefficient or decommissioned plant, underground dc cable transmission is a viable means to import electricity.

• Increasing the capacity of existing ac transmission by conversion to dc transmission. New transmission rights-of-way may be impossible to obtain. Existing overhead ac transmission lines upgraded to or overbuilt with dc transmission can substantially increase the power transfer capability on the existing right-of-way.

• Power flow control. Ac networks do not easily accommodate desired power flow control. Power marketers and system operators may require the power flow control capability provided by HVDC transmission.

• Stabilization of electric power networks. Some wide spread ac power system networks operate at stability limits well below the thermal capacity of their transmission conductors. HVDC transmission is an option to consider to increase utilization of network conductors along with the various power electronic controllers which can be applied on ac transmission.

• An HVDC transmission line has lower losses than ac lines for the same power capacity. The losses in the converter stations have of course to be added, but above a certain break-even distance, the total HVDC transmission losses become lower than the ac losses. HVDC cables also have lower losses than ac cables.

Although thyristor-based HVDC systems represent mature technology, there are still exciting developments worth mentioning such as:

• active ac and dc filtering.

• capacitor commutated converter(CCC) based systems[9].

An improvement in the thyristor-based commutation, the CCC concept is characterized by the use of commutation capacitors inserted in series between the converter transformers and the thyristor valves. The commutation capacitors reduce the risk of commutation failure of the converters when connected to weak networks.

• air-insulated outdoor thyristor valves.

• new and advanced cabling technology.

• direct connection of generators to HVDC converters.

2.5 VSC-HVDC system

2.5.1 Configuration of VSC-HVDC system

VSC-HVDC is a new dc transmission system technology. It is based on the voltage source converter, where the valves are built by IGBTs and PWM is used to create the desired voltage waveform. With PWM it is possible to create any waveform (up to a certain limit set by the

switching frequency), any phase angle and magnitude of the fundamental component. Changes in waveform, phase angle and magnitude can be made by changing the PWM pattern, which can be done almost instantaneously.

Thus, the voltage source converter can be considered as a controllable voltage source. This high controllability allows for a wide range of applications. From a system point of view VSC-HVDC acts as a synchronous machine without mass that can control active and reactive power almost instantaneously. In this chapter, the topology of the investigated VSC-HVDC is discussed.

2.5.2 System description

The main function of the VSC-HVDC is to transmit constant dc power from the rectifier to the inverter. As shown in Figure 2.20, it consists of dc-link capacitors C_{dc}, two converters, passive high-pass filters, phase reactors, transformers and dc cable.

2.5.2.1 Physical structure

The converters are VSCs employing IGBT power semiconductors, one operating as a rectifier and the other as an inverter. The two converters are connected either back-to-back or through a dc cable, depending on the application.

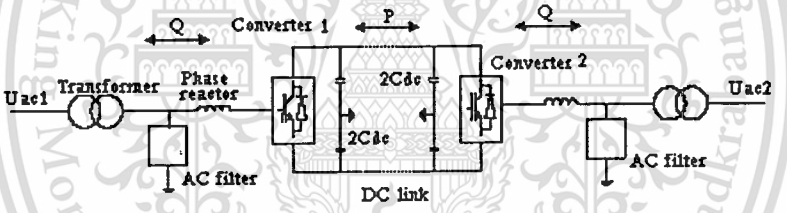

Figure 2.20 Topology of VSC-HVDC.

2.5.2.2 Transformers

Normally, the converters are connected to the ac system via transformers. The most important function of the transformers is to transform the voltage of the ac system to a value suitable to the converter. It can use simple connection (two-winding instead of three to eight-winding transformers used for other schemes [5]). The leakage inductance of the transformers is usually in the range 0.1-0.2pu.

2.5.2.3 Phase reactors

The phase reactors are used for controlling both the active and the reactive power flow by regulating currents through them. The reactors also function as ac filters to reduce the high

frequency harmonic contents of the ac currents which are caused by the switching operation of the VSCs. The reactors are essential for both the active and reactive power flow, since these properties are determined by the power frequency voltage across the reactors. The reactors are usually about 0.15pu impedance.

2.5.2.4 AC filters

The ac voltage output contains harmonic components, derived from the switching of the IGBT's. These harmonics have to be taken care of preventing them from being emitted into the ac system and causing malfunctioning of ac system equipment or radio and telecommunication disturbances. High-pass filter branches are installed to take care of these high order harmonics. With VSC converters there is no need to compensate any reactive power consumed by the converter itself and the current harmonics on the ac side are related directly to the PWM frequency. The amount of low-order harmonics in the current is small. Therefore the amount of filters in this type of converters is reduced dramatically compared with natural commutated converters.

2.5.2.5 DC capacitors

On the dc side there are two capacitor stacks of the same size. The size of these capacitors depends on the required dc voltage. The objective for the dc capacitor is primarily to provide a low inductive path for the turned-off current and energy storage to be able to control the power flow. The capacitor also reduces the voltage ripple on the dc side.

2.5.2.6 DC cables

The cable used in VSC-HVDC applications is a new developed type, where the insulation is made of an extruded polymer that is particularly resistant to dc voltage. Polymeric cables are the preferred choice for HVDC, mainly because of their mechanical strength, flexibility, and low weight[25].

2.5.3 Converters

The converters so far employed in actual transmission applications are composed of a number of elementary converters, that is, of three-phase, two-level, six-pulse bridges, as shown in Figure 2.21, or three-phase, three-level, 12-pulse bridges, as shown in Figure 2.22.

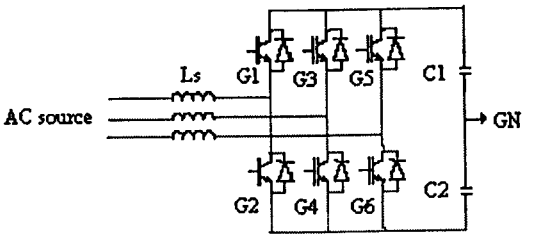

Figure 2.21 Two-level VSC converter.

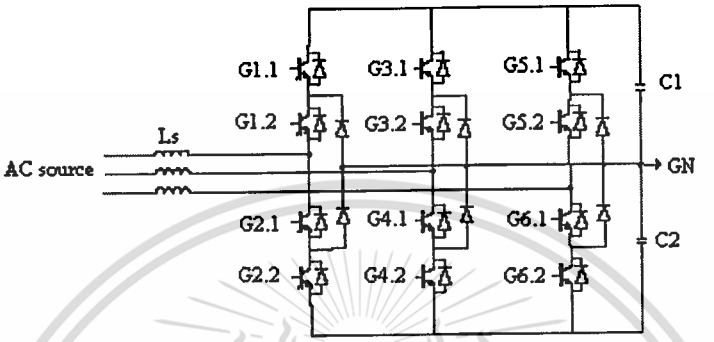

Figure 2.22 Three-level VSC converter.

The two-level bridge is the most simple circuit configuration that can be used for building up a three-phase forced commutated VSC bridge. It has been widely used in many applications at a wide range of power levels. As shown in Figure 2.21, the two-level converter is capable of generating the two-voltage levels $-0.5.U_{dc}N$ and $+0.5.U_{dc}N$. The two-level bridge consists of six valves and each valve consists of an IGBT and an anti-parallel diode. In order to use the two-level bridge in high power applications series connection of devices may be necessary and then each valve will be built up of a number of series connected turn-off devices and anti-parallel diodes. The number of devices required is determined by the rated power of the bridge and the power handling capability of the switching devices.

With a present technology of IGBTs a voltage rating of 2.5kV has recently become available in the market and soon higher voltages are expected. The IGBTs can be switched on and off with a constant frequency of about 2kHz. The IGBT valves can block up to 150kV. A VSC equipped with these valves can carry up to 800A (rms) ac line current. This results in a power rating of approximately 140MVA of one VSC and a ±150kV bipolar transmission system for power ratings up to 200MW[25].

2.5.4 Advantages and applications of VSC-HVDC

The main difference in operation between classic HVDC and VSC-HVDC is the higher controllability of the latter. This leads to a number of new advantages and applications, some of which are given below. This is a very new technology and the number of installations in use is still very limited. Most of the examples given below are only potential applications [9,25-26]. The general agreement appears that the technical potential is very large, the limitations are mainly on the economic side.

- Independent control of active and reactive power without any needs for extra compensating equipment.

With PWM, VSC-HVDC offers the possibility to control both active and reactive power independently. While the transmitted active power is kept constant the reactive power controller can automatically control the voltage in the ac-network.

Reactive power generation and consumption of a VSC-HVDC converter can be used for compensating the needs of the connected network within the rating of a converter.

- Mitigation of power quality disturbances.

The reactive power capabilities of VSC-HVDC can be used to control the ac network voltages, and thereby contribute to an enhanced power quality. Furthermore, the faster response due to increased switching frequency (PWM) offers new levels of performance regarding power quality control such as flicker and mitigation of voltage dips, harmonics etc. Power quality problems are issues of priority for owners of industrial plants, grid operators as well as for the general public [4].

- No contribution to short circuit currents.

The converter works independently of any ac source, which makes it less sensitive for disturbances in the ac network and ac faults do not drastically affect the dc side. If ac systems have ground faults or short circuits, whereupon the ac voltage drops, the dc power transmitted is automatically reduced to a predetermined value.

- Reduced risk of commutation failures.

Disturbances in the ac system may lead to commutation failures in classic HVDC system. As VSC-HVDC uses self-commutating semiconductor devices, the presence of a sufficiently-high ac voltage is no longer needed. This significantly reduces the risk of commutation failures, and extends the use of the HVDC system in stability control.

- Communication not needed.

The control systems on rectifier and inverter side operate independently of each other. They do not depend on a telecommunication connection. This improves the speed and the reliability of the controller.

- Feeding islands and passive ac networks.

The VSC converter is able to create its own ac voltage at any predetermined frequency, without the need for rotating machines. It may be used to supply industrial installations or large wind farms.

- Multi-terminal dc grid.

VSC converters are very suitable for creating a dc grid with a large number of converters, since very little coordination is needed between the interconnected VSC-HVDC converters.

Chapter 3

Modeling for Voltage Source Converter Controlled Power Transfer for HVDC Applications

3.1 Introduction

In recent years, voltage source converter technology has made a great progress through the development of high power self-turn off type semiconductor devices. The rating for converter of this type in practical application has already reached as a high power capacity. Because of its advantage over the line commutated type in performance characteristics and compactness, various applications of the voltage source converter have been developed and researched [27].

In this thesis, a model for PWM VSC Controlled Power Transfer for HVDC Application is developed. The control variables based on mathematical model are determined and vector control strategy is proposed.

Under steady state conditions, the 3-phase quantities when expressed in the synchronously rotating frame become dc quantities. If one of the axes, usually the d-axis, arbitrarily aligned with supply voltage vector, then he d and q axis supply current components automatically represent the active (P) and the reactive (Q) power flow respectively. Thus it is possible to have decoupled control of the active and reactive control. The DC-link voltage controller sets the active power demand whereas the reactive power demand can be set by an outer reactive power controller or by the required displacement angle between the phase current and voltages.

Therefore, the main advantages of the vector control technique are the direct control of the active and reactive power flow in the converter during transient, steady state and the fast dynamics of the current control loops. Additionally, the current controllers deal with dc quantities which, using PI controllers, ensure zero current error in steady state. These are the main reasons for selecting the control strategy for the implementation of the VSC. The validity of proposed model and control strategy has been verified by digital simulation using SIMULINK MATLAB version 6.5.

3.2 Basic system configuration of VSC

The system configuration of the VSC connected to the on side of an ac network is shown in Figure 3.1. The 3-phase supply voltages are v_a, v_b, v_c and the 3-phase converter voltages are v_{a1}, v_{b1} and v_{c1}. The PWM control block is adopted to control IGBT, this control not only can manage the active power, but also reactive power, allowing this type of VSC to correct power factor.

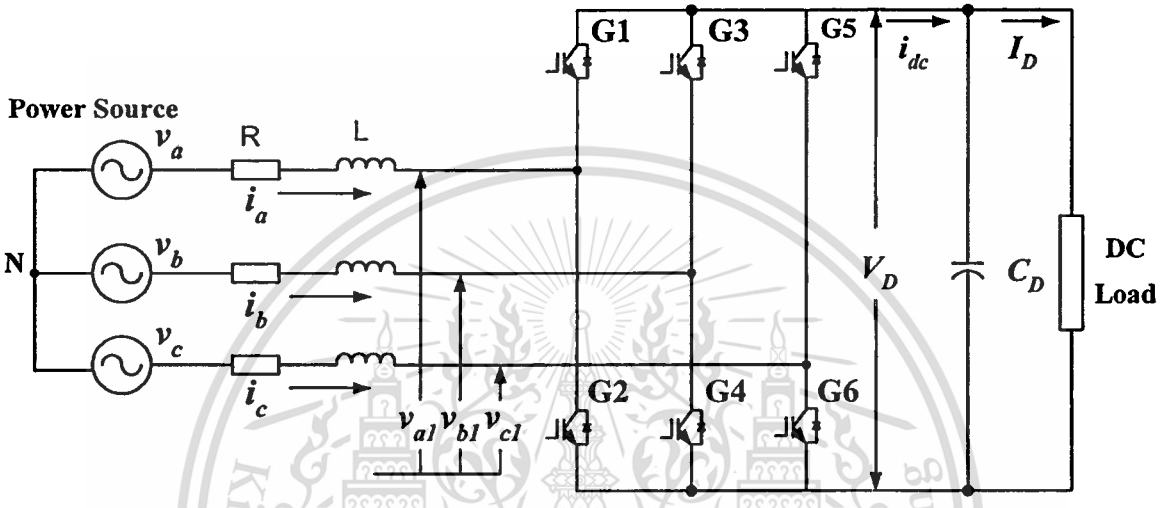

Figure 3.1 Schematic diagram of a three-phase voltage source converter.

3.3 VSC model and its vector control structure for side 1 of HVDC system

According to Figure 3.1, assuming ideal commutation and neglecting the effect of current harmonics, the equations that model side 1 of VSC can be derived as follows. Considering that V_{a1},V_{b1} and V_{c1} are the fundamental voltages per phase at the input of converter, the following equation can be written:

$$\begin{bmatrix} v_a \\ v_b \\ v_c \end{bmatrix} = R\begin{bmatrix} i_a \\ i_b \\ i_c \end{bmatrix} + L\frac{d}{dt}\begin{bmatrix} i_a \\ i_b \\ i_c \end{bmatrix} + \begin{bmatrix} v_{a1} \\ v_{b1} \\ v_{c1} \end{bmatrix} \tag{3.1}$$

From the reference frame transformations, stationary ABC reference frame to stationary reference frame for voltages are[28]:

$$v_\alpha = \sqrt{3}v_{ab} + \frac{\sqrt{3}}{2}v_{bc} \tag{3.2}$$

$$v_\beta = \frac{3}{2}v_{bc} \tag{3.3}$$

and for currents are:

$$i_\alpha = \frac{3}{2}i_a \tag{3.4}$$

$$i_\beta = \frac{\sqrt{3}}{2}(i_b - i_c) \tag{3.5}$$

and stationary αβ reference frame to rotating d-q reference frame for voltages (and currents) are :

$$v_d = \frac{1}{k}(v_\alpha \cos\theta - v_\beta \sin\theta) \tag{3.6}$$

$$v_q = \frac{1}{k}(v_\beta \cos\theta + v_\alpha \sin\theta) \tag{3.7}$$

where θ is the angle position of the d-q reference frame. The scaling factor k is introduced so that the d-q variables are scaled to have the same amplitude as the rms phase quantities as follows:

For the voltages:

$k = \frac{3}{2}\sqrt{2}$ for Delta Connection and

$k = \frac{3}{2}\sqrt{6}$ for Star Connection.

For the currents:

$k = \frac{3}{2}\sqrt{6}$ for Delta Connection and

$k = \frac{3}{2}\sqrt{2}$ for Star Connection.

Using the transformation given above, equation (3.1) can be transformed into a synchronously rotating (angular frequency, ω_e) d-q reference frame, to yield the following expressions:

$$v_d = Ri_d + L\frac{di_d}{dt} - \omega_e L i_q + v_{dl} \tag{3.8}$$

$$v_q = Ri_q + L\frac{di_q}{dt} + \omega_e L i_d + v_{ql} \tag{3.9}$$

And the following equivalent circuit is obtained as shown in Figure 3.2.

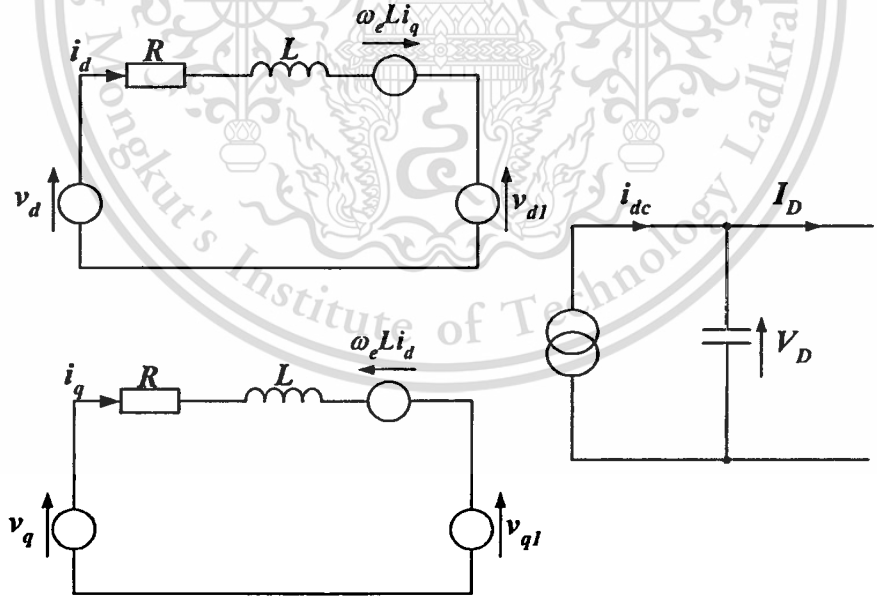

Figure 3.2 VSC equivalent circuit in d-q coordination.

Using the scaling factor for the transformations as shown above, i_{dc} is given by:

$$i_{dc} = 3\frac{i_d v_{d1} + i_q v_{q1}}{V_D} \tag{3.10}$$

The expressions for the active and reactive power flowing from the supply to converter are given by:

$$P = 3(v_d i_d + v_q i_q) \tag{3.11}$$

$$Q = 3(v_d i_q + v_q i_d) \tag{3.12}$$

If the d-axis of the reference frame is aligned along the supply voltage vector position, vq is zero and since the amplitude of the supply voltage is constant, v_d is constant. Therefore the active and reactive power flow from the supply to converter will be proportional to id and iq respectively. To calculate the supply voltage vector position θ_e, the 3-phase voltages are transformed to a stationary 2-axis (α,β) reference frame as described above to give:

$$\theta_e = \arctan\frac{V_\beta}{V_\alpha} \tag{3.13}$$

$$\omega_e = \frac{d\theta_e}{dt} \tag{3.14}$$

Where v_α , v_β , are the supply voltage components. Neglecting the losses in the filter resistance and the DC-link (i.e. $v_{d1} = v_d$ and $v_{q1} = v_q = 0$) the following relations can be written:

$$V_D i_{dc} = 3 v_d i_d \tag{3.15}$$

$$m_1 = \frac{2\sqrt{2}v_d}{V_D} \tag{3.16}$$

$$i_{dc} = \frac{3}{2\sqrt{2}} m_1 i_d \tag{3.17}$$

$$C\frac{dV_D}{dt} = i_{dc} - I_D \tag{3.18}$$

where m_1 is the PWM modulation index for converter. From (3.15)-(3.18) it is seen that the DC-link voltage can be controlled by i_d.

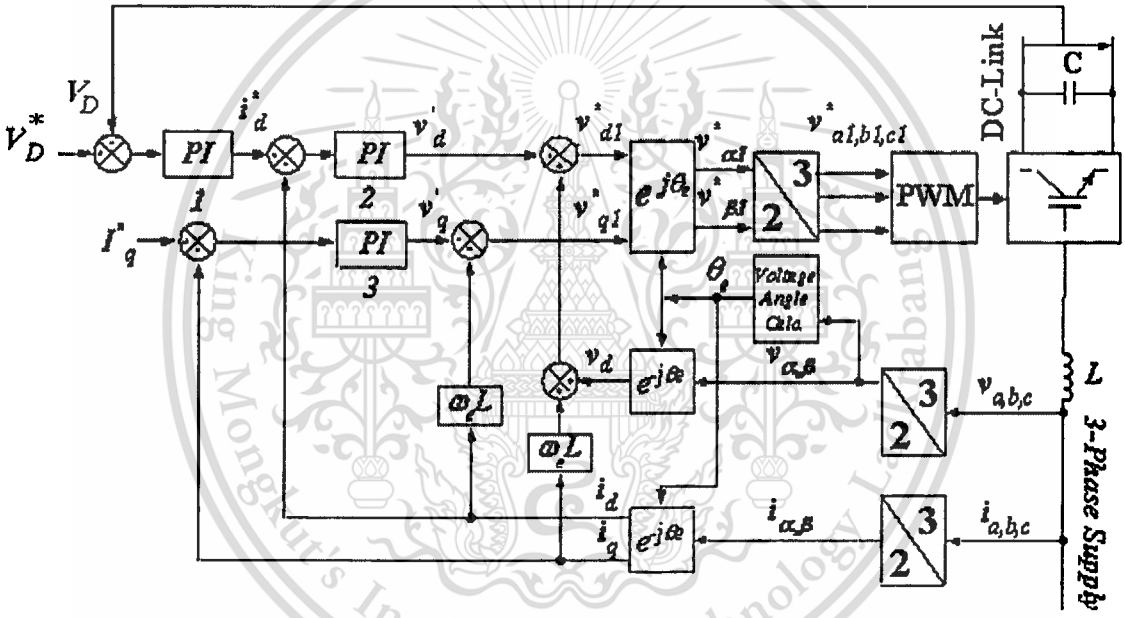

Figure 3.3 Vector control structure for VSC.

The control scheme thus utilizes current control loops for i_d and i_q, with the i_d demand being derived from the DC-link voltage error through a standard PI controller. The design of the vector control structure for VSC shown in Figure 3.3.

3.4 Control loop design

Considering equation (3.8) and (3.9) with the d-axis of the reference frame align along the supply voltage vector position, the following relationship can be written:

$$v_d = Ri_d + L\frac{di_d}{dt} - \omega_e Li_q + v_{d1} \tag{3.19}$$

$$0 = Ri_q + L\frac{di_q}{dt} + \omega_e Li_d + v_{q1} \tag{3.20}$$

In order to decouple the d and q axis, equation compensation terms are introduced by defining:

$$v_{d1} = -v_d' + (\omega_e Li_q + v_d) \tag{3.21}$$

$$v_{q1} = -v_q' - (\omega_e Li_d) \tag{3.22}$$

to give

$$v_d' = Ri_d + L\frac{di_d}{dt} \tag{3.23}$$

$$v_q' = Ri_q + L\frac{di_q}{dt} \tag{3.24}$$

or

$$F(s) = \frac{i_d(s)}{v_d'(s)} = \frac{i_q(s)}{v_q'(s)} = \frac{1}{Ls + R} \tag{3.25}$$

A PI current control loop is used to determine the demand values for v'_d and v'_q. The actual values for v^*_{d1} and v^*_{q1} are given by:

$$v^*_{d1} = -v'_d + (\omega_e L i_q + v_d) \tag{3.26}$$

$$v^*_{q1} = -v'_q - (\omega_e L i_d) \tag{3.27}$$

and are then transformed to provide the 3-phase modulating waves (v^*_{a1}, v^*_{b1} and v^*_{c1}) for the PWM generation. The line inductor used in the simulation has a value of 5mH/phase.

3.3.1 DC-link voltage controller design

The design of the DC-link voltage controller follows directly from equation (3.15)-(3.18) and the transfer function of the plant is given by:

$$\frac{V_D(s)}{I_d(s)} = \frac{3m_1}{2\sqrt{2}Cs} \tag{3.28}$$

The closed loop block diagram for the DC-link voltage control [29] is shown in Figure 3.3. In which I_D is represented as a disturbance.

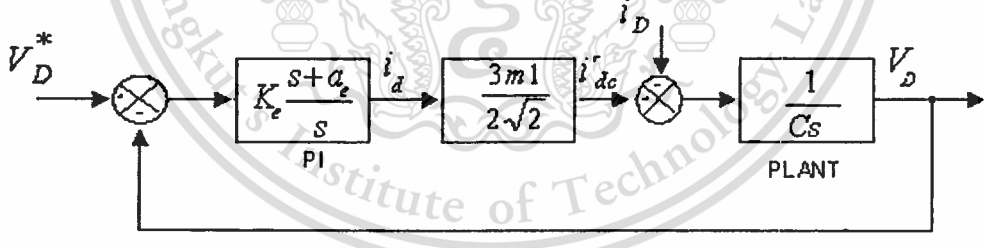

Figure 3.4 Block diagram of the DC-link Voltage control loop

From Figure 3.4, the characteristic equation for the DC-link voltage controller is given by:

$$S^2 + \frac{3m_1K_e}{2\sqrt{2}C}S + \frac{3K_e a_e m_1}{2\sqrt{2}C} = 0 \tag{3.29}$$

The controller parameters are given by:

$$K_e = \frac{4\sqrt{2}C\zeta\omega_n}{3m_1} \tag{3.30}$$

$$a_e = \frac{2\sqrt{2}\omega_n^2 c}{3m_1 K_e} \tag{3.31}$$

3.3.2 Current loop controller design

The design of the PI current controller [30] follows directly from (3.24). The closed loop block diagram for the current control is shown in Figure 3.5

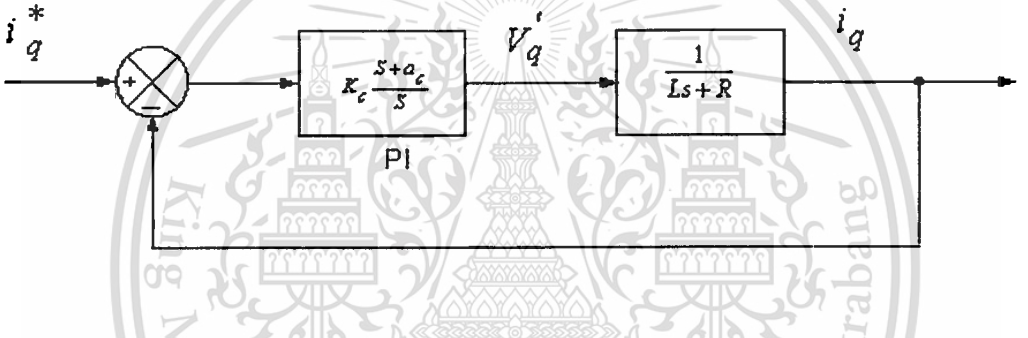

Figure 3.5 Block diagram of the current control loop

From Figure 3.5. The characteristic equation for the current controller is given by:

$$S^2 + \frac{R + K_c}{L}S + \frac{K_C a_c}{L} = 0 \tag{3.32}$$

The controller parameters are given by:

$$K_c = 2\zeta\omega_n L - R \tag{3.33}$$

$$a_c = \frac{\omega_n^2 - L}{K_c} \tag{3.34}$$

A standard design procedure can be applied to the block diagram of Figure 3.3 . All the basic equations for VSC (side 2) of HVDC system are similarly to the equations shown above.

3.5 Simulation results

The simulation results were performed just only for side1 of VSC-HVDC system by connecting to load (for rectifying mode) and to dc source (for inverting mode). And also a Bode plot has been conducted. The controller gains are initially calculated by equations (3.28) to(3.34). A design for a closed loop natural frequency (ω_n = 20 Hz) and a damping ratio (ζ=0.707) have been chosen.

Figure 3.6 shows the typical line current and supply voltage of the converter in rectifying mode (P > 0, Q = 0). Figure 3.7 shows the typical line current and supply voltage of the converter in inverting mode (P < 0, Q = 0) and Figure 3.8 shows the results at different load. To control the reactive power, Iq* has been controlled, Figure 3.9. Figure 3.10, Figure 3.11, show the Bode plot diagram, and Pole Zero diagrams of DC-link voltage control loop.

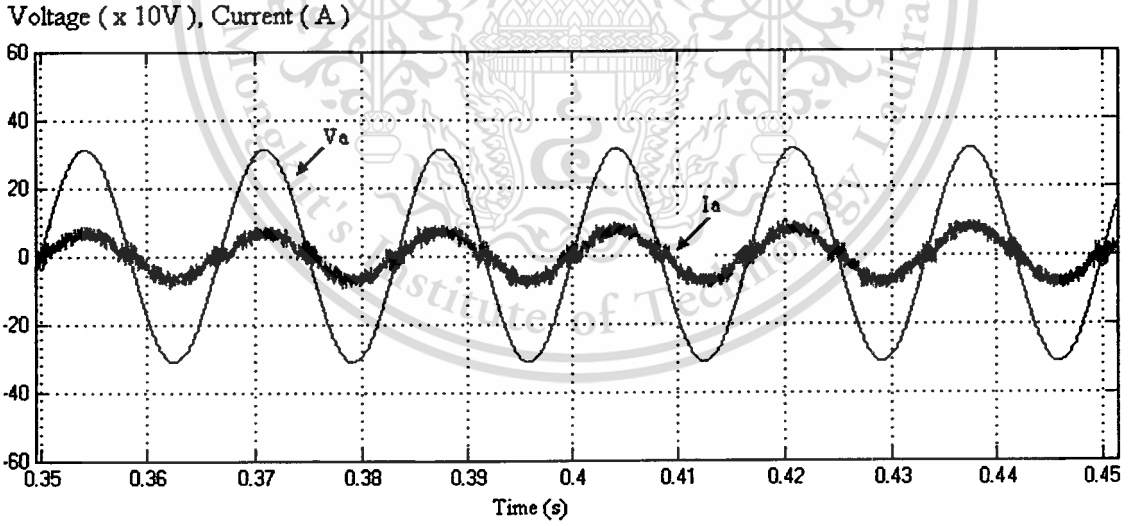

Figure 3.6 Typical line current and supply voltage (rectifying mode, P > 0, Q = 0).

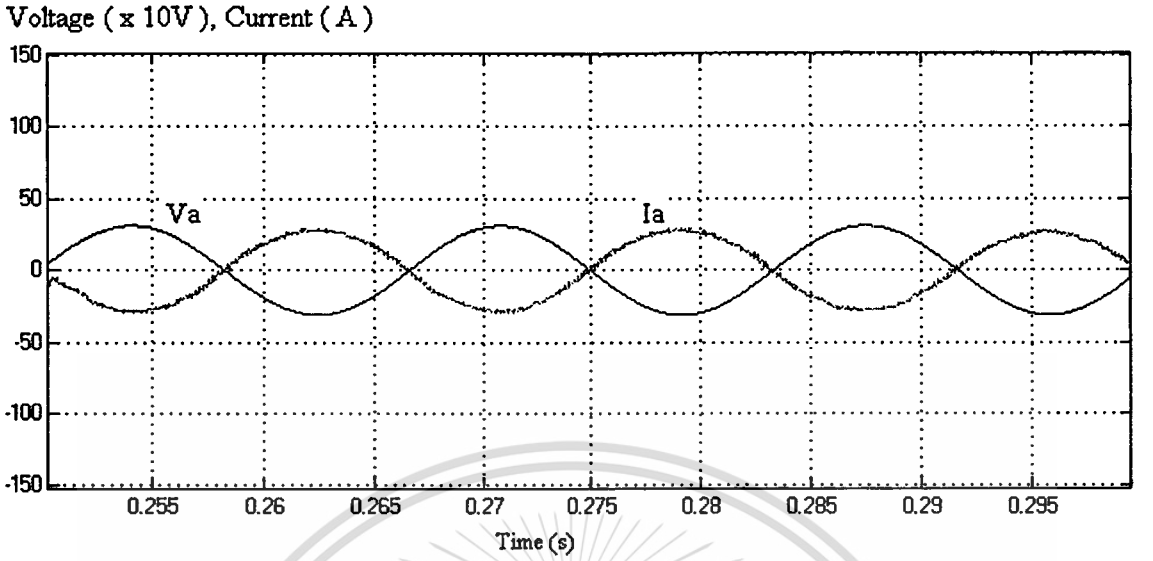

Figure 3.7 Typical line current and supply voltage (inverting mode, $P < 0$, $Q = 0$)

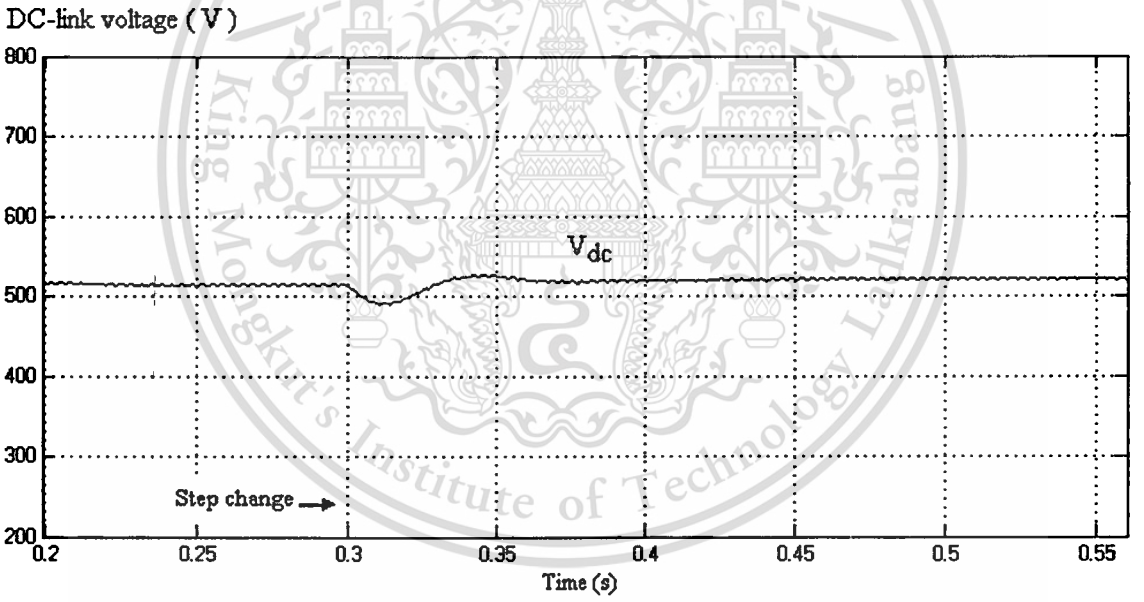

Figure 3.8 Dynamic response performance with increasing load current 5A to 10 A

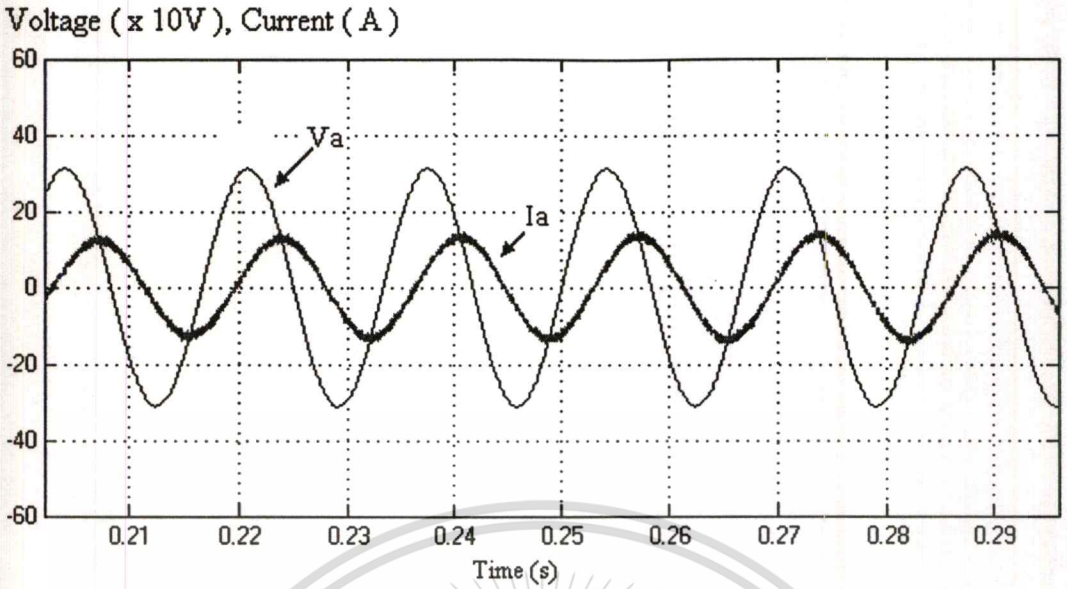

Figure 3.9 Line current and voltage (P > 0, Q > 0)

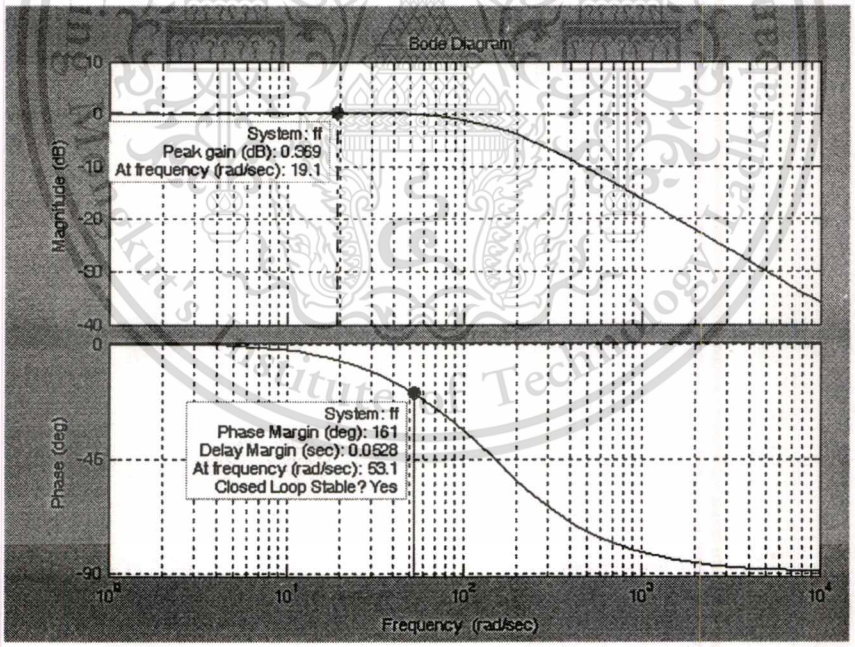

Figure 3.10 Bode plot diagram of DC-link voltage control loop

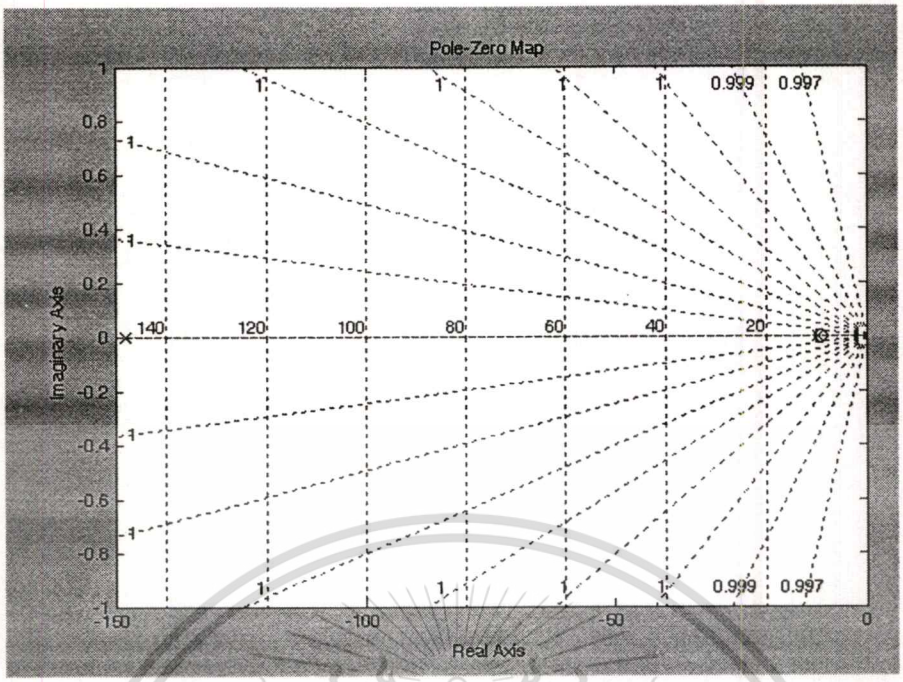

Figure 3.11 Pole Zero plot diagram of DC-link voltage control loop

3.6 Conclusion

A model of the Voltage Source Converter Controlled Power Transfer for HVDC Applications is developed by using the d-q transformation. The characteristic equation of the DC-link voltage and current control loops are second order (Equation 3.29 and 3.32). The controller gains are chosen based on the natural frequency and damping factor. The simulation results show that the line current can be calculated to be in phase or out of phase by controlling the reactive power as shown in Figure 3.9. The DC-link voltages maintained while the load has changed as shown in Figure 3.8.

Chapter 4

VSC between two grids

4.1 Introduction

To analyze the designed control system, the system shown in Figure 4.1 is simulated and the control system is implemented using vector control strategy. Simulation results are presented in this chapter. The study is focused on the performance of the VSC at steady state, with load changes. Here, four study cases of the system simulation are investigated.

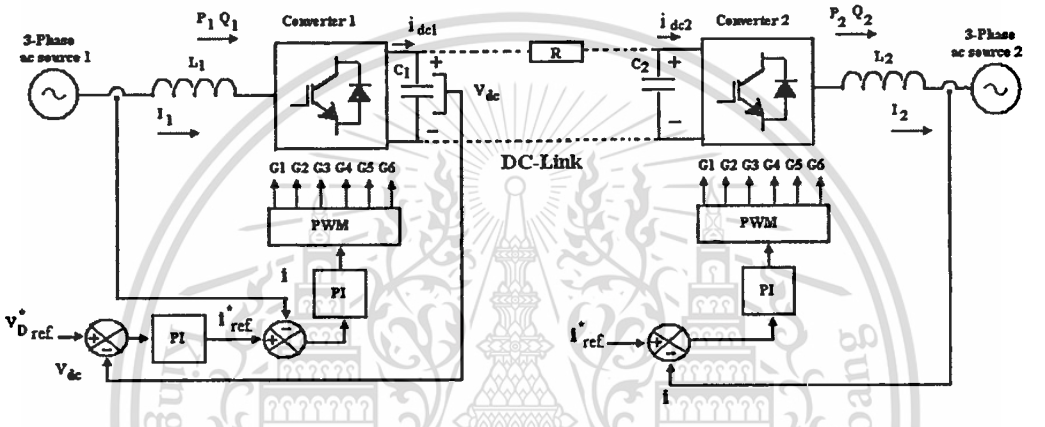

Figure 4.1 Block diagram of the studied systems with the control algorithm

4.2 DC-link control between two grids with proposed control strategy

The studied system consists of two voltage source converters, one of which operates as a power dispatcher and the other as a power receiver. Four study cases are explained in this chapter.

4.2.1 Case I: The same frequency, different voltage

As shown in Figure 4.1, all simulations have been performed with two two-level converters. The converter bridge valves are represented as a turn-off IGBT and an anti-parallel diode with ideal switches in Simulink models. State losses and switching losses are neglected. The ac system voltages at both sides are 220V and 110V, respectively. The rated dc voltage is 500V, the set reference value of the dc voltage is 500V, the rated power flow of P is set to 2500 W and the reactive power flow (Q) steps from 1500 Var to 3000 Var, the line inductance are 5mH, the

switch frequency used in the VSC is 5kHz, the fundamental frequency of the ac systems is 60Hz. Two dc capacitors are 5000 μF.

The control loop implemented will depend on the application. To control reactive power and active power flow via DC-link, the control strategy as stated below is implemented to evaluate their performances:

The control strategy is:

- Converter 1 controls dc voltage and reactive power.

In order to control dc voltage, the value of the dc voltage can be chosen by setting the reference value V_D^* directly to the DC-link voltage control loop (inner loop) as shown in the vector control structure for VSC in chapter 3. To control the reactive power, the value of the reactive power can be chosen by setting the reference value (i_q^*) directly to the reactive control loop (outer loop).

- Converter 2 controls the active power and reactive power.

In order to control the active power, the value of the reactive power can be chosen by setting the reference value (i_d^*) directly to the active control loop (inner loop) as there is no DC-link control loop in this side. To control the reactive power, the value of the reactive power can be chosen by setting the reference value (i_q^*) directly to the reactive control loop (outer loop).

4.2.1.1 Converter side1 (sending side)

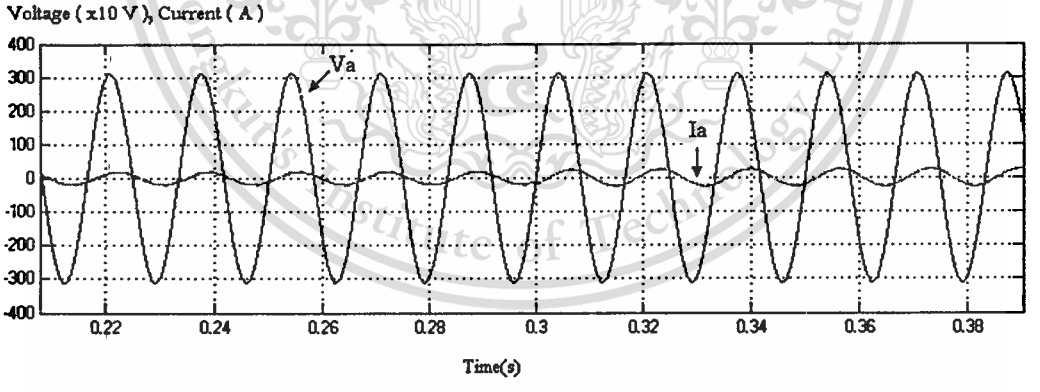

Figure 4.2 Typical line current and supply voltage of converter 1

Figure 4.2 illustrates the voltage and current from the ac source side 1 and Figure 4.3 shows the dc voltage under steady state operation conditions. From figure 4.4, 4.5 and 4.6, it can be seen that high quality balanced three phase ac voltages and currents are obtained at the converter side

1. The step changes in power flow occurs at Ts= 0.3s for many cases. The dc voltage is a constant equal to the set reference value. In fact dc voltage includes ±0:5% ripple at steady state due to the use of small capacitors on the dc side and the recovery time is about 0.04s. From Figure 4.3, it can be seen that the V_{dc} slightly dropped at the moment of step change in power flow.

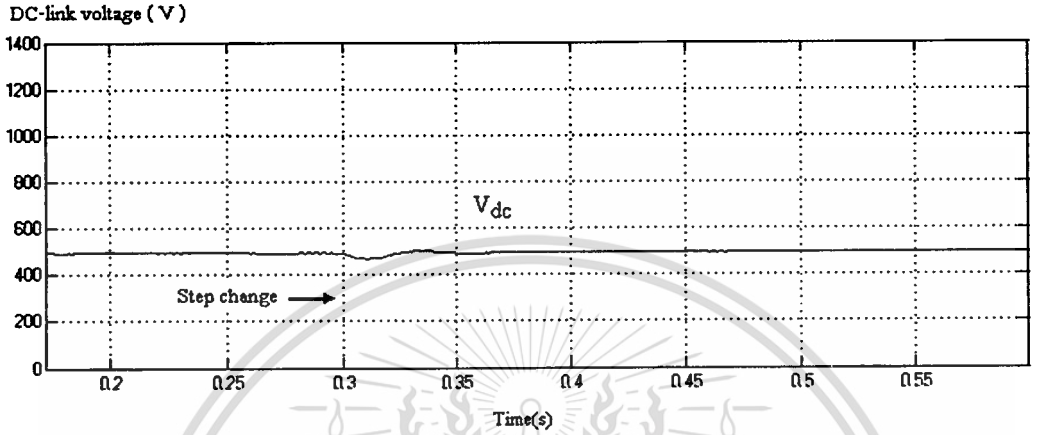

Figure 4.3 Dynamic response performance with step change in power flow

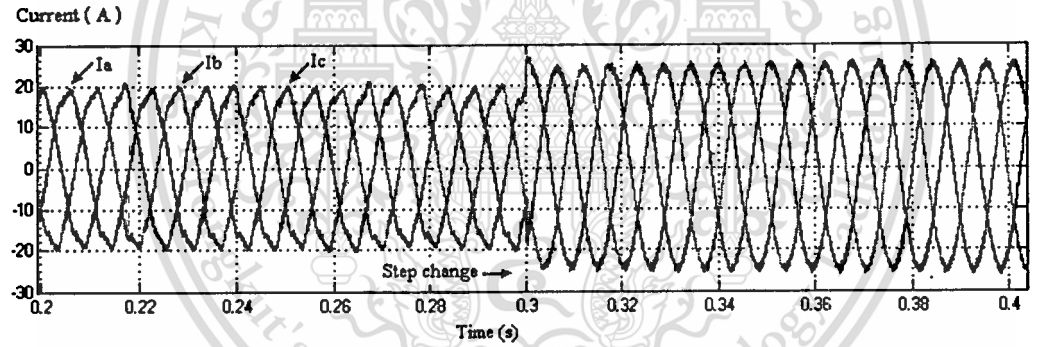

Figure 4.4 Three-phase line currents at converter side1during the reactive power step change

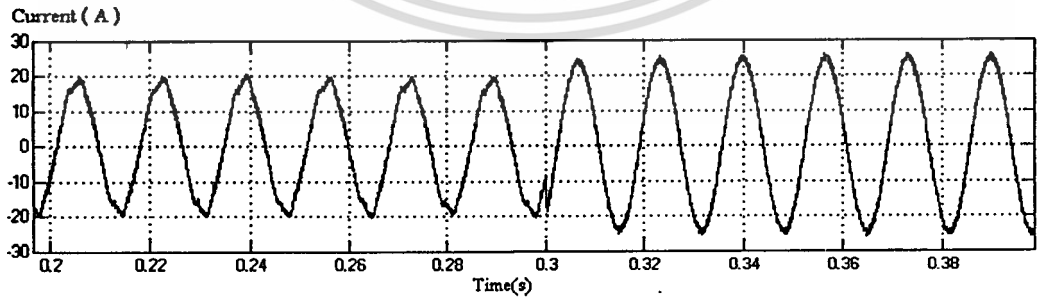

Figure 4.5 Phase current at converter side1during the reactive power step change

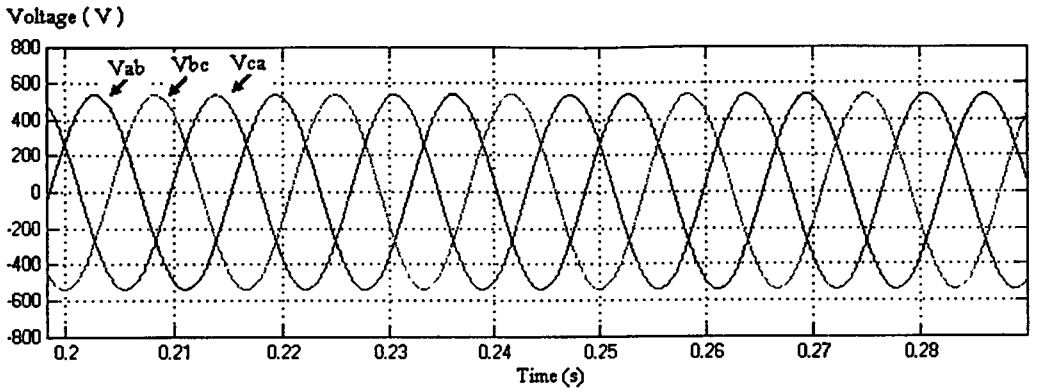

Figure 4.6 Line-to- line voltage waveforms at converter side 1

From Figure 4.6, it is clearly that the line-to- line voltages waveforms at converter side 1 are kept constant during the reactive power step change.

The active and reactive powers are measured by using equation 4.1and equation 4.2.

$$P = 3(v_d i_d + v_q i_q) \tag{4.1}$$

$$Q = 3(v_d i_q + v_q i_d) \tag{4.2}$$

Figure 4.7 shows the graph of active power flow from converter side 1 at the rated of 2500 W and the reactive power flow with initial rate of 1500 Var and then it steps to 3000 Var at Ts = 0.3s. It takes about 0.015s to reach the reference value. The active power flow, which is transmitted from converter 1 to converter 2, changes slightly when the step is applied and then it become steady again after 0.05s.

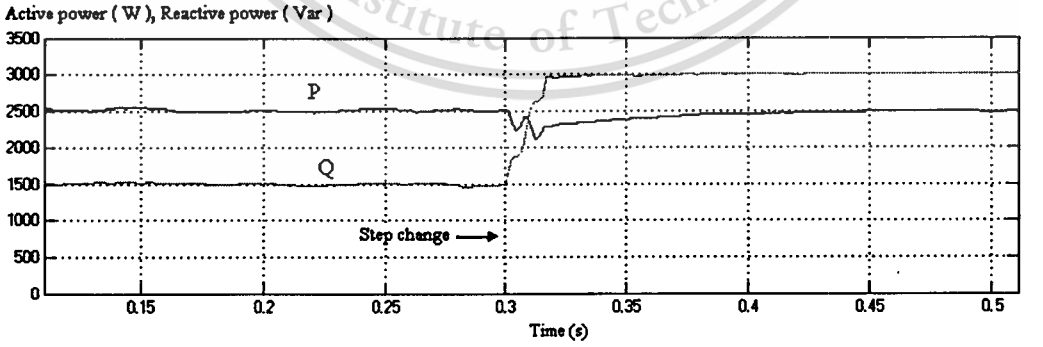

Figure 4.7 Step change of reactive power from 1500 Var to 3000 Var at the converter side 1

The PWM line-to-neutral voltage waveform shown in Figure 4.8 is the voltage measured between the corresponding phase voltage near converter and neutral point. It can be seen that the fundamental voltage reduce and the number of pulses increases to meet the step change of reactive power flow. Figure 4.9 presents PWM phase voltage and corresponding harmonics. Harmonics appear at multiple of switching frequency.

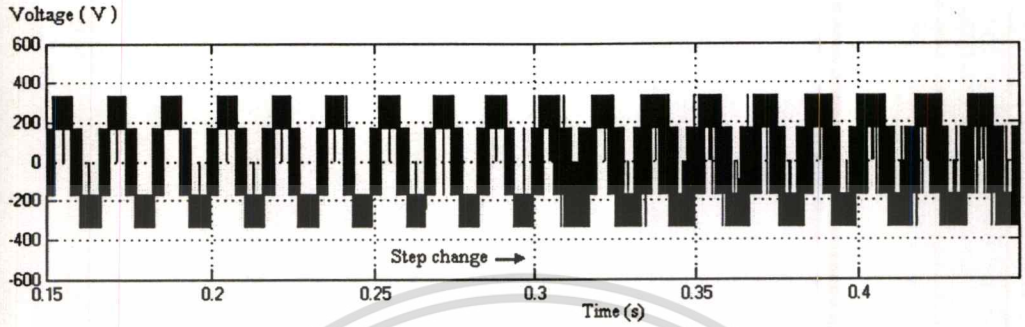

Figure 4.8 PWM line-to neutral voltage waveform

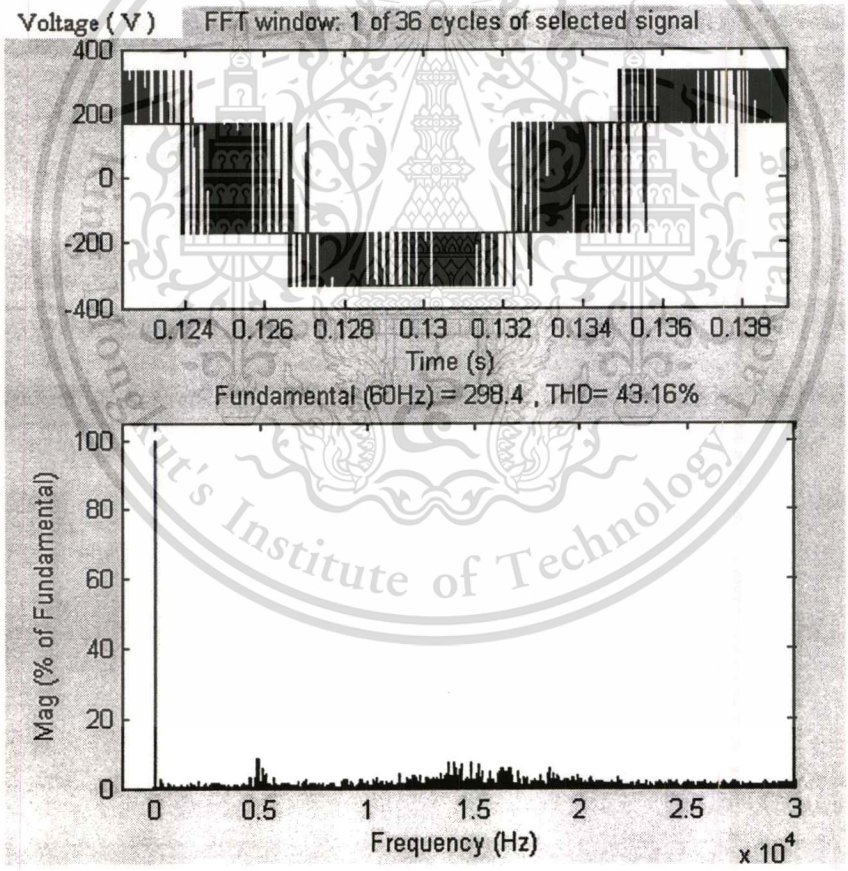

Figure 4.9 PWM line-to neutral voltage spectra (switching frequency of 5 kHz)

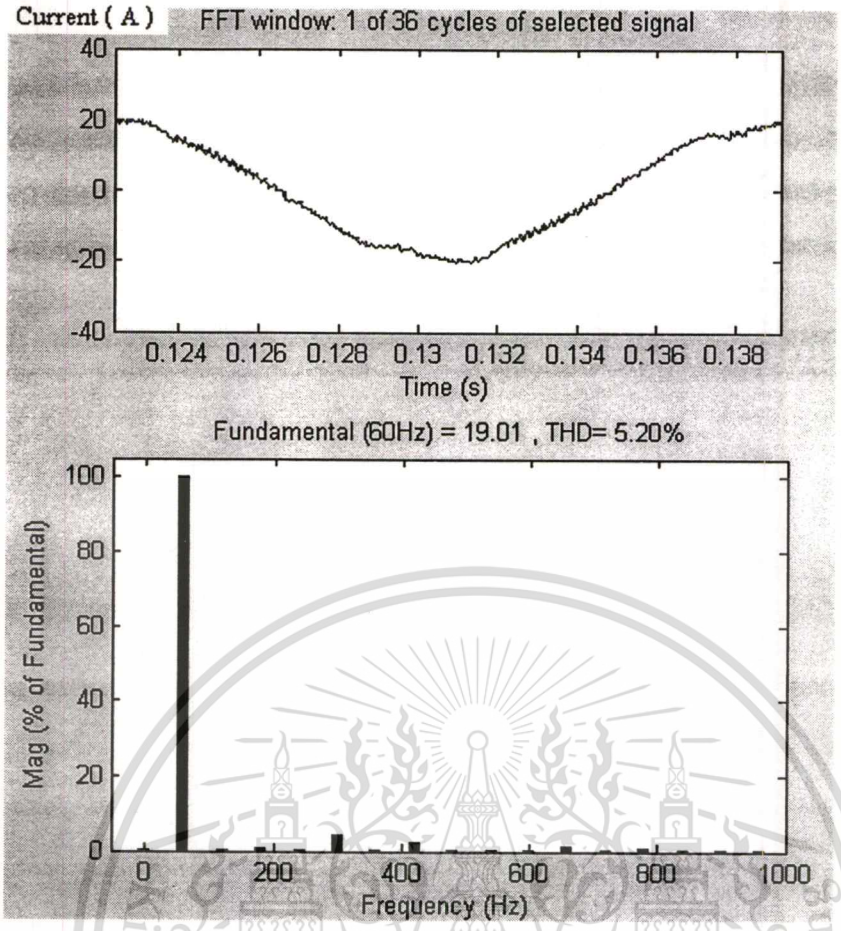

Figure 4. 10 PWM current spectra at converter side 1

Figure 4.10 shows the PWM current spectra at converter side1, it can be seen that the lower order harmonic appears and current waveform is nearly sinusoidal wave with THD of 5.20 %.

4.2.1.2 Converter side 2 (receiving side)

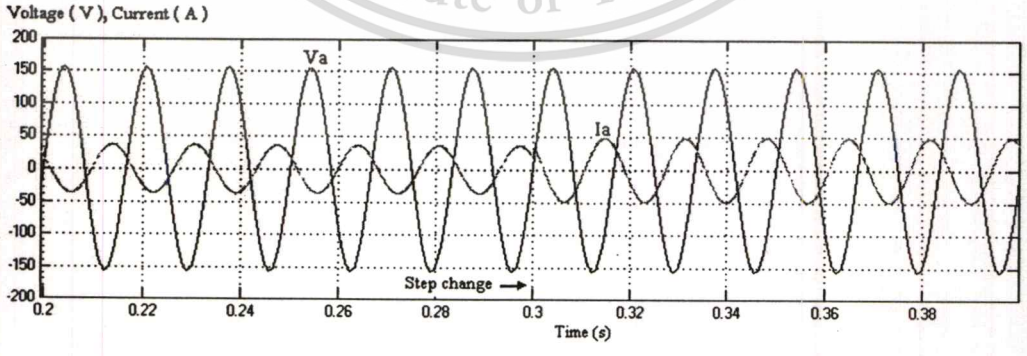

Figure 4.11 Typical line current and supply voltage of converter side 2

Figure 4.11 illustrates the voltage and current at the ac source side 2. From Figure 4.12, 4.13 and 4.14, it can be seen that high quality balanced three phase ac voltages and currents are obtained at the converter side 2. The currents are slightly changed due to the changing of reactive power flow, but the voltage waveforms are maintained constant.

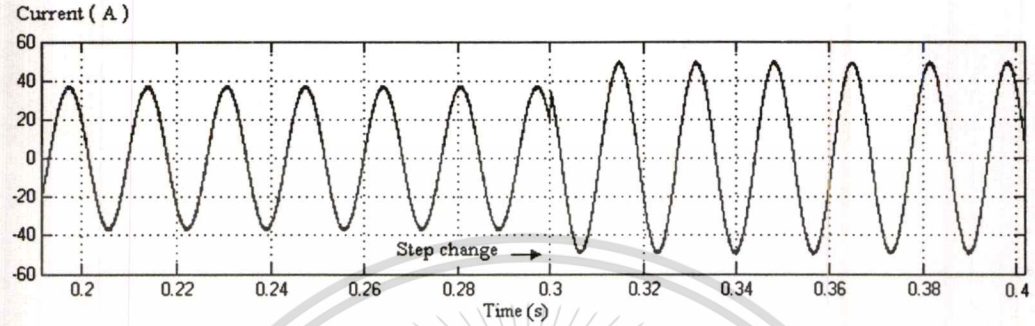

Figure 4.12 Phase current at converter side 2

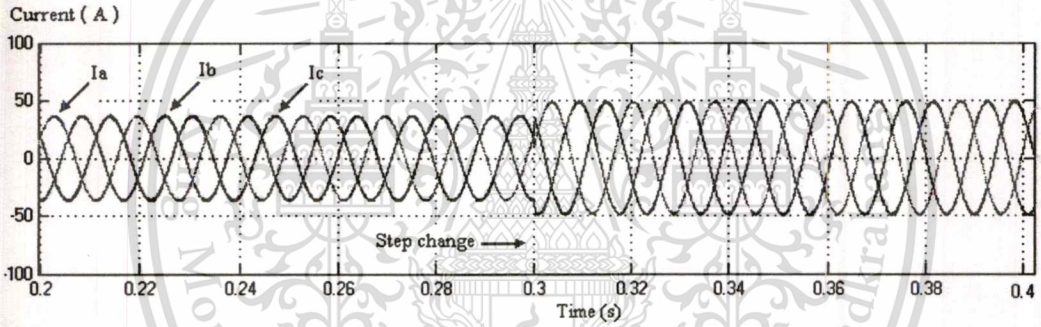

Figure 4.13 Three-phase line current at converter side 2

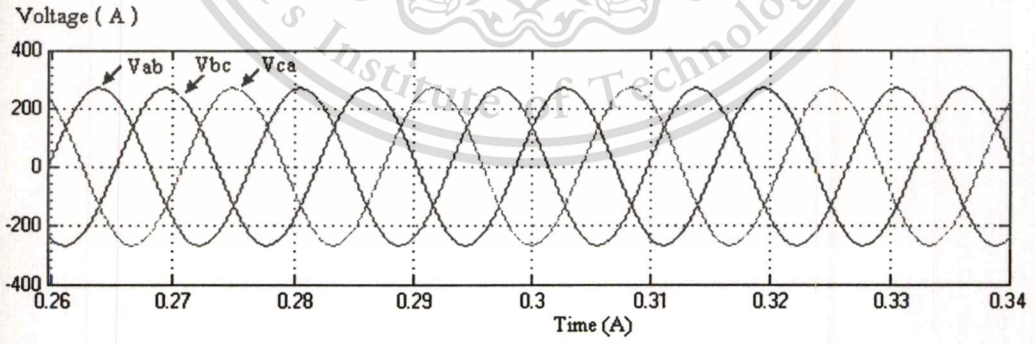

Figure 4.14 Line-to- line voltage waveform at converter side 2

The measured active power and reactive power levels at the converter side 2 are slightly changed due to the step change in power flow as shown in Figure 4.15. The active power slightly changes during the step change of Q and it recovers again after 0.02s.

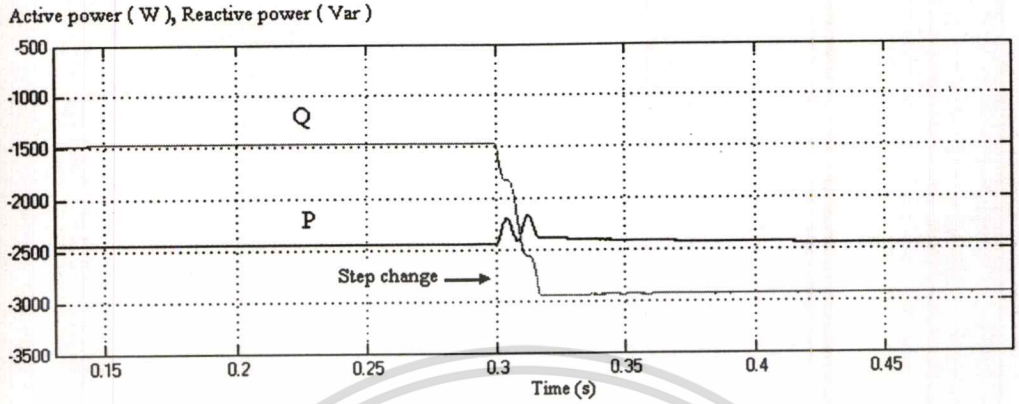

Figure 4.15 Step change of the active power at the converter side 2

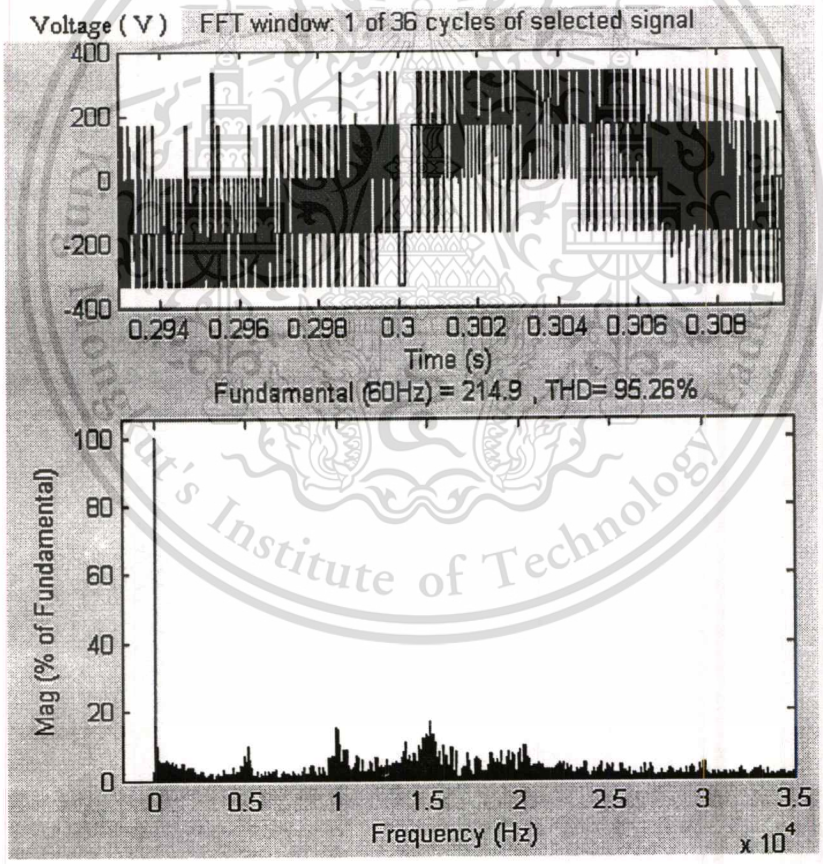

Figure 4.16 PWM line-to neutral voltage spectra (switching frequency of 5 kHz)

Figure 4.16 presents PWM line-neutral voltage waveform and its corresponding harmonics. Harmonics appear at multiple of switching frequency (i.e. 5 kHz, 15 kHz, etc.) Figure 4.17 shows the PWM line-to- neutral voltage waveform and it can be seen that the pulse with of PWM waveform increases after the moment of step change of reactive power flow.

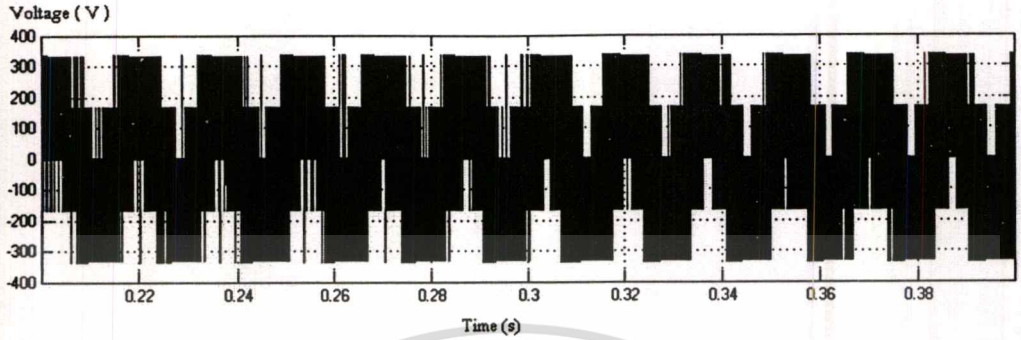

Figure 4.17 PWM line-to- neutral voltage waveform at converter side 2

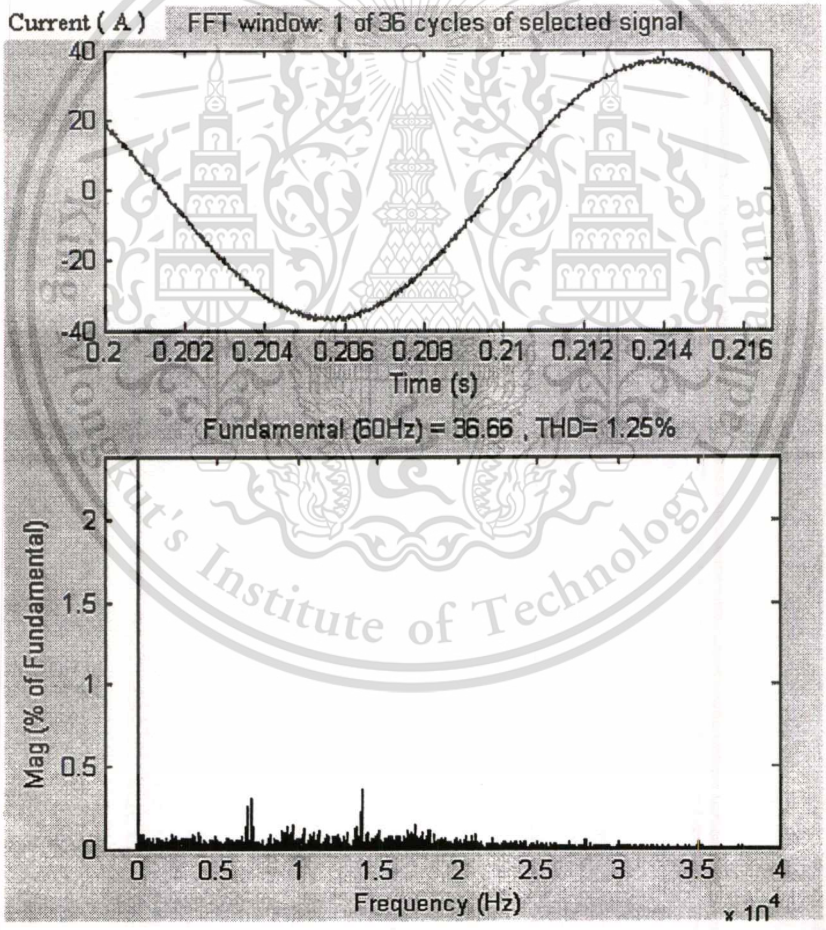

Figure 4.18 PWM current spectra at converter side 2

Figure 4.18 shows the PWM current spectra at converter side 2, it is clearly that the current waveform is nearly sinusoidal wave with THD of 1.25 %.

4.2.2 Case II: The same voltage and frequency

All simulations have been performed according to Figure 4.1, the ac system voltages at both sides are 110V . The rated dc voltage is 500V, the set reference value of the dc voltage is 500V, the rated power flow of Q is set to 3750 Var and the active power flow (P) steps from 1250 W to 2500 W , the line inductance are 5000mH, the switch frequency used in the VSC is 5kHz, the fundamental frequency of the ac systems is 60Hz. Two dc capacitors are 5000 μF. The same control strategy as in case I is also implemented here.

The control strategy is:

- converter 1 controls dc voltage and reactive power.
- converter 2 controls the active power and reactive power.

4.2.2.1 Converter side1 (sending side)

The Figure 4.19 shows the curve of power transmission from converter side 1 to converter side 2, the reactive power is kept constant at about 3750 Var, meanwhile the active power is changed at Ts = 0.6s from 1250 W to 2500 W. During this transient time, Q slightly changes and become steady state again after about 0.03s. Clearly that controllers work well. The AC voltage waveform maintained constant at the moment of step change in power as shown in Figure 2.20.

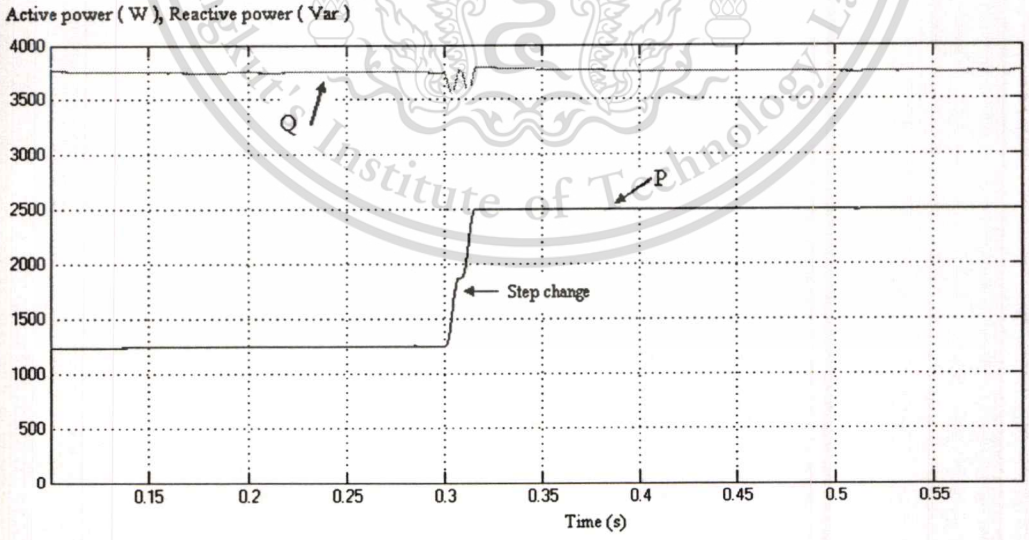

Figure 4.19 Step change of the reactive power at the converter side 1 from 1250 W to 2500 W

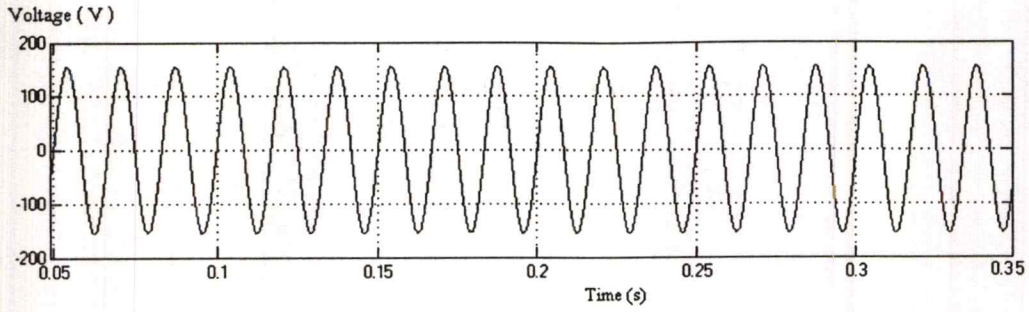

Figure 4.20 Typical line voltage of converter side 1

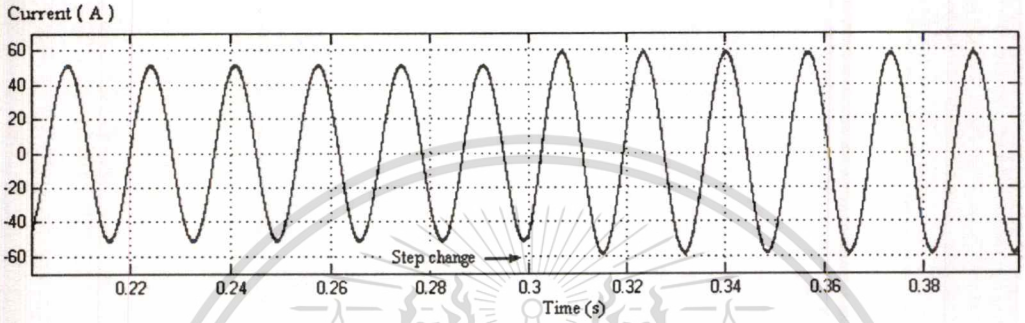

Figure 4.21 Typical line current of converter side 1

Figure 4.21 and Figure 4.22 show the typical line currents of the converter side 1, the line current changes from the moment of the active power flow changing (Ts = 0.3s). From Figure 4.23, it can be seen that the changing of the active power flow is not affect to voltages waveforms. The changing of the active power flow causes in changes of the current amplitude and phase shift between voltage and current as shown in Figure 4.24.

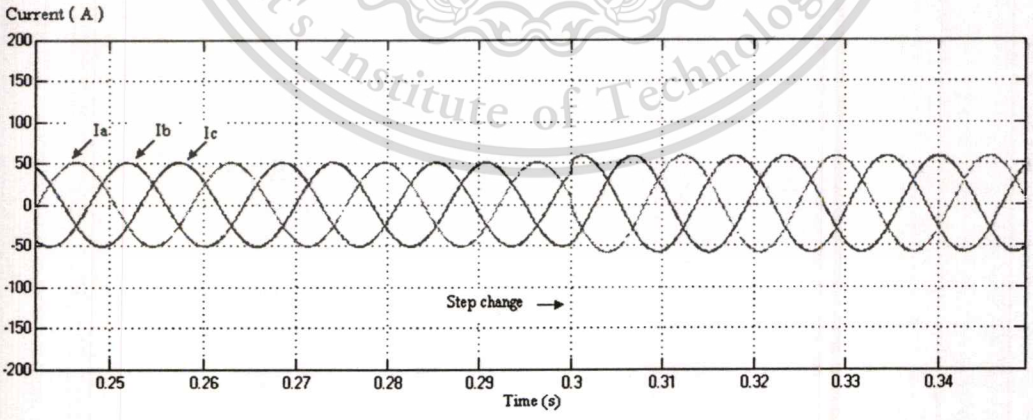

Figure 4.22 Three-phase line currents at converter side 1

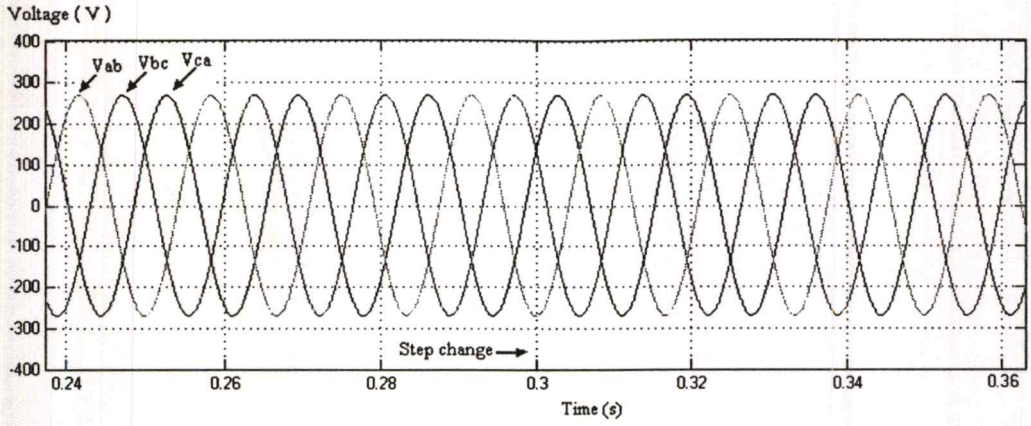

Figure 4.23 Line-to- line voltages waveforms at converter side 1

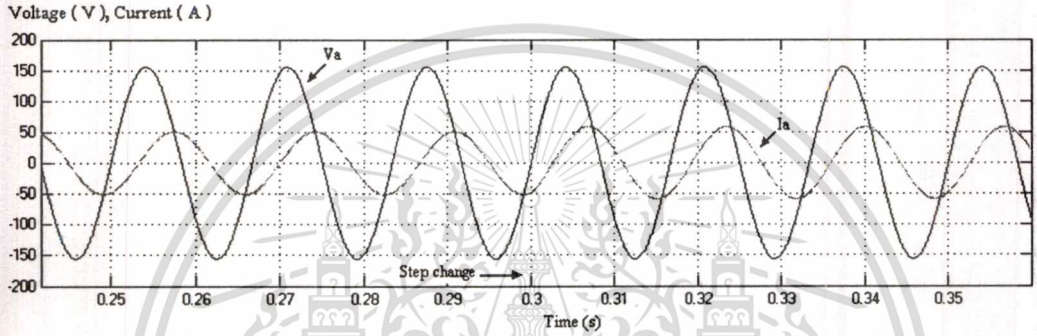

Figure 4.24 Typical line current and supply voltage of converter side 1

All of the figures shown below are obtained at converter side 1 of case studied 2, but with different levels of the active and reactive power flow. As in Figure 4.25, P is kept constant at about 2500 W and Q steps from 1250 Var to 3750 Var. The active power flow changes slightly when the step is applied and then it becomes steady again after about 0.05s.

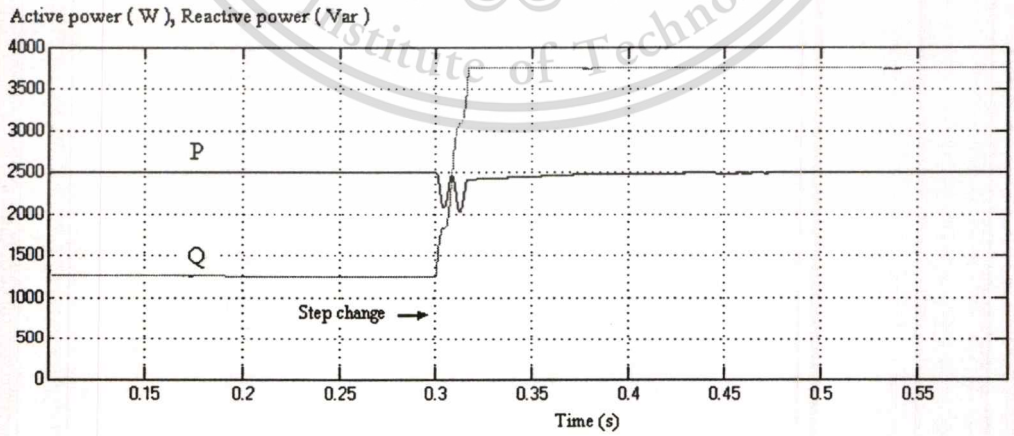

Figure 4.25 Step change of the active power at the converter side 1

From Figure 2.26, it can be seen that the dc voltage is constant equal to the set reference value. But it drops during the step change of reactive power flow and recovers again after about 0.04s. One more thing that we can see is that the current phase angle is shifted from the moment of reactive power changing (Figure 4.27 and Figure 4.28)

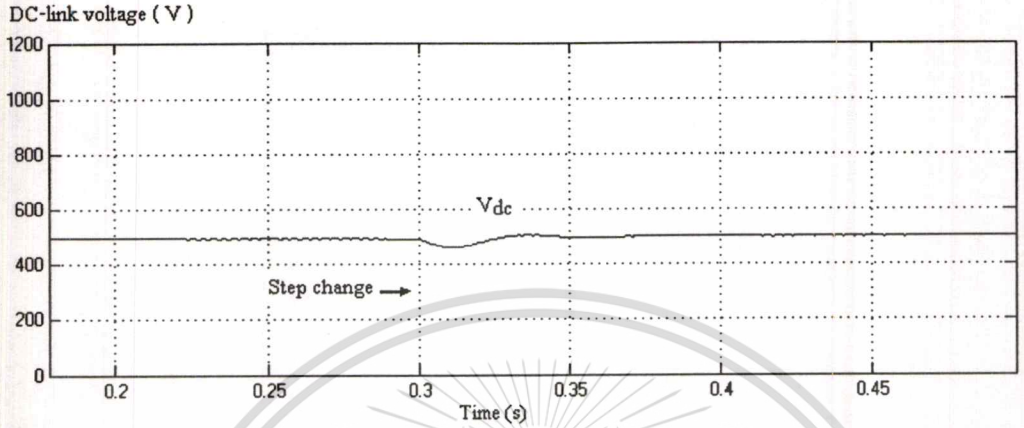

Figure 4.26 Dynamic response performance with step change in power flow

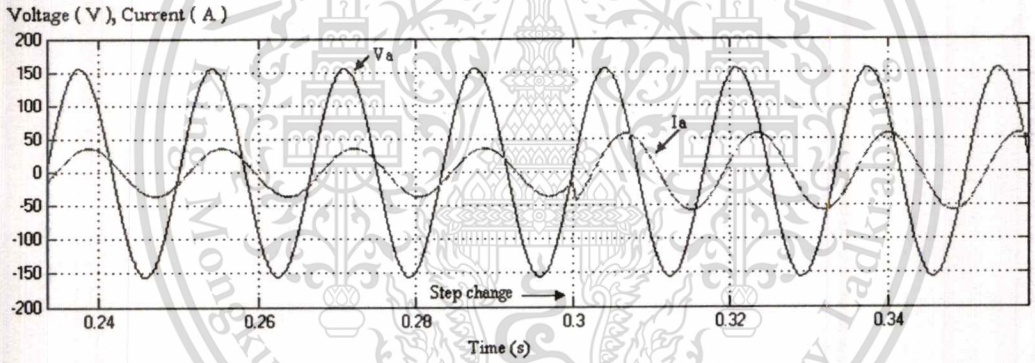

Figure 4.27 Typical line current and supply voltage of converter side 1

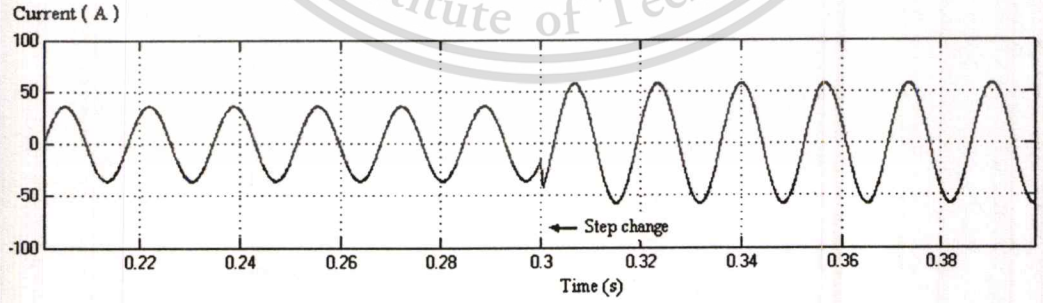

Figure 4.28 Typical line current of converter side 1

Figure 4.29 shows the changes of three-phase line currents after step change in power flow. And Figure 4.30 shows the PWM current spectra at converter side1; it is clearly that the current waveform is nearly sinusoidal wave with THD of 1.50 %.

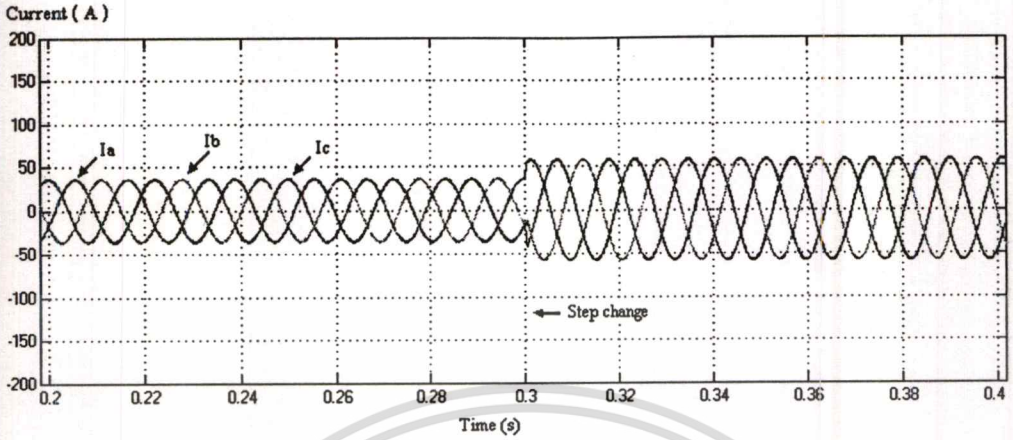

Figure 4.29 Three-phase line currents at converter side 1

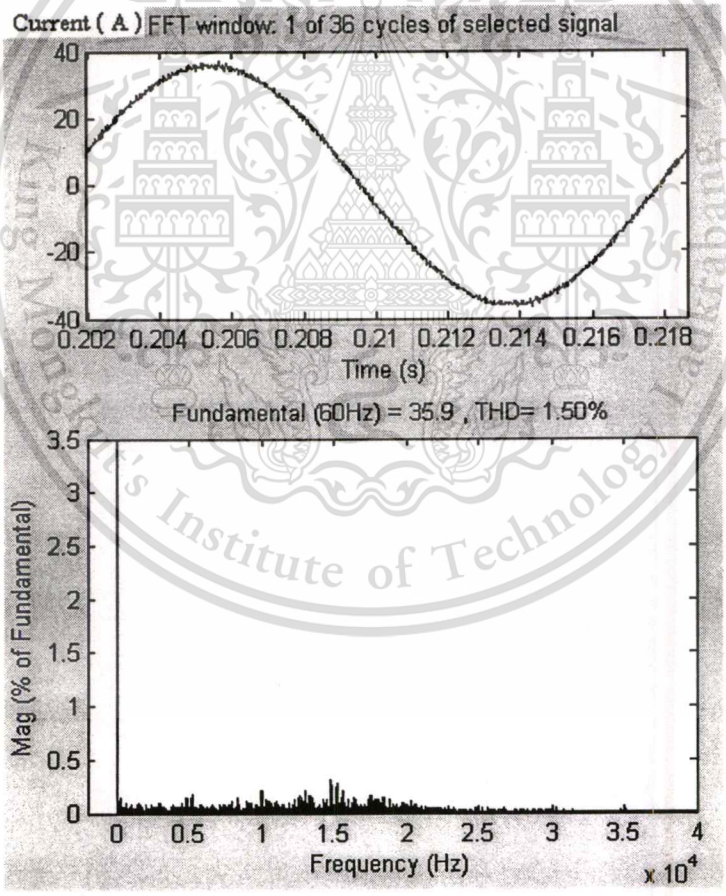

Figure 4. 30 PWM current spectra at converter side 1

Figure 4.31 presents the PWM line-to-neutral voltage waveform at converter1 and Figure 4.32 presents PWM phase voltage waveform and its corresponding harmonics.

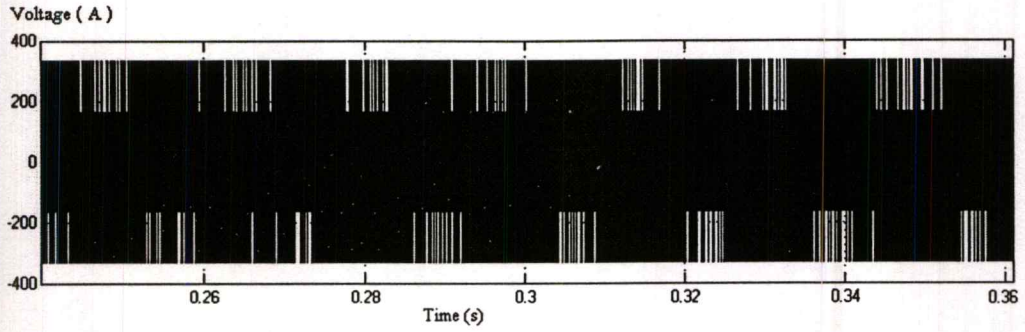

Figure 4.31 PWM line-to neutral voltage waveform at converter side 1

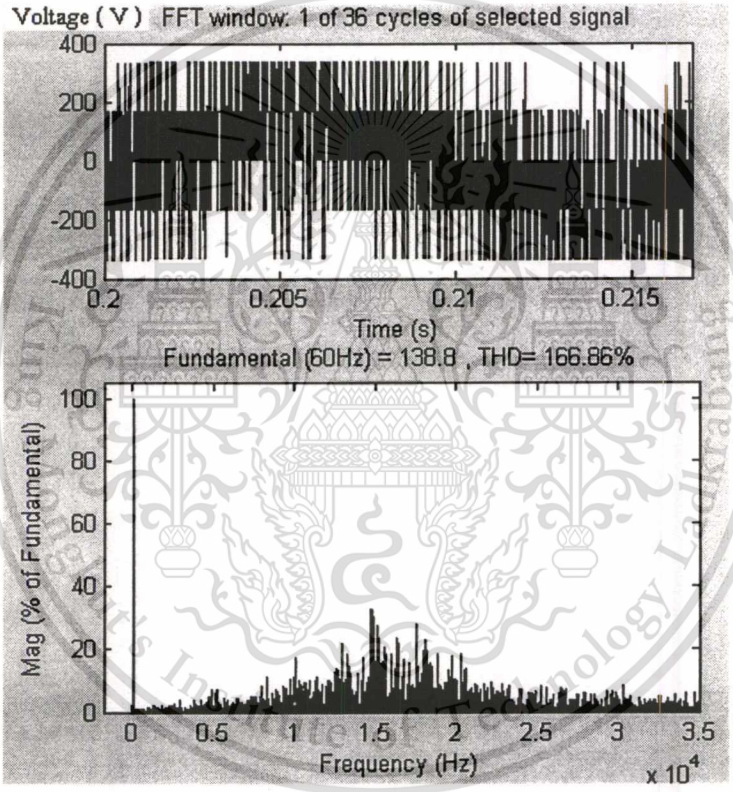

Figure 4.32 PWM line-to neutral voltage spectra (switching frequency of 5 kHz)

4.2.2.2 Converter side 2 (receiving side)

The measured active power and reactive power levels at the converter side 2 are slightly dropped due to transmission impedance and converter absorptions as shown in Figure 4.33. Similarity figures are obtained at the study case 1 in this chapter.

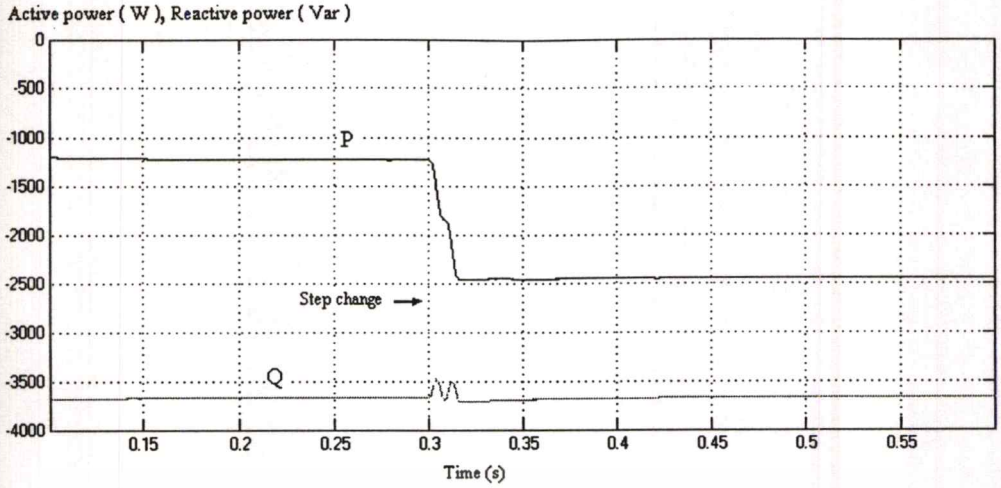

Figure 4.33 Step change of the active power at the converter side 2

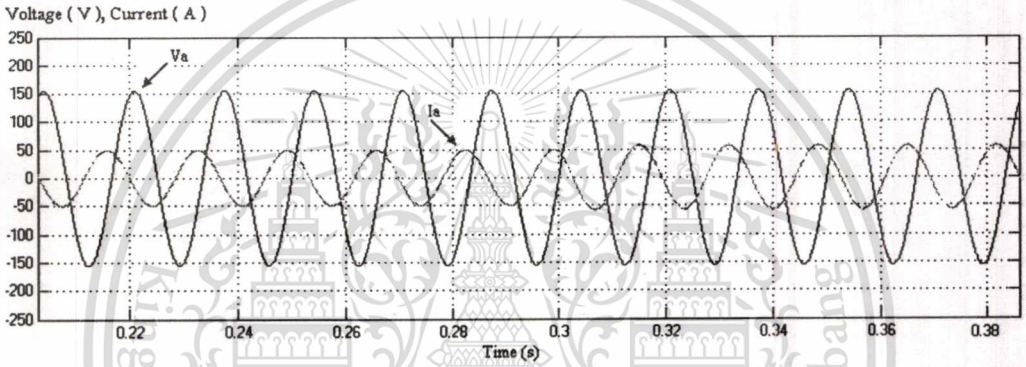

Figure 4.34 Typical line current and supply voltage of converter side 2

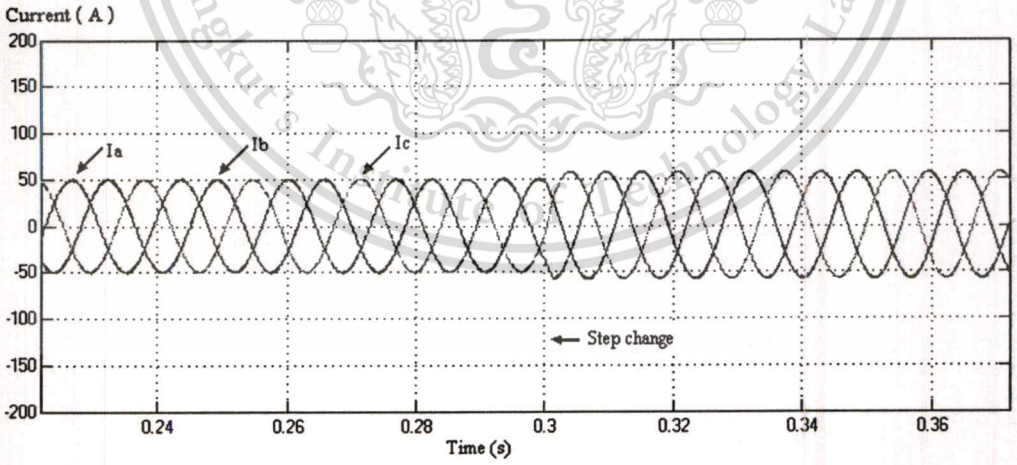

Figure 4.35 Three-phase line currents at converter side 2

The changing of the active power flow causes in changes of the current amplitude and phase shift between voltage and current as shown in Figure 4.34 and Figure 4.35.). From Figure 4.36, it can be seen that the changing of the active power flow is not affect to voltages waveforms. Figure 4.37 presents PWM voltage spectra at converter side 2 with THD=75.98%.

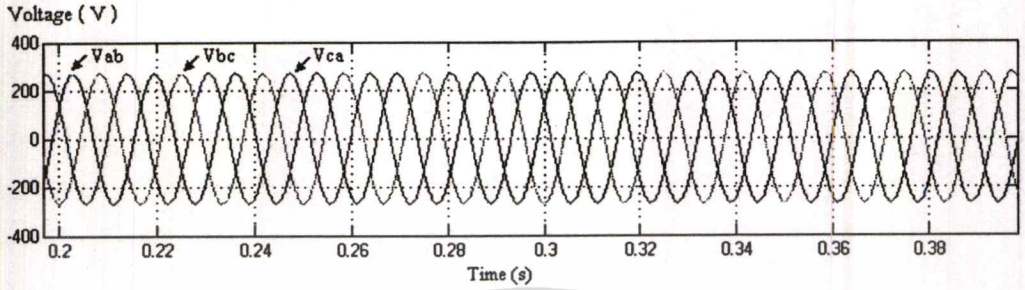

Figure 4.36 Line-to- line voltages waveform at converter side 2

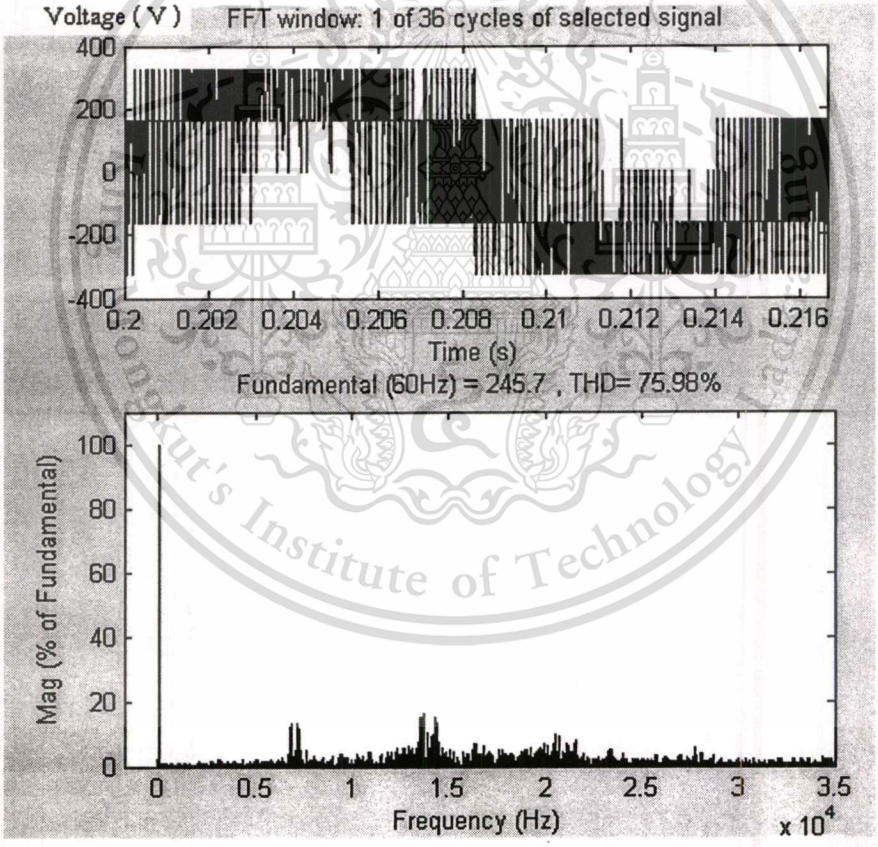

Figure 4. 37 PWM voltage spectra at converter side 2

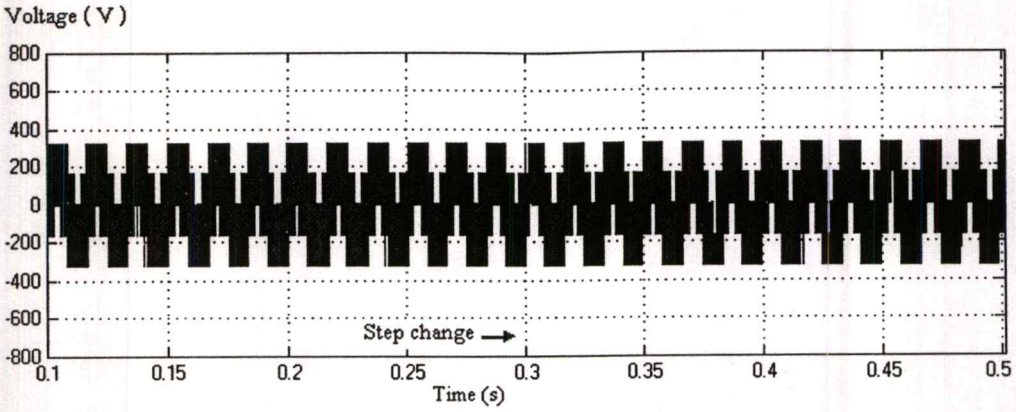

Figure 4.38 PWM line-to neutral voltage waveform at converter side 2

Figure 4.38 presents the PWM line-to neutral voltage waveform at converter side 2 and it can be seen that the fundamental voltage reduce and the number of pulses increases to meet the step change (T_s = 0.3s) of reactive power flow.

Figure 4.39 shows the step change of the reactive power flow in converter side 2 (receiving side) with initial rate of -1250 Var and then it steps to -3750 Var at Ts = 0.3s. It takes about 0.015s to reach the reference value. The active power flow, which is transmitted from converter 1 to converter 2, changed slightly when the step is applied and then it became steady again after 0.05s.

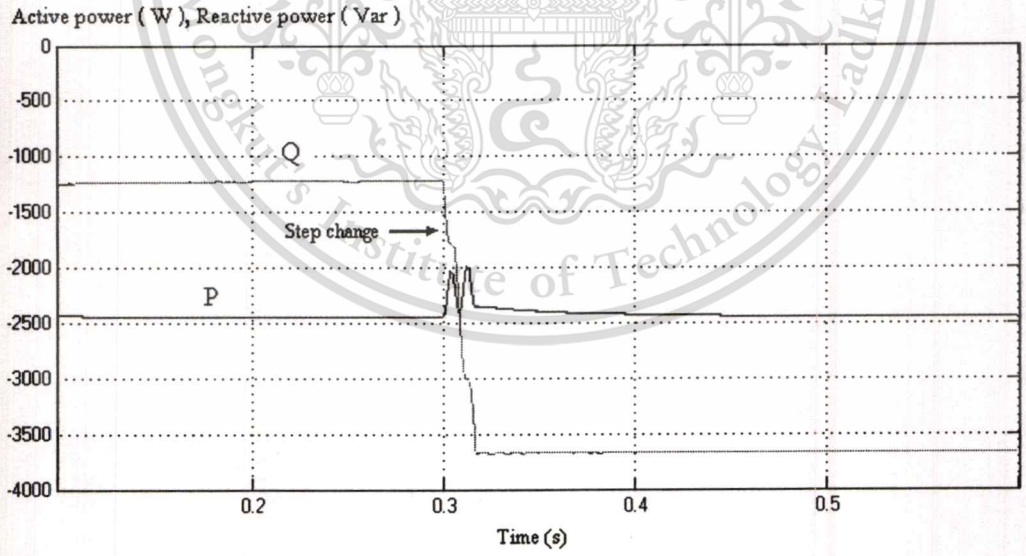

Figure 4.39 Step change of the active power at the converter side2

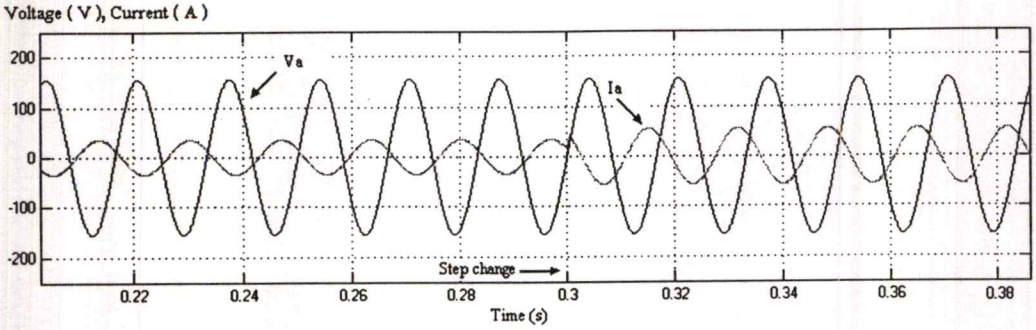

Figure 4.40 Typical line current and supply voltage of converter side 2

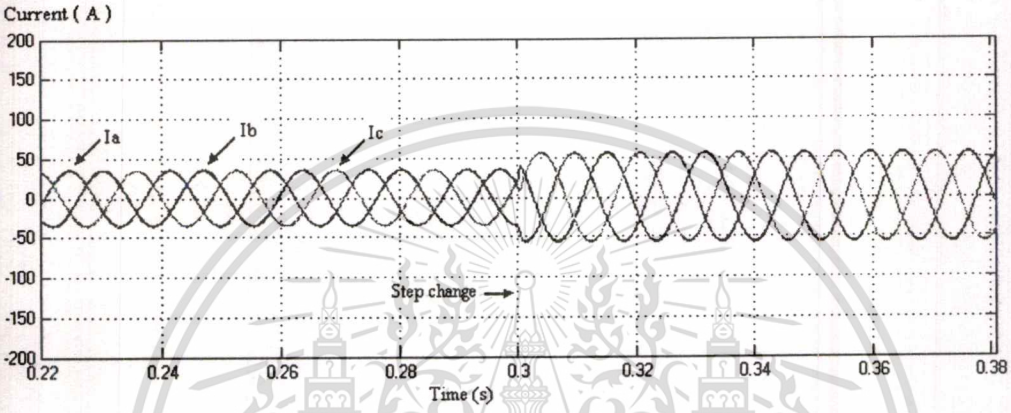

Figure 4.41 Three-phase line currents at converter side 2

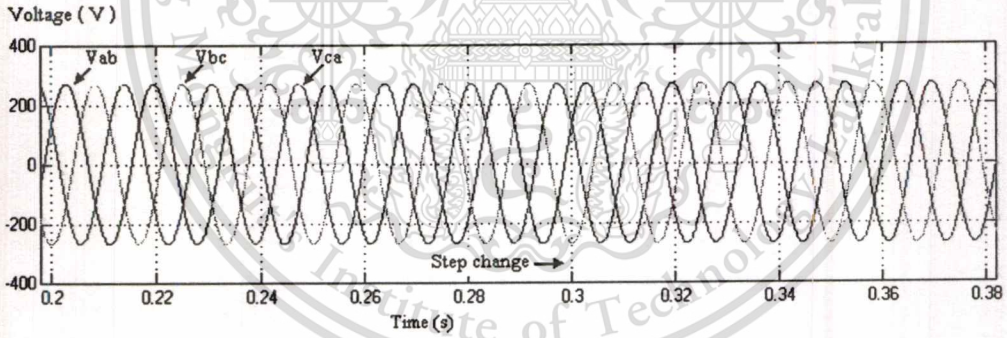

Figure 4.42 Line-to- line voltages waveform at converter side 2

Figure 4.40 and Figure 4.41 show the changes of the line currents due to the step change of reactive power flow. The amplitude of the currents is changed and the phase angle between voltage and current is shifted. But the Line-to- line voltages waveform is maintained as shown in Figure 4.42. From Figure 4.43, it can be seen that the current sidebands appear at multiple of

switching frequency (5 kHz, 10 kHz, 15 kHz, etc.), the current waveform is nearly sinusoidal with THD = 1.52%.

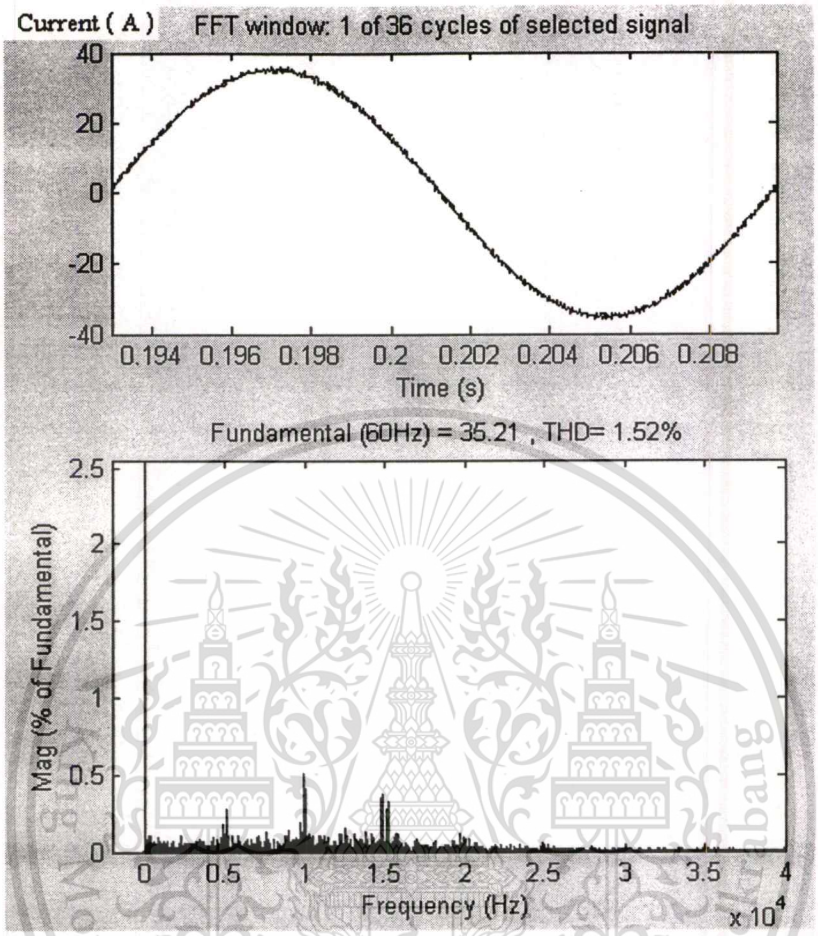

Figure 4. 43 PWM current spectra at converter side 2

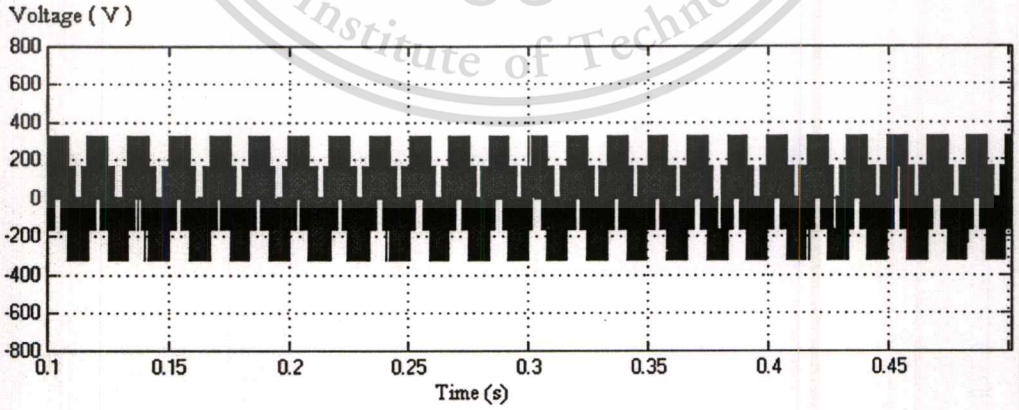

Figure 4.44 PWM phase-to neutral voltage waveform at converter side 2

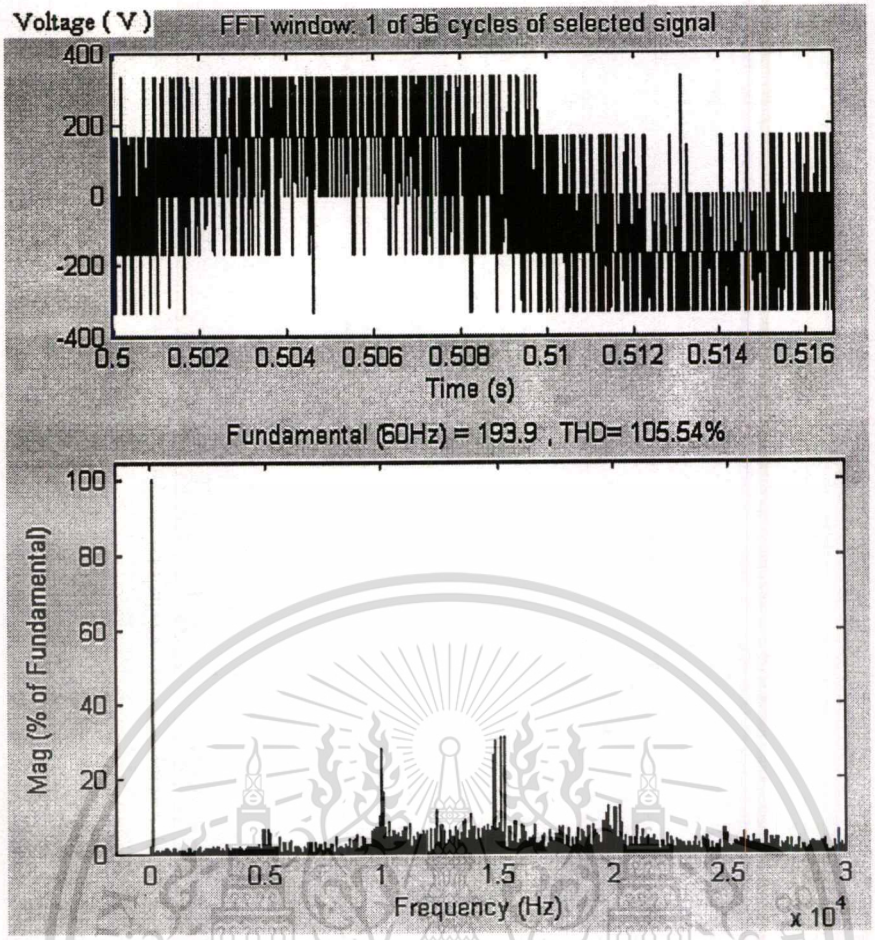

Figure 4. 45 PWM voltage spectra at converter side 2

Figure 4.45 presents PWM phase voltage waveform and corresponding harmonics. Harmonics appear at multiple of switching frequency (i.e. 10 kHz, 15 kHz, 20 kHz, 25 kHz, etc.).

4.2.3 Case III: Different voltage and different frequency

All simulations have been performed according to Figure 4.1, the ac system voltages at both sides are 220V and 110V, respectively. The rated dc voltage is 500V, the set reference value of the dc voltage is 500V, the line inductance are 5000mH, the switch frequency used in the VSC is 5kHz, the fundamental frequency of converter1 is 50Hz and the fundamental frequency of converter2 is 60Hz. Two dc capacitors are 5000μF. The same control strategy as in case studied 1 is also implemented here.

The control strategy is :

- converter 1 controls dc voltage and reactive power.

• converter 2 controls the active power and reactive power.

4.2.3.1 Converter side 1

The Figure 4.46 shows the curve of power transmission from converter side 1 to converter side 2, the reactive power is kept constant at about 2800 Var, meanwhile the reactive power is changed at T_s = 0.3s from 2000 W to 4000 W. The reactive power slightly changes during the step change of P and it recovers again after about 0.02s.

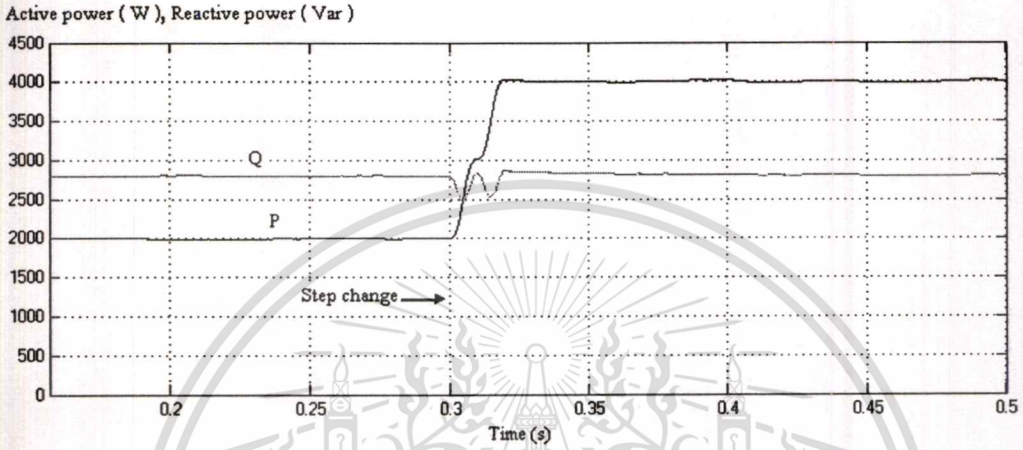

Figure 4.46 Step change of the active power at the converter side 1

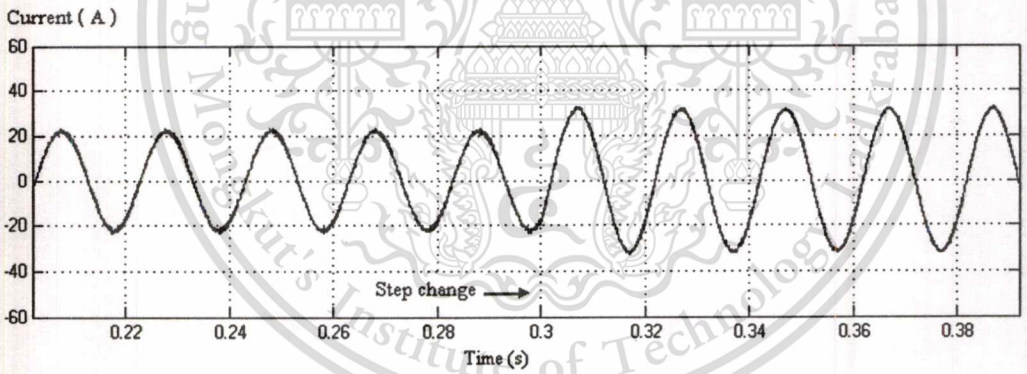

Figure 4.47 Typical line current of converter side 1

Figure 4.47 shows the typical line current of the converter side 1, the line current slightly changes its amplitude while the reactive power is stepping up at T_s = 0.3s. Figure 4.48 also shows the changes of three-phase line currents due to the step change in power flow. Figure 4.49 presents the line-to- line voltages waveforms at converter side 1, there is no any changes in

voltage waveform during the step change. From Figure 4.50, it can be seen that the phase shift angle between voltage and current is larger in case of P<Q, but it is smaller in case of P>Q.

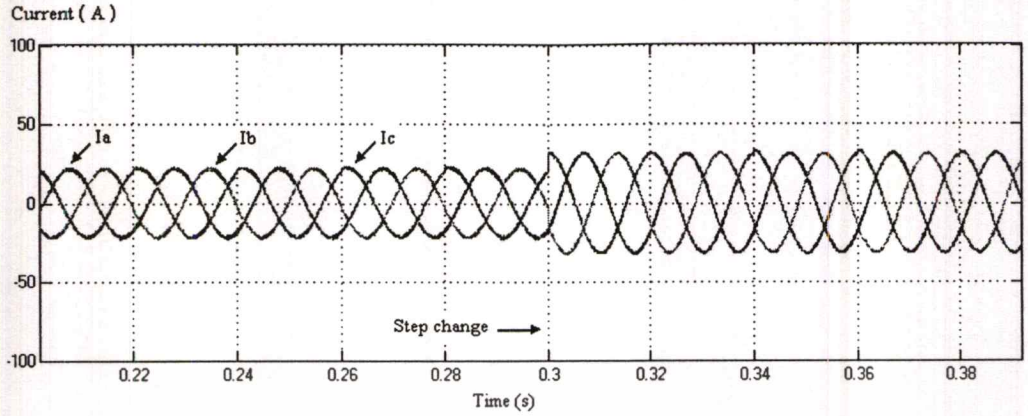

Figure 4.48 Three-phase line currents at converter side 1

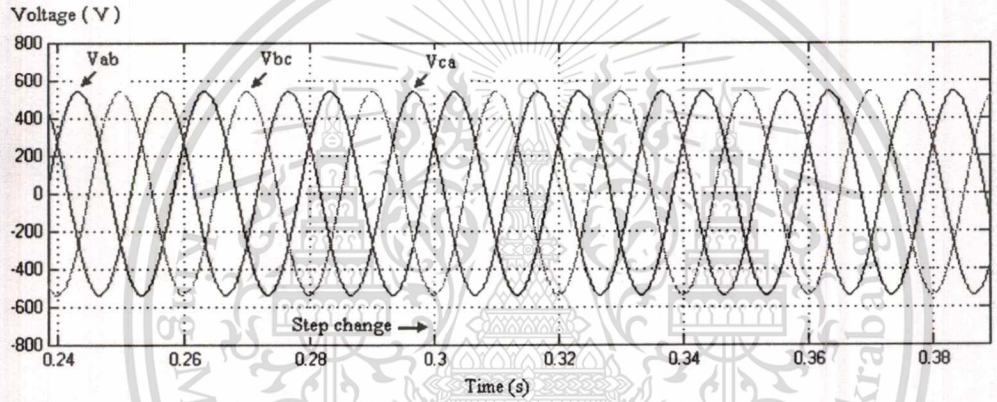

Figure 4.49 Line-to- line voltages waveforms at converter side 1

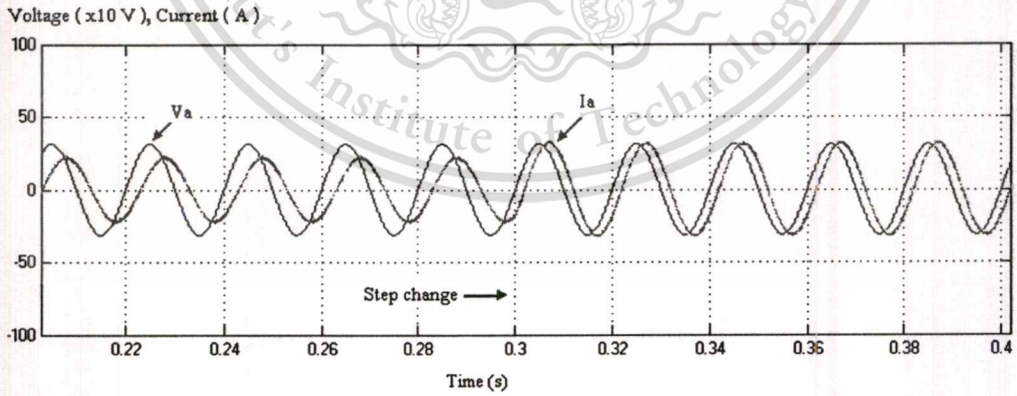

Figure 4.50 Typical line current and supply voltage of converter side 1

Figure 4.51 and Figure 4.52 presents PWM phase voltage and corresponding harmonics. Harmonics appear at multiple of switching frequency (i.e. 5 kHz, 15 kHz, etc.)

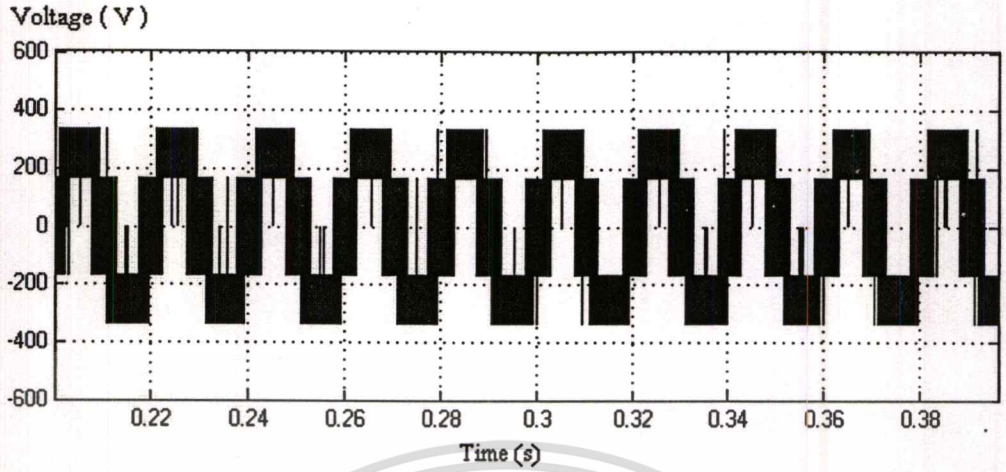

Figure 4.51 PWM phase-to neutral voltage waveform

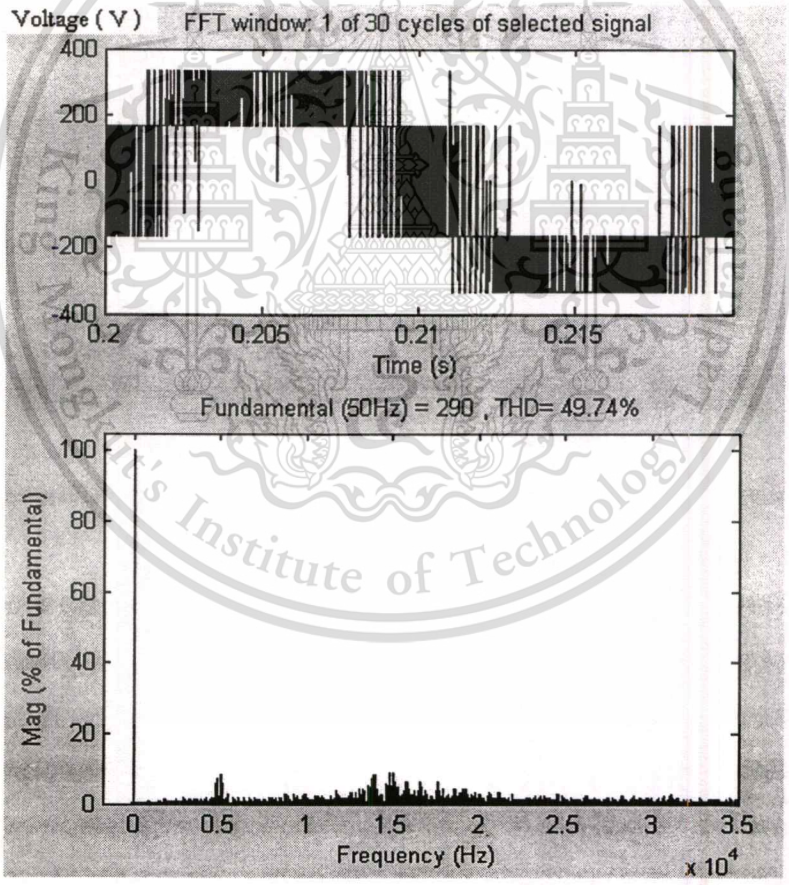

Figure 4.52 PWM phase-to neutral voltage spectra (switching frequency of 5 kHz)

Figure 4.52 PWM phase-to neutral voltage spectra (switching frequency of 5 kHz)

Figure 4.53 presents the PWM current spectra at converter side 1, the current waveform is nearly sinusoidal with THD = 2.84%.

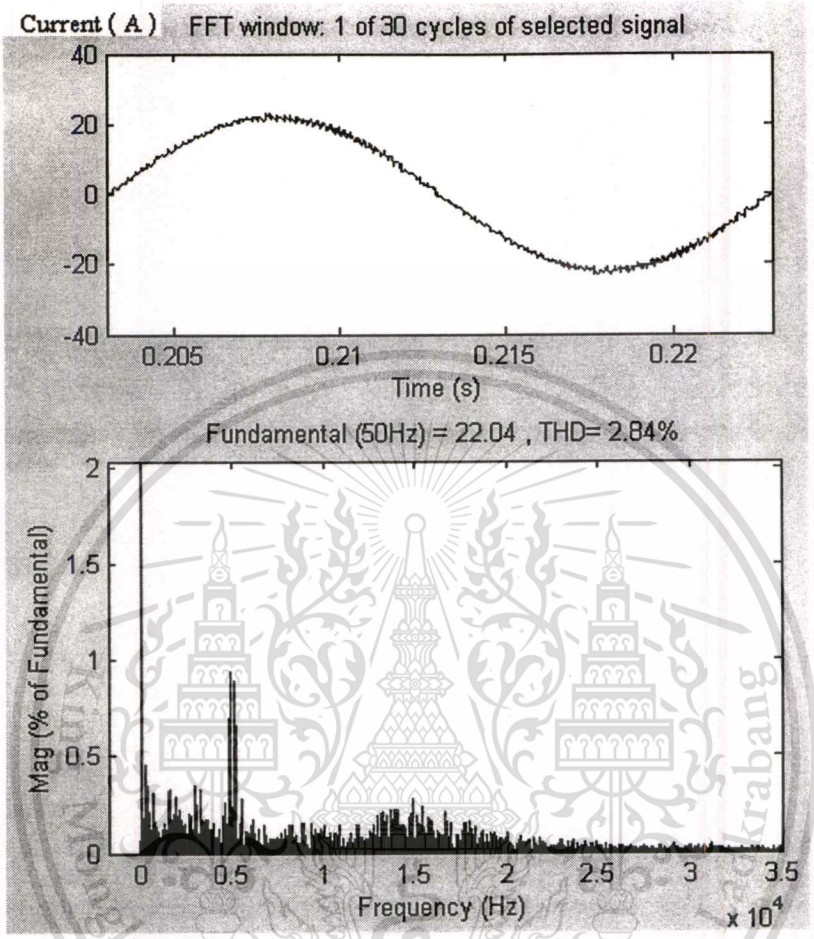

Figure 4. 53 PWM current spectra at converter side 1

All of the figures shown below are obtained at converter side 1 of case III, but with different levels of the active and reactive power flow. The Figure 4.54 shows the curve of power transmission from converter side 1 to converter side 2, the active power is kept constant at about 2800 W, meanwhile the reactive power is changed at T_s = 0.3s from 2000 Var to 4000 Var. From the graph, it can be seen that the real power slightly changes at the moment of reactive power flow step change. It recovers again after about 0.05s. Figure 4.55 shows the disturbance of reactive power step change. The phase shift between voltage and current due to the reactive power step change can be seen in Figure 4.56.

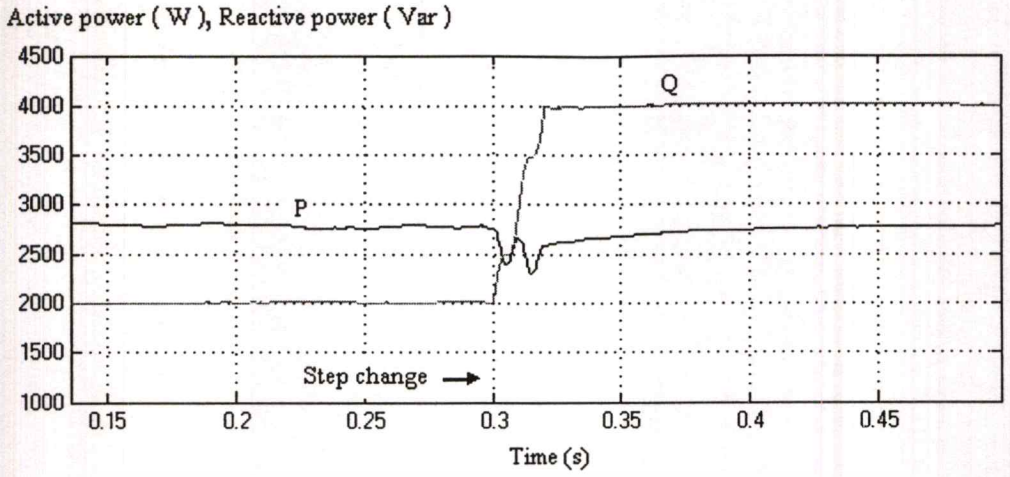

Figure 4.54 Step change of the reactive power at the converter side 1

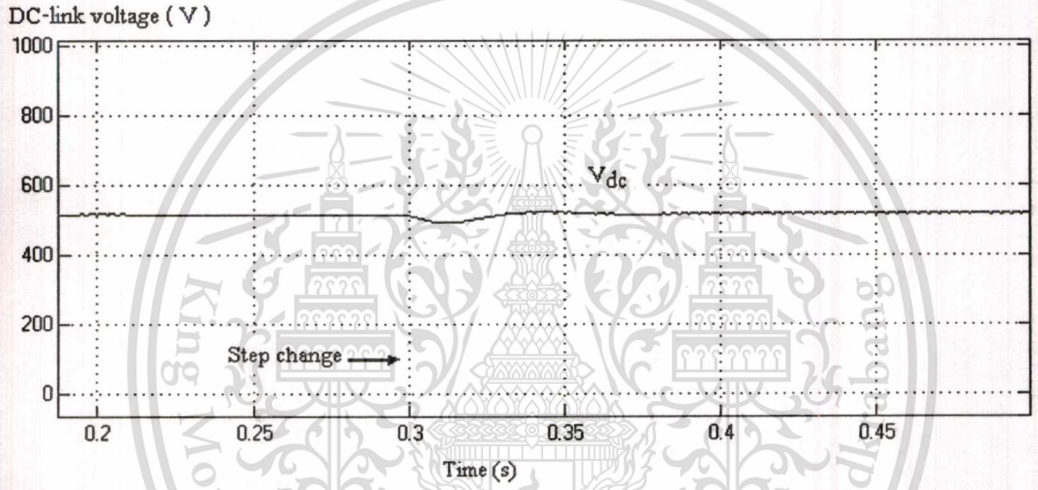

Figure 4.55 Dynamic response performance with step change in power flow

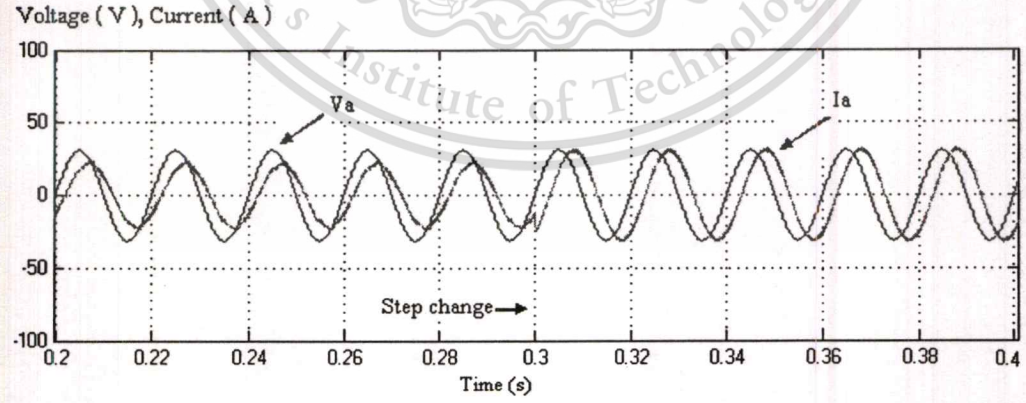

Figure 4.56 Typical line current and supply voltage of converter side 1

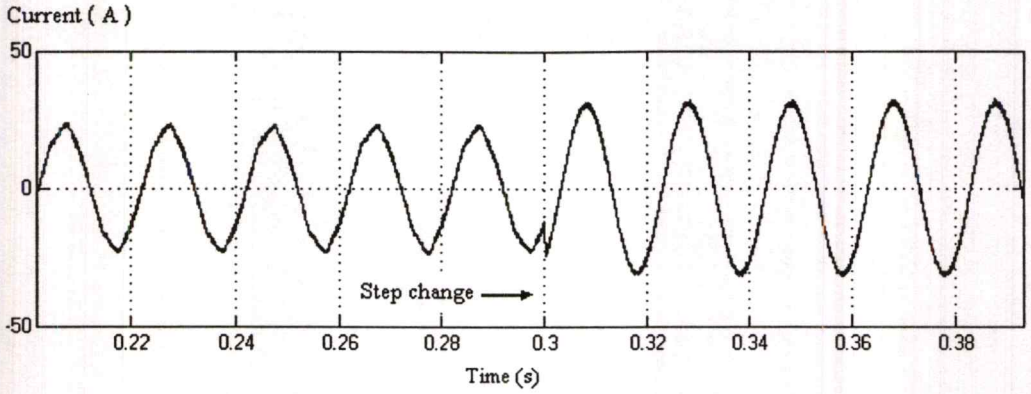

Figure 4.57 Typical line current of converter side 1

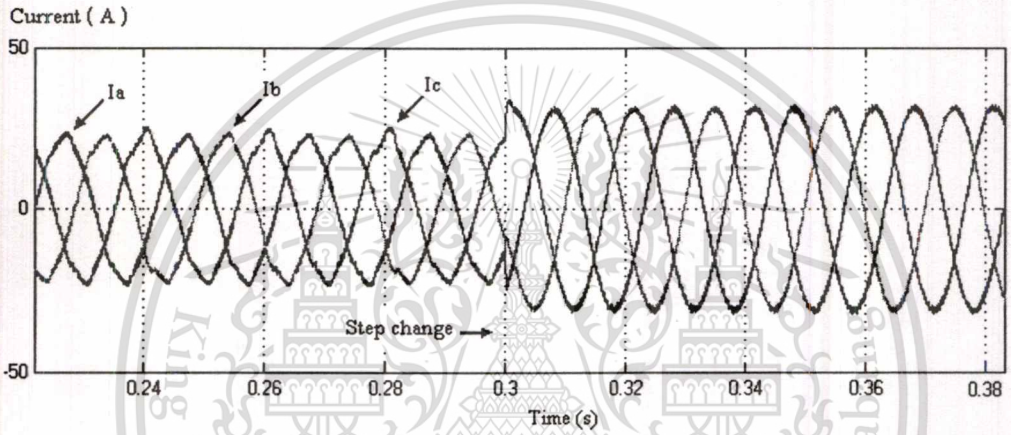

Figure 4.58 Three-phase line currents at converter side 1

Figure 4.57 shows the typical line current of the converter side 1, it can be seen that the line current after step change is slightly shifted and the current amplitude is changed. Figure 4.58 also shows the changes of three-phase line currents due to the power changes. Figure 4.59 shows the PWM line-to-neutral voltage waveform, It can be seen that the fundamental voltage reduce and the number of pulses increases to meet the step change in power flow. Figure 4.60 presents PWM phase voltage waveform and corresponding harmonics. Harmonics appear at multiple of switching frequency (i.e.5 kHz, 15 kHz, etc.). Figure 4.61 presents the PWM current spectra at converter side 1, the current waveform is nearly sinusoidal with THD=4.27%.

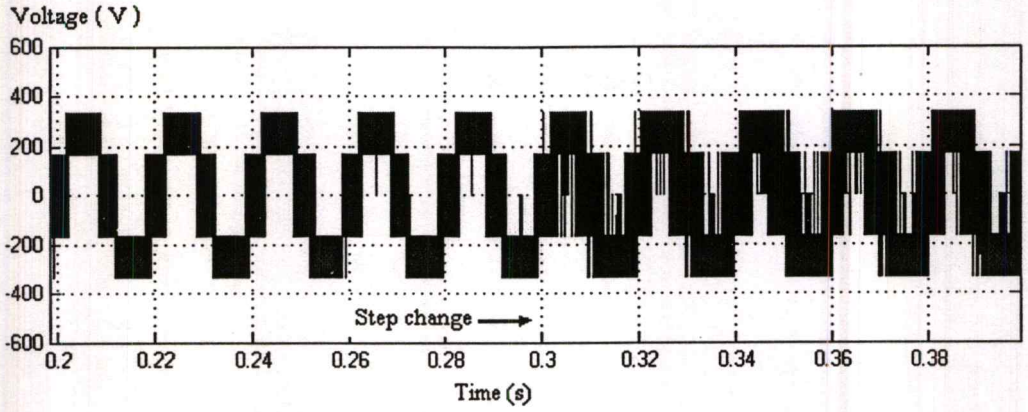

Figure 4.59 PWM phase-to neutral voltage waveform

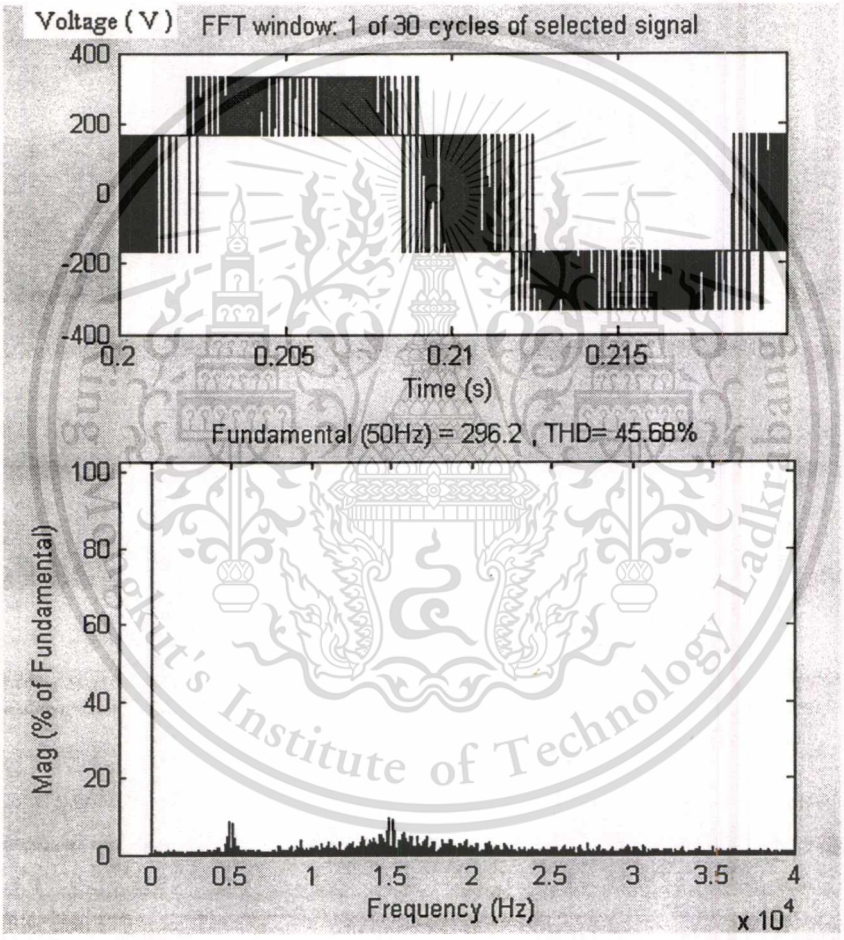

Figure 4.60 PWM phase-to neutral voltage waveform at converter side 1

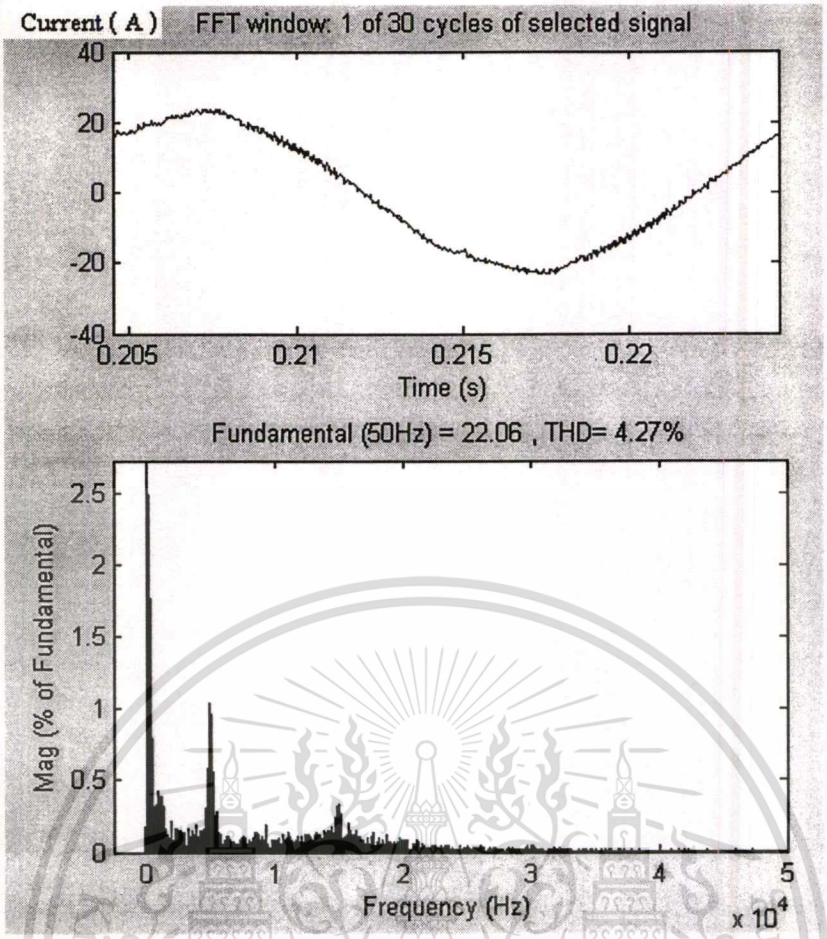

Figure 4. 61 PWM current spectra at converter side 1

4.2.3.2 Converter side 2

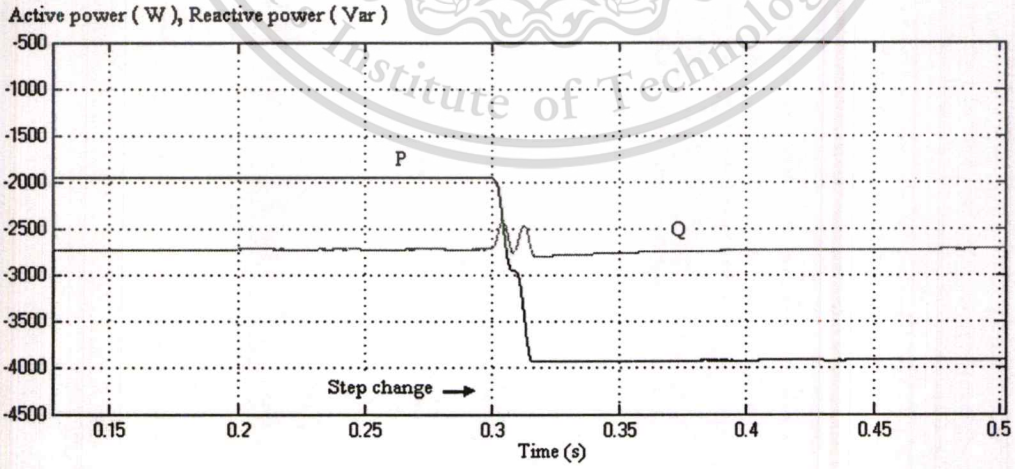

Figure 4.62 Step change of the active power at the converter side 2 from -2000 W to -4000 W

The measured active power and reactive power levels at the converter side 2 are slightly changed due the step change of power transfer as shown in Figure 4.62. Similarly to figures at the previous study cases are obtained here.

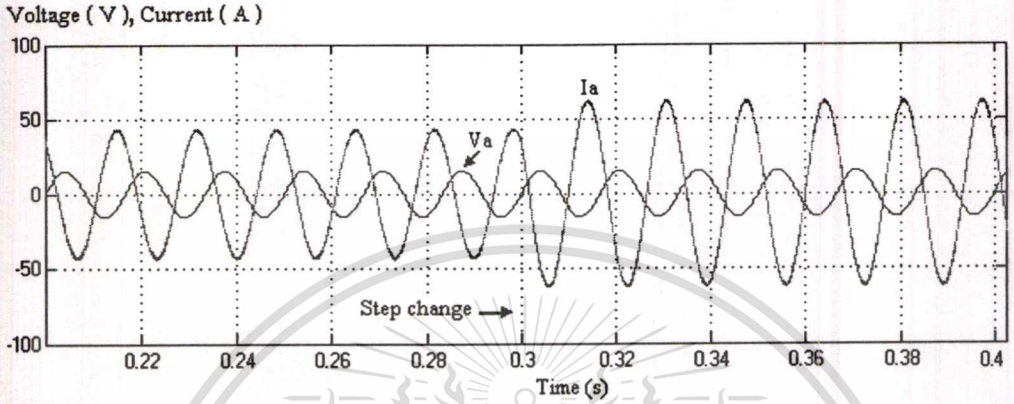

Figure 4.63 Typical line current and supply voltage of converter side 2

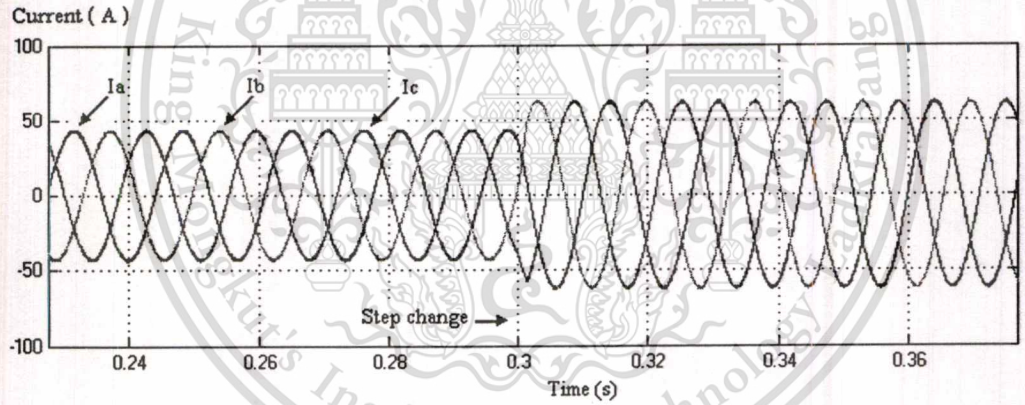

Figure 4.64 Three-phase line currents at converter side 2

Figure 4.63 and Figure 4.64 show the changes of currents from the moment of the active power changing. The line-to- line voltage waveforms at converter side 2 maintained sinusoidal as shown in Figure 4.65. Figure 4.66 presents PWM phase voltage waveform and corresponding harmonics. Harmonics appear at multiple of switching frequency (i.e.5kHz, 10 kHz, 15 kHz, 20 kHz, 25 kHz, etc.).

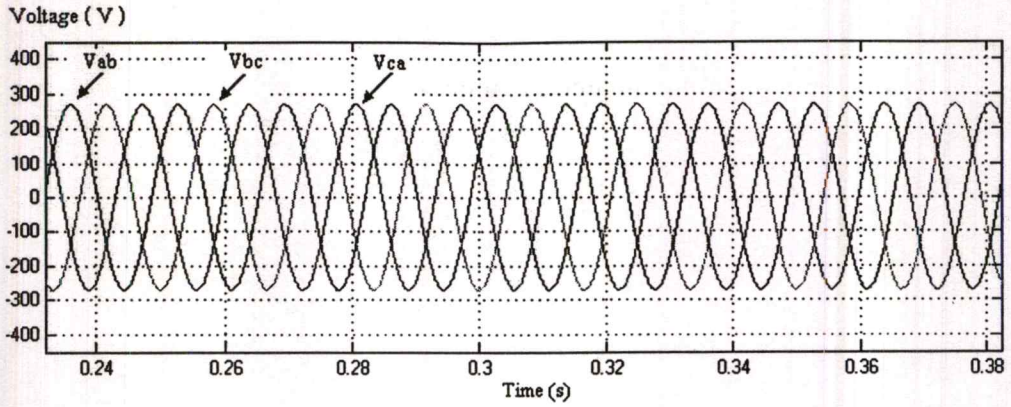

Figure 4.65 Line-to- line voltages waveform at converter side 2

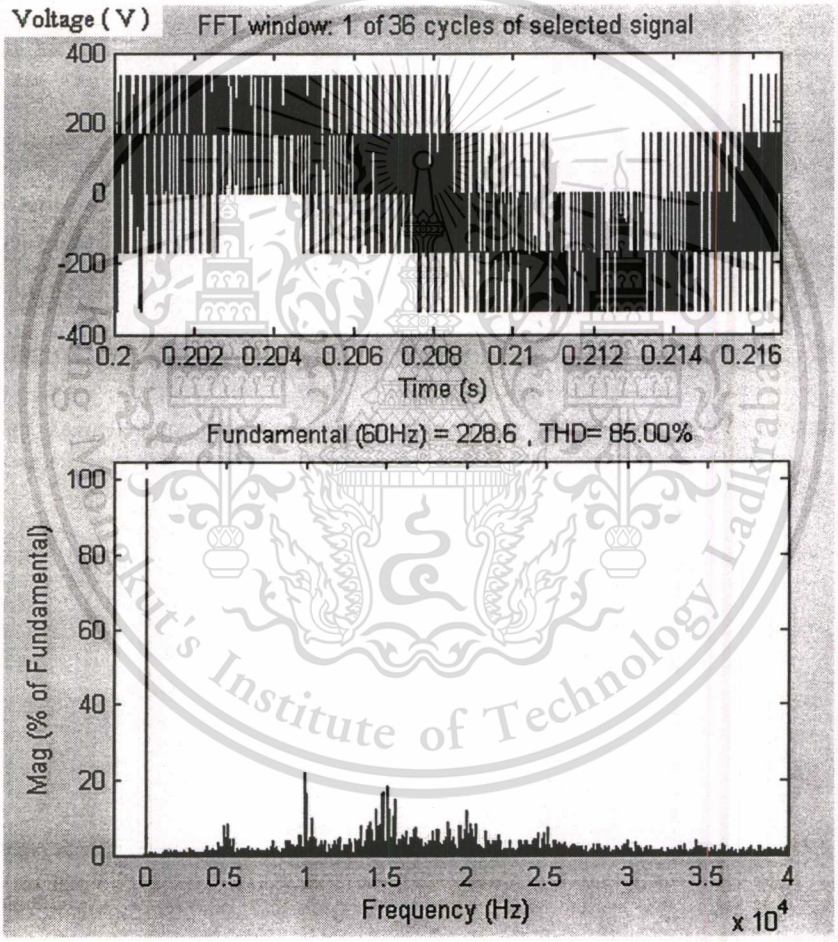

Figure 4. 66 PWM voltage spectra at converter side 2

From Figure 4.67, it can be seen that the fundamental voltage reduce and the number of pulses increases to meet the step change (Ts=0.3s) of power flow. Figure 4.68 presents the PWM current spectra at converter side 2, the current waveform is nearly sinusoidal with THD=1.26%.

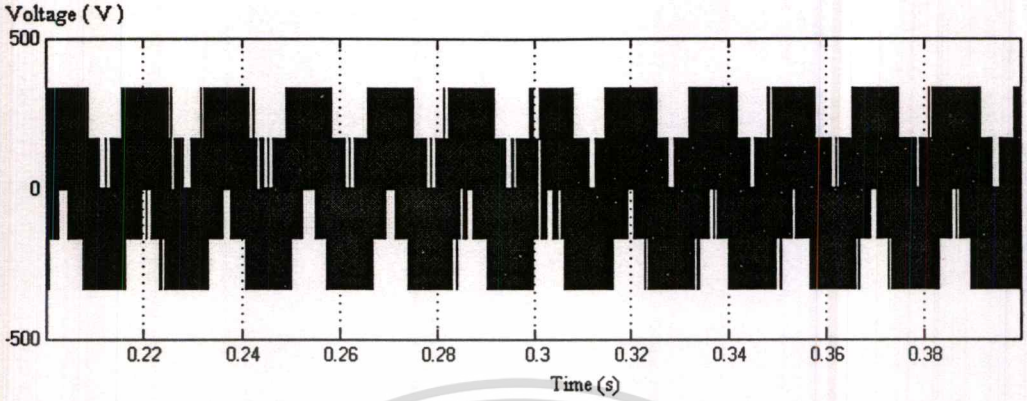

Figure 4.67 PWM line-to neutral voltage waveform at converter side 2

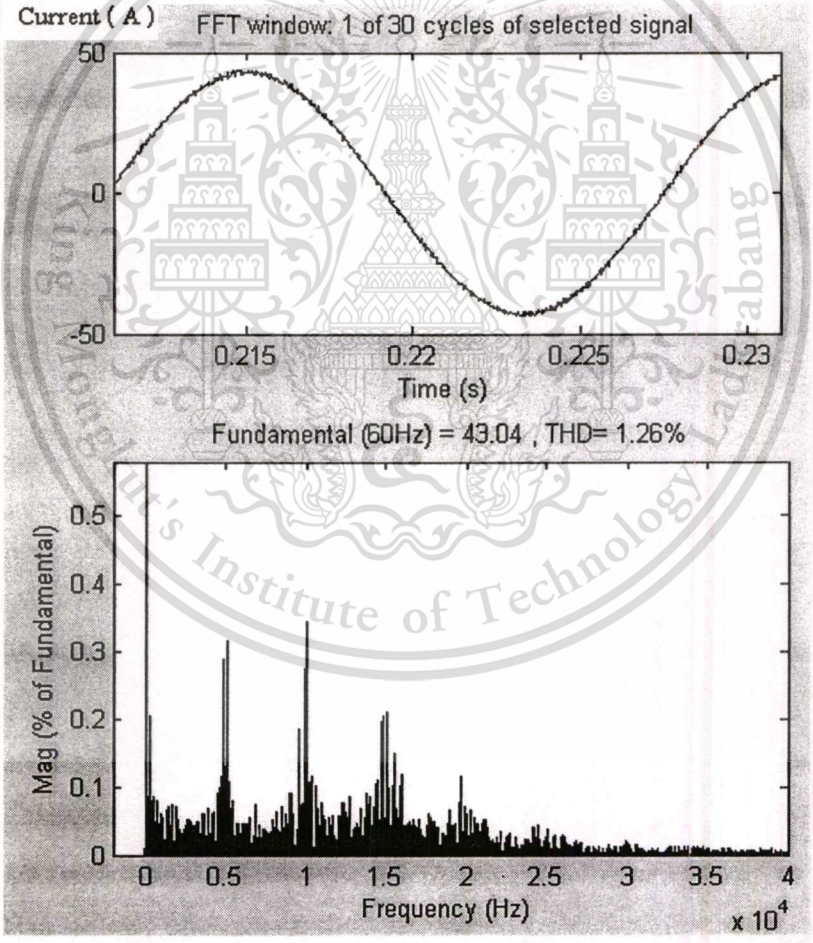

Figure 4.68 PWM current spectra at converter side 2

All of the figures shown below are obtained at converter side 2 of case III, but with different levels of the active and reactive power flow. The measured active power is slightly changed due to the step change in power flow as shown in Figure 4.69.

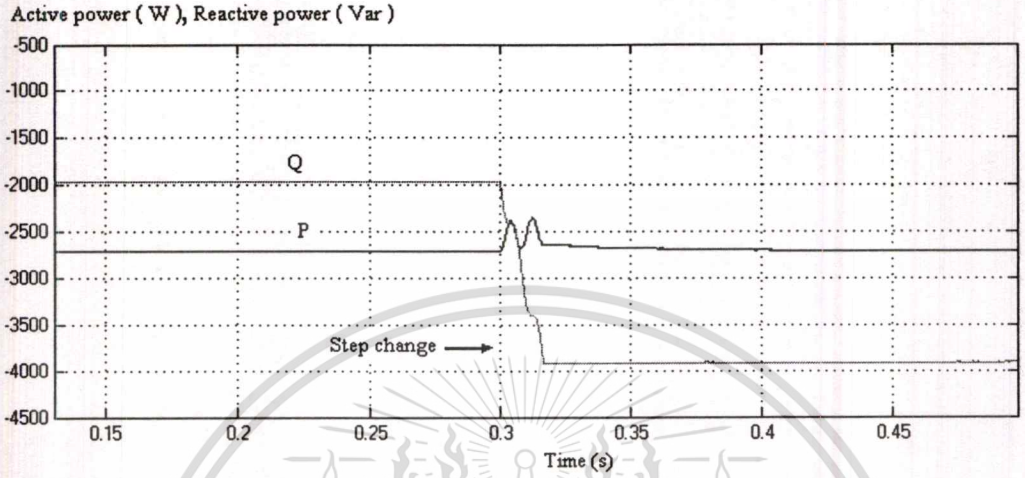

Figure 4.69 Step change of the reactive power at the converter2 side from -2000Var to -4000 Var

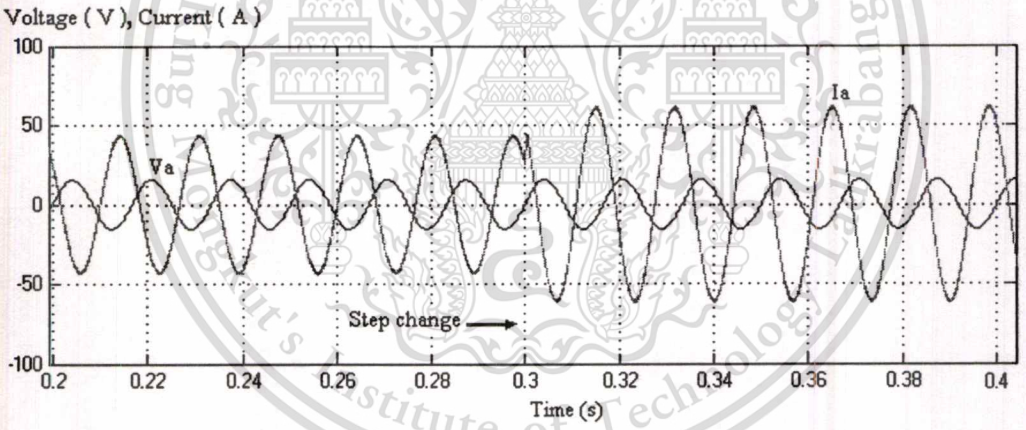

Figure 4.70 Typical line current and supply voltage of converter side 2

Figure 4.70 shows the phase shift between voltage and current and the change of current amplitude due to the step change of power flow. Figure 4.71 and Figure 4.72 present the changes of one typical line current and three-phase line currents at converter side 2 according to the step change of power flow. But the line-to- line voltages waveform as shown in Figure 4.73 maintain.

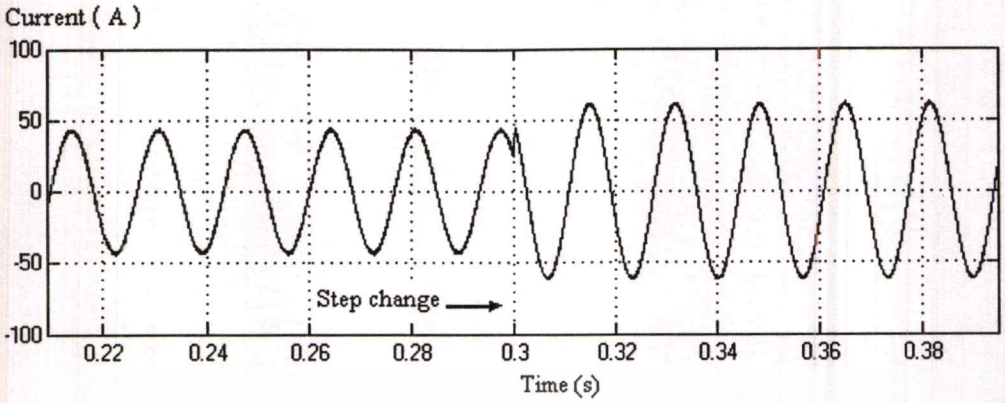

Figure 4.71 Typical line current of converter side 2

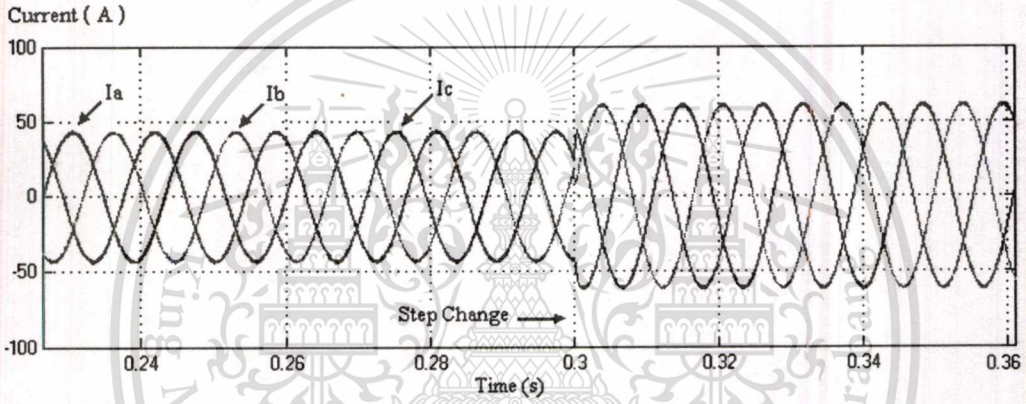

Figure 4.72 Three-phase line currents at converter side 2

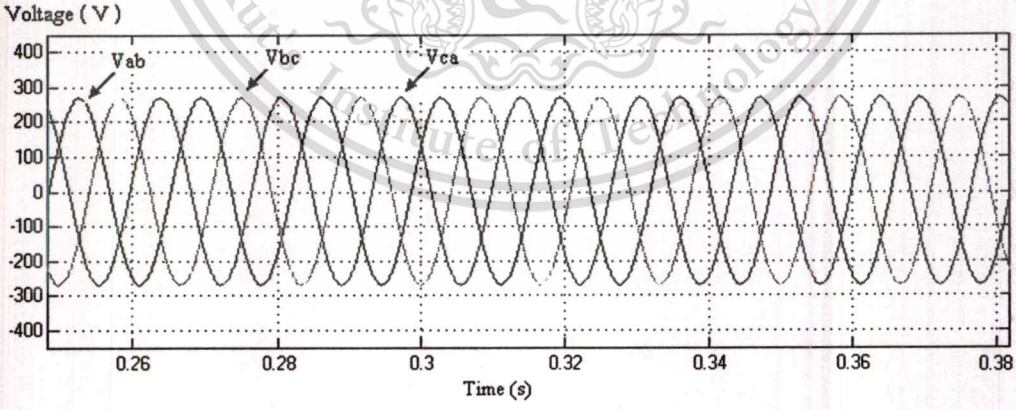

Figure 4.73 Line-to- line voltages waveform at converter side 2

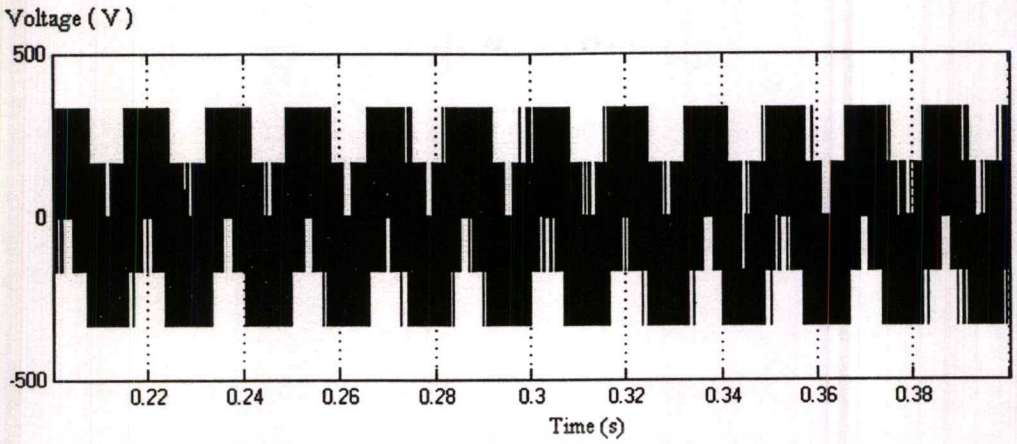

Figure 4.74 PWM phase-to neutral voltage waveform at converter side 2

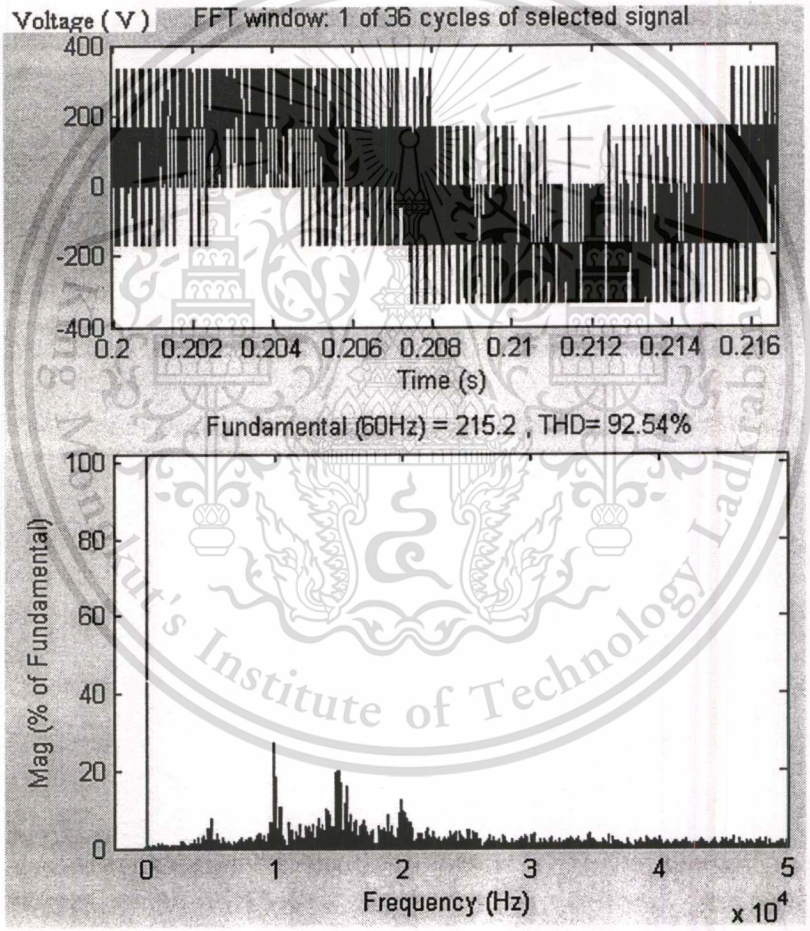

Figure 4. 75 PWM voltage spectra at converter side 2

Figure 4.66 presents PWM phase voltage waveform at converter side2. Harmonics appear at multiple of switching frequency (i.e.5kHz, 10 kHz, 15 kHz, etc.) as shown in Figure 4.75.

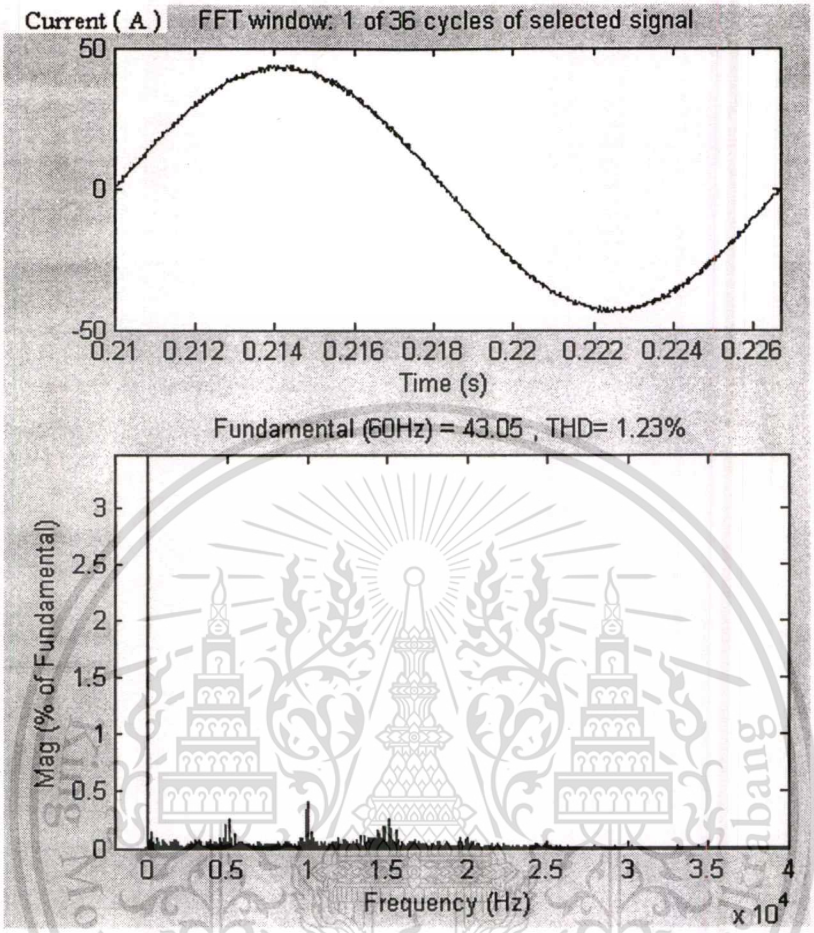

Figure 4. 76 PWM current spectra at converter side 2

Figure 4.76 presents the PWM current spectra at converter side 2, the current waveform is nearly sinusoidal with THD=1.23%.

4.2.4 Case IV: The same voltage and frequency with high DC-link voltage

All simulations have been performed according to Figure 4.1, the ac system voltages at both sides are 220V. The rated dc voltage is 1200V; the fundamental frequency of the ac systems is 50Hz. Other elements of the systems are the same as in the previous cases.

4.2.4.1 Converter side 1

The Figure 4.77 shows the curve of power transmission from converter side 1 to

converter side 2, the active power is kept constant at about 4150 W, meanwhile the reactive power is changed at Ts = 0.25 s from 3000 Var to 6000 Var. During the transient time, the active power slightly changes due to the disturbance of reactive power step change.

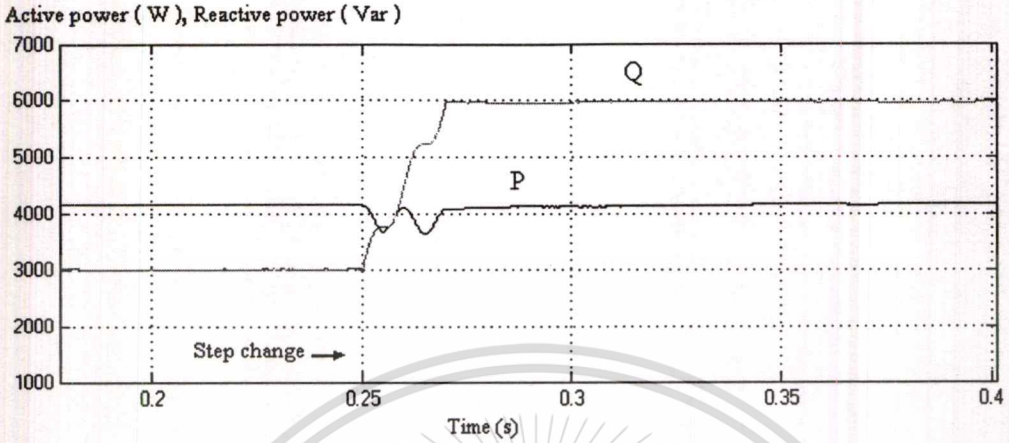

Figure 4.77 Step change of the reactive power at the converter side1 from 3000W to 6000W

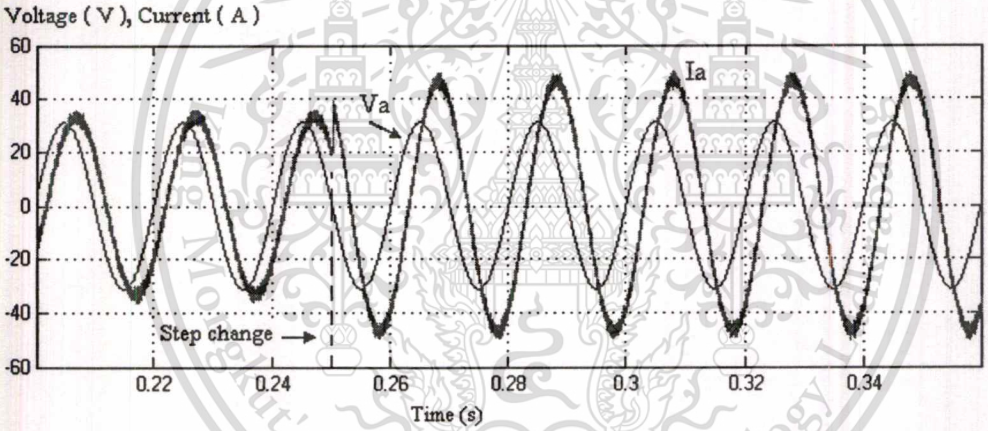

Figure 4.78 Typical line current and supply voltage of converter side 1

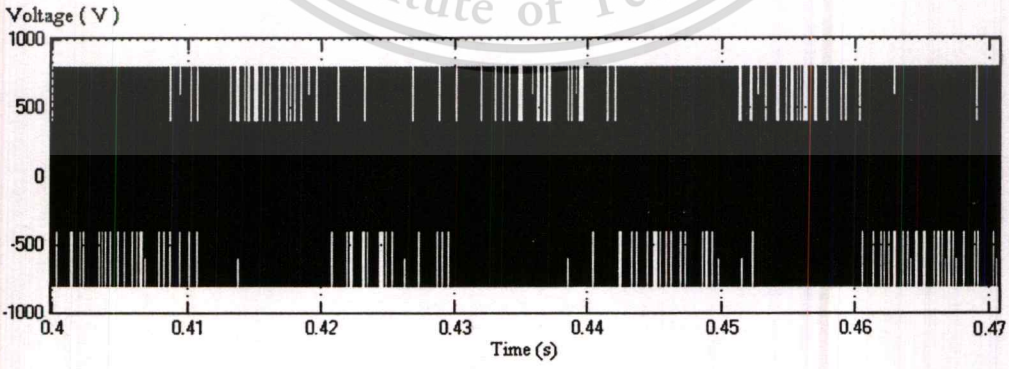

Figure 4.79 PWM phase-to neutral voltage waveform at converter side 1

Figure 4.78 shows the typical line voltage and current of the converter side 2, the line current slightly changes while the reactive power is stepping up at Ts = 0.25 S and the current amplitude increases. The PWM line-to-neutral voltage waveform shown in Figure 4.79 is the voltage measured between the corresponding phase voltage near converter and neutral point. It can be seen that the fundamental voltage reduce and the number of pulses increases to meet the step change of power flow.

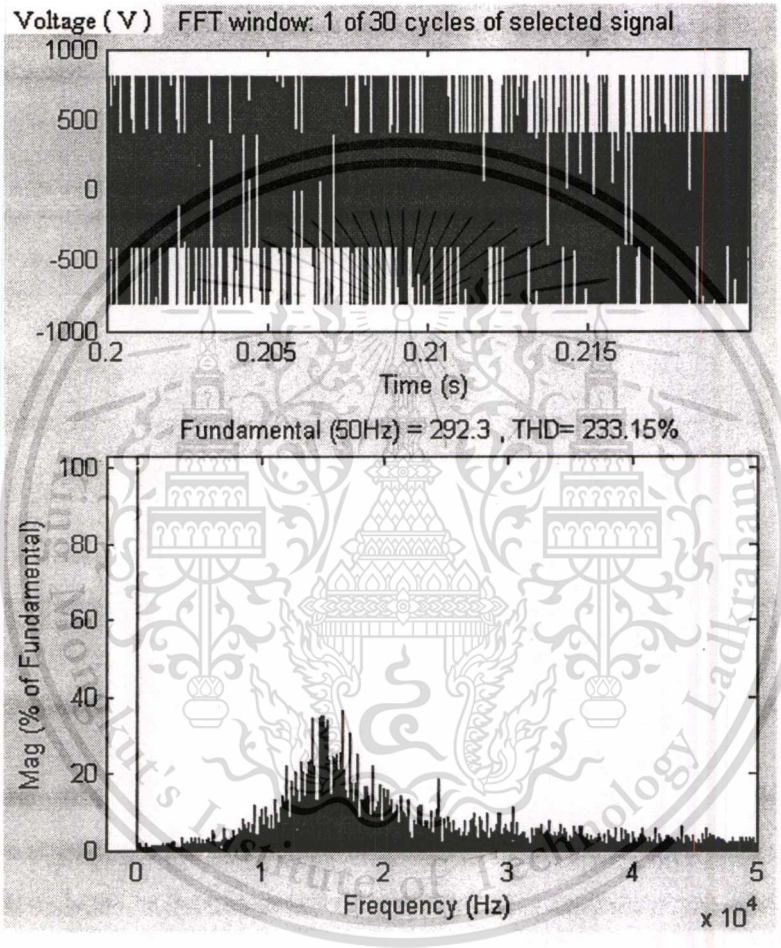

Figure 4. 80 PWM voltage spectra at converter side 1

Figure 4.80 presents PWM phase voltage waveform at converter side 1 and its corresponding harmonics.

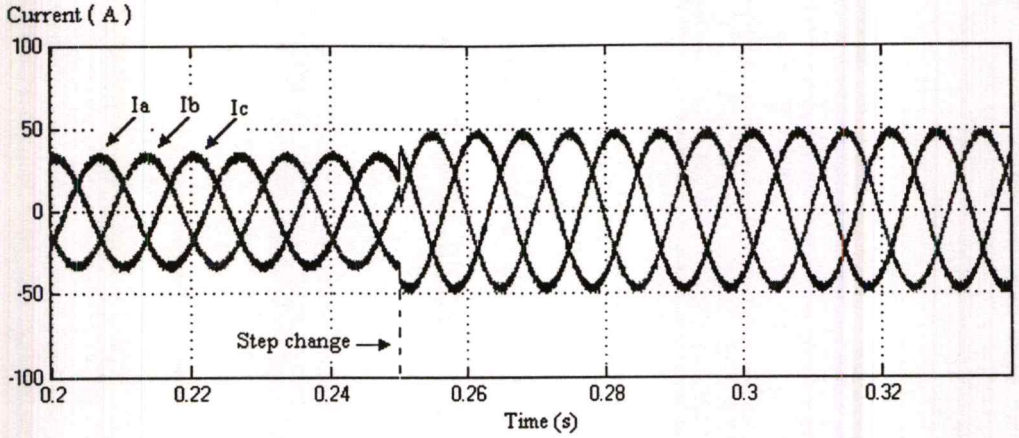

Figure 4.81 Three-phase line currents at converter side 1

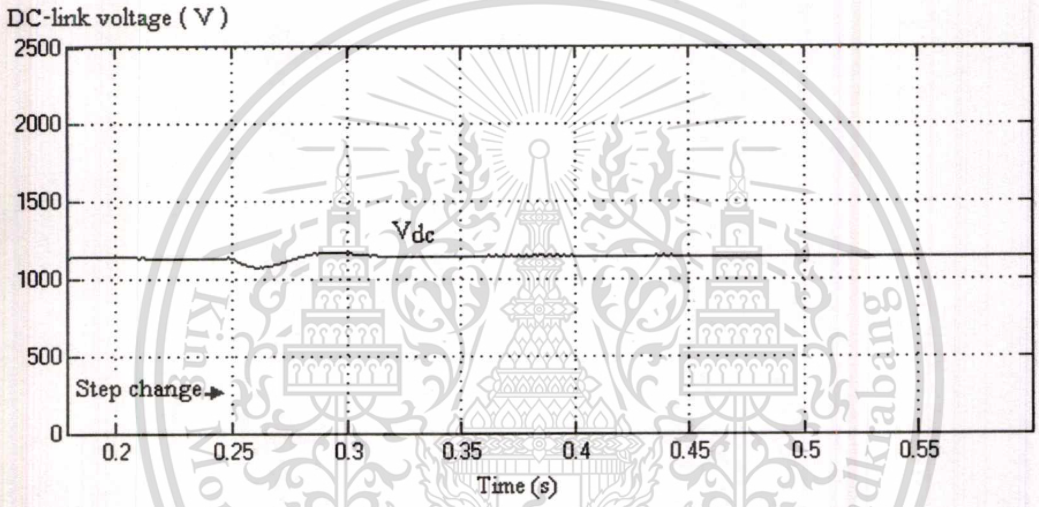

Figure 4.82 Dynamic response performance with step change in power flow

From Figure 4.81, it can be seen the phase shift angle between voltage and current due to the step change of power flow. The DC-link voltage of the system shown in Figure 4.82, slightly drops at the moment of the reactive power step change. It becomes steady again after 0.04 S. It can be concluded that the DC-link controller works well. Figure 4.83 presents the PWM current spectra at converter side 1, the current waveform is nearly sinusoidal with THD = 5.44%.

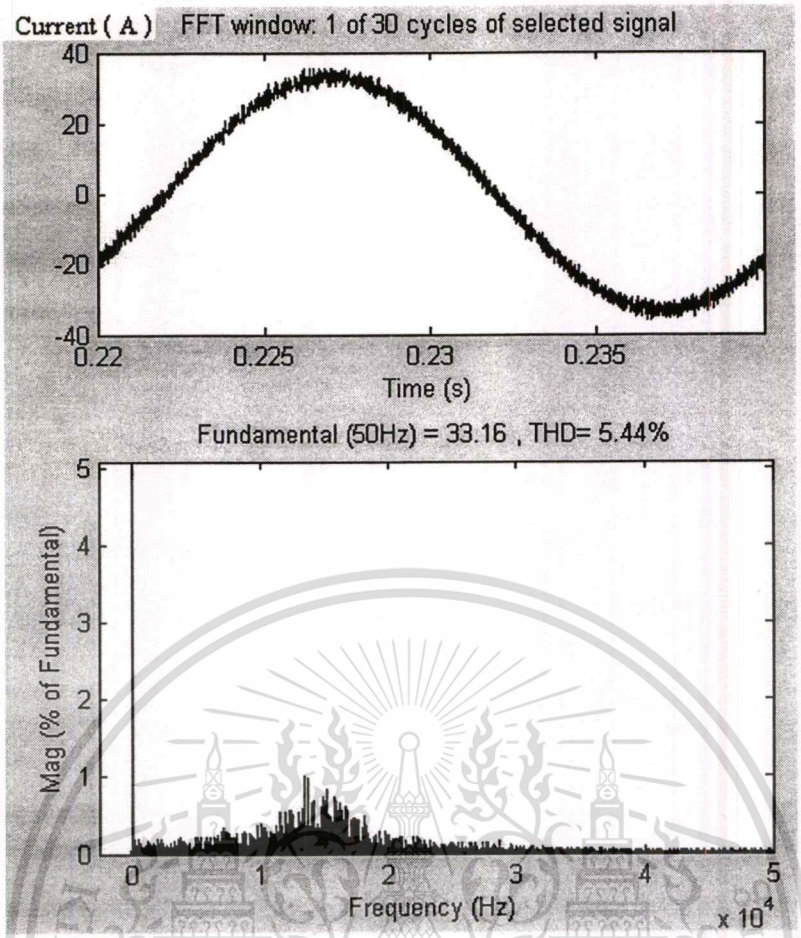

Figure 4. 83 PWM current spectra at converter side 1

4.2.4.2 Converter side 2

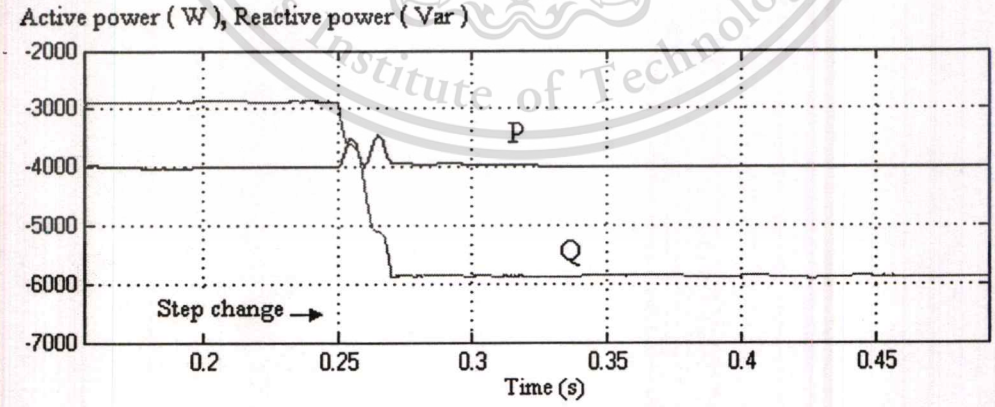

Figure 4.84 Step change of the active power at the converter side 2

The measured active power and reactive power levels at the converter side 2 as shown in Figure 4.84 are slightly changed due to the step change of power transfer. Similarity figures to other cases are obtained here. The changing of the reactive power flow causes in changes of the current amplitude and phase shift between voltage and current as shown in Figure 4.85. The changes in three-phase line currents at converter side 2 because of the step change in power flow are shown in Figure 4.86.

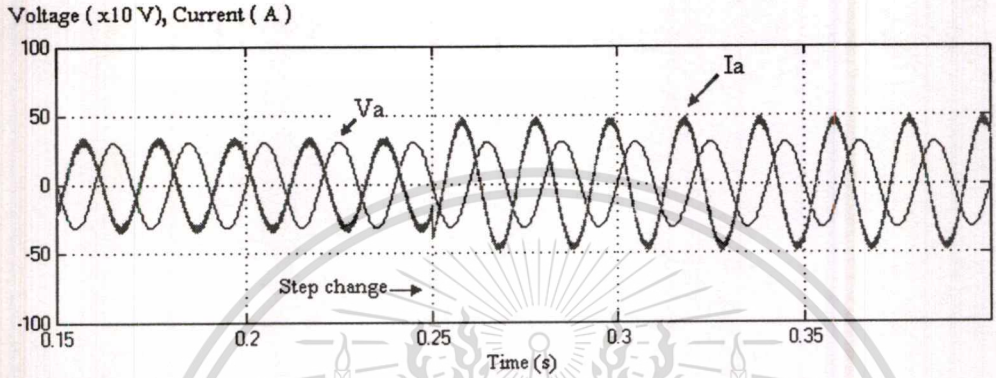

Figure 4.85 Typical line current and supply voltage of converter side 2

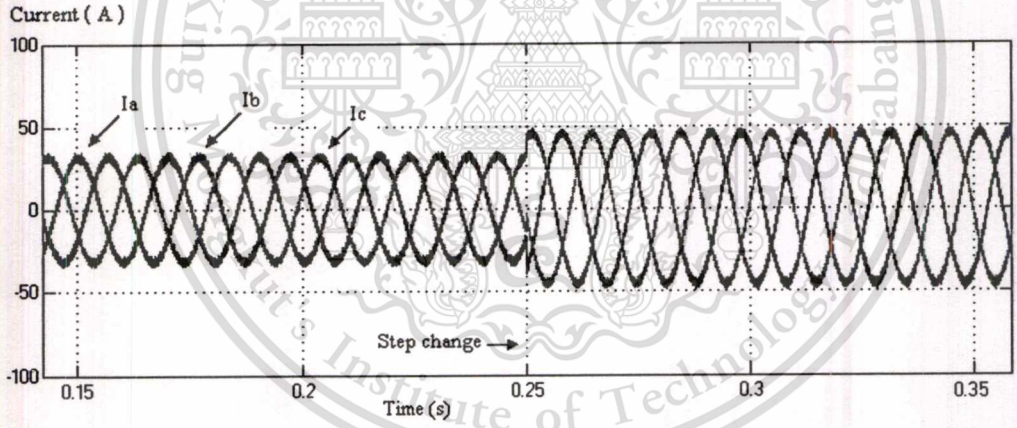

Figure 4.86 Three-phase line currents at converter side 2

Figure 4.87 presents PWM phase voltage waveform at converter side 2 and its corresponding harmonics. Figure 4.88 presents the PWM line-to neutral voltage waveform at converter side 2 and it can be seen that the fundamental voltage reduce and the number of pulses increases to meet the step change (T_s = 0.25s) of power flow.

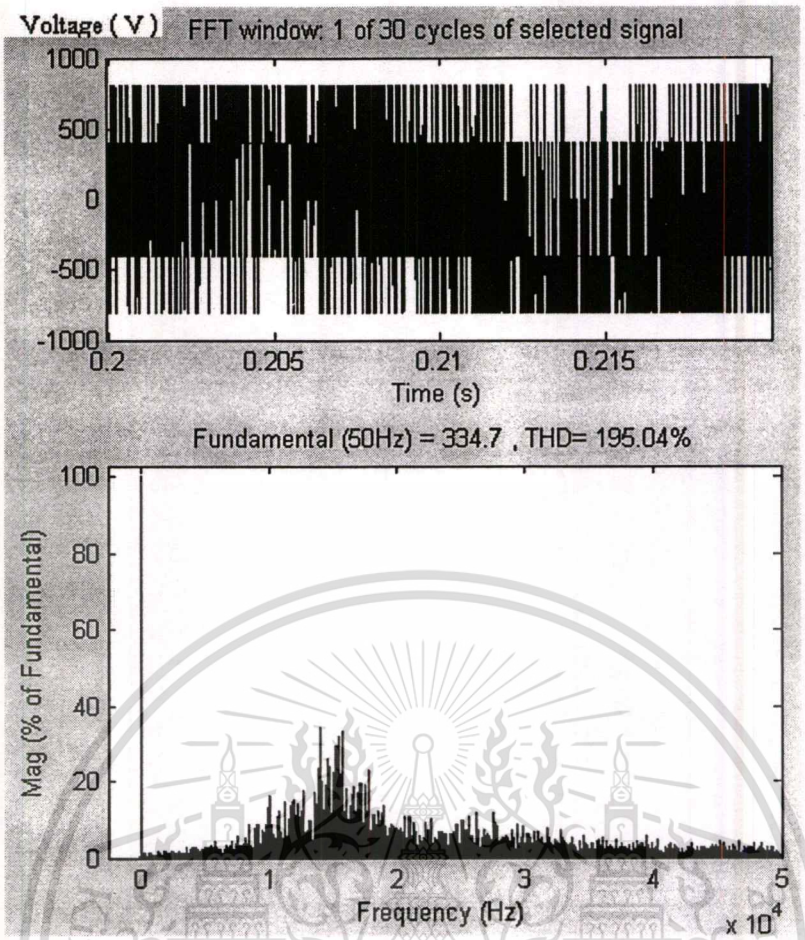

Figure 4. 87 PWM voltage spectra at converter side 2

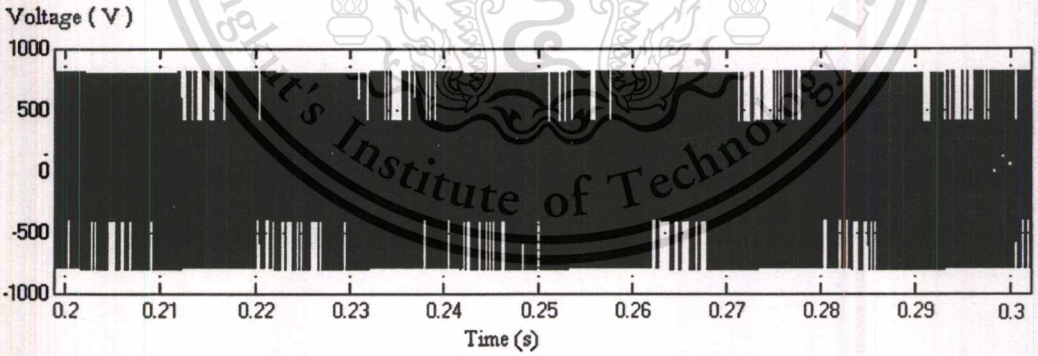

Figure 4.88 PWM phase-to neutral voltage waveform at converter side 2

Figure 4.89 presents the PWM current spectra at converter side 2, the current waveform is nearly sinusoidal with THD = 5.46%.

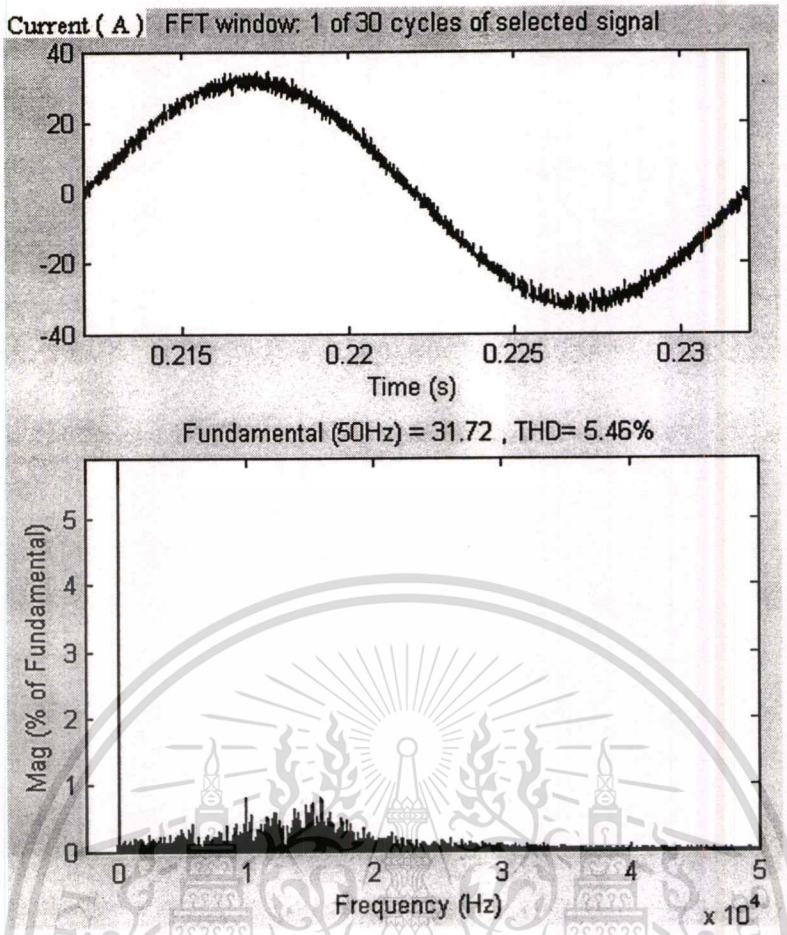

Figure 4. 89 PWM current spectra at converter side 2

4.3 Summary

This chapter presents Simulink Matlab implementation of the VSC between two grids. Four study cases are investigated in this chapter. As described before, the VSC control strategies can be varied regarding different objectives. The control strategy is used for simulation as bellows:

- Converter 1 controls dc voltage and reactive power.
- Converter 2 controls reactive power and active power.

From the simulation results, it is verified that

- VSC can control both active and reactive power independently.
- Due to the use of the PWM the high quality ac voltages (Figure 4.14) and ac currents (Figure 4.13) can be obtained from the source sides, and the harmonics caused by disturbances in the power system are reduced compared with thyristor converter as described in chapter 2.

Chapter 5

Conclusions and suggestions.

5.1 Conclusions

A model of a PWM VSC Controlled Power Transfer for HVDC Applications and vector control strategies are presented in this thesis. Four study cases were investigated. This control strategy is described and implemented in SIMULINK/MATLAB.

5.1.1 Control system

Using pulse-width modulation (PWM) for voltage-source converters enables independent control of real and reactive power within the equipment limits. The HVDC control objectives and schemes will change significantly because of this. Different kinds of controllers can be used depending on the application. A decision on which controller to use may require advanced power system study. But the active power flow through the dc link must be the same with both terminals, the dc voltage controller is necessary to achieve this balance.

The control system of the VSC-HVDC is based on DC-link voltage control loop controlling the dc voltage and current control loops controlling the active and reactive power flow.

In the sending side of the system, the reference value (V_D^*) for the DC-link voltage control is set directly to the DC-link voltage control loop (inner loop) as shown in the vector control structure for VSC in chapter 4. To control the reactive power, the reference value (i_q^*) is set directly to the reactive control loop (outer loop). And at the same time in the receiving side of the system, the reference value (i_d^*) and the reference value (i_q^*) for controlling P and Q, are set directly to active and reactive control loops respectively. The validity of the proposed control has been confirmed in MATLAB/SIMULINK.

From the simulation results, it is concluded that the system response is fast; control accuracy can be achieved and high quality ac voltages and ac currents can be obtained. The active power and the reactive power can be controlled independently. But fast transient variations of the operating point of the converter may cause transients in the dc voltage.

5.2 Suggestions

As described before, VSC distribution and transmission have some disadvantages, which include potentially high losses and costs, but the technology continues to evolve. To further assess the potential and limitation of VSC distribution and transmission for industrial power systems, a number of possible applications and advancements in the VSC technology are required.

For the case studies, the level of system voltages must be set to be much closed to the level of the real system voltages with bidirectional controlling technique. All of transmission line parameters must be included.

It is necessary to establish an ac controller for the ac side, the frequency control and other controllers to protect the system from faults also should be implemented. Keeping the dc voltage constant in the sending side is very importance for power transfer processes.

As not all of device parameters were implemented in this model, it is also necessary to take in to account some conditions for improvement this model such as:

- Blanking time effect. The blanking time prevents the upper and lower switched devices in the same leg of converter from short circuit. In this work, the model converters have ideal characteristic. However, in practice they have some delay time of banking.
- Snubber effects to reduce the switching losses and current spikes.
- DC filter, the filters are needed to take care of the harmonics generated on the dc end
- Minimized rated dc capacitor in terms of the cost reason.

Literature Cited

[1] M. M. de oliveira. Power Electronics for Mitigation of Voltage Sags and Improved Control of ac Power Systems. PhD thesis, Ph.D. thesis, Royal Institute of Technology, ISSN-1100-1607, TRITA-EES-0003, Stockholm, Sweden, 2000.

[2] Hingorani and N.G. Introducing custom power. IEEE Spectrum, 1995.

[3] E.Acha, V.G. Agelidis, O.Anaya-lara, and T.J.E. Miller. Power electric control in electrical system. Newnes, 2002.

[4] M.H.J. Bollen. Understanding power quality problems: voltage sags and interruptions. IEEE Press, New York, 2000.

[5] N.G.Hingorani L.gyugyi. Understanding FACTS. IEEE Press, New york, 2000.

[6] A Ghosh and G Ledwich. Power quality enhancement using custom power devices. Uluwer Academic Publishers, 2002.

[7] Jos Arrillaga. High Voltage Direct Current Transmission. The Institution of Electrical Engineers, 1998.

[8] Dennis A. Woodford. Hvdc transmission. Technical report, Manitoba HVDC Research Centre, 1998.

[9] Navid R,Zargari and Zeza Joos,"Performance Investigation of a Current-Controlled Voltage-Regulated PWM Rectifier in Rotating and Stanary Frames",in IEEE Trans.on Ind. Electronics, Vol. 42, No. 42, August 1995.

[10] Roberto Rudervall, J.P. Charpentier, and Raghuveer Sharma. High voltage direct current (hvdc)transmission systems technology review paper. In Energy Week 2000, 2000.

[11] Kjell Eriksson. Operational experience of hvdc light. AC-DC Power Transmission, 2001.

[12] F.Schettler, H.Huang, and N.Christl. Hvdc transmission systems using voltage sourced converters-design and applications. In IEEE power Engineering Society Summer Meeting, 2000.

[13] Urban Axelsson, Anders Holm, and Kjell Eriksson Christer Liljegren. Gotland hvdc light transmission-world's first commercial small scale dc transmission. In CIRED Conference, Nice, France, 1999.

[14] Anna-Karin Skytt, Per Holmberg, and Lars Erik Juhlin. Hvdc light for connection of wind farms. In Second International Workshop on Transmission Networks for Off Shore Wind Farms, Royal Institute of Technology, Stockholm, Sweden, 2001.

[15] Kjell Eriksson Lar Stendius. Hvdc light an excellent tool for city center infeed. In PowerGen Conference, Singapore, 1999.

[16] Ned Mohan, Tore M.Undeland, and William P. Robbins. Power electronics converters, application and design. John Wiley and Sons, New York, 1995.

[17] Feir Biledt John Graham Don Menzies. Electrical system considerations for the argentina-brazil 1000mw interconnection. In CIGRE Conference, Paris, France, 2000.

[18] Mannheim Michael HÄausler. Mutiterminal hvdc for high power transmission in europe. In CEPEX99, Poland, 1999.

[19] B.J.Cory B.M.Weedy. Electric Power Systems. Wiley, 1998.

[20] W.P. Robbins N.Mohan, T.M.Undeland. Power electronics: converters, applications and design. Wiley, New York, 1989.

[21] D.A.Paice. Power electronic converter harmonics. In IEEE Press, New York, 1996.

[22] Ingvar Hagman and Tomas Jonsson. Verification of the ccc concept in a high power test plant. In CIGRE Study Committee 14 International Colloquium on HVDC and FACTS Proceedings, 1997.

[23] Lena Kjellin and Niclas Ottosson. Modular back-to-back hvdc with capacitor commutated converters (ccc). In Cigre Suceava Conference,, 2001.

[24] W.Zhang. Modern harmonicfiltering techniques in power systems. electricity delivery and power quality, 1996.

[25] Lars Weimers. New markets need new technology. In Powercon 2000 Conference, Western Australia, 2000.

[26] Rolf GrÄunbaum, Bruno Halvarsson, and Aleksander Wilk-Wilczynski. Facts and hvdc light for power system interconnections. In PowerDelivery Confrerence, 1999.

[27] A. Khanthee, V. Kinnares," Analysis and Design of IGBT Converters for AC Power Transfer via DC-link", EECON-26, P 648-653, 2003

[28] Peter Vas, "Parameter Estimation, Condition Monitoring and Diagnosis of Electrical Machines" Clarendon Press, Oxford 1993

[29] Andrzej M. Trzynadlowski, " The Field Orientation Principle in Control of Induction Motors"

[30] Prof. J.T Boys, A.W Green,BE, " Current-forced single- phase reversible rectifier", in IEE PROCEEDINGS,Vol. 136, Pt. B,No. 5,September 1989.

Appendices

Appendix A

The Publication

S. Douangsyla, P.Indarack , A.Kanthee, M.Kando, S. Kittiratsatcha and V. kinnares "Modeling for PWM Voltage Source Converter Controlled Power Transfer," International Symposium on Communication and Information Technologies 2004 (ISCIT 2004) , Sapporo. Japan, October 26-29, 2004.

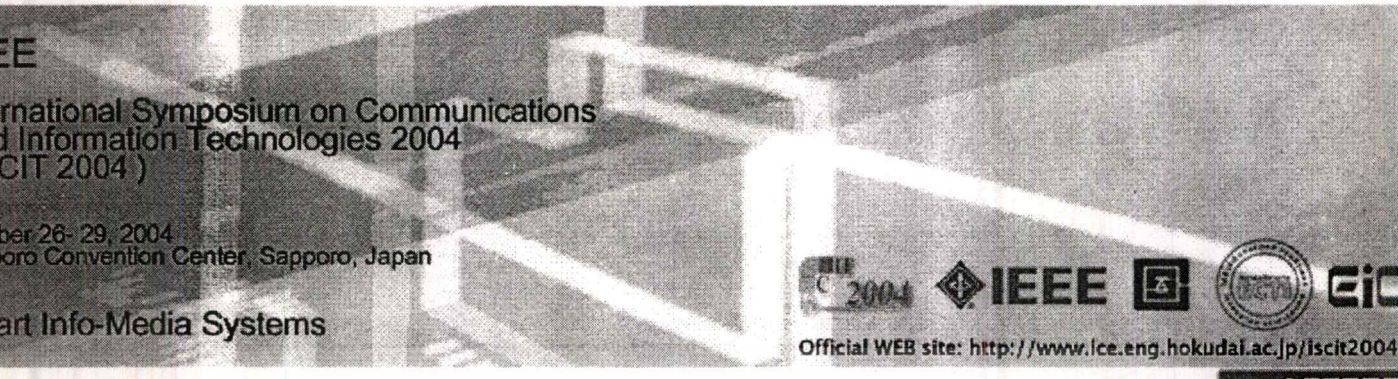

Sponsored by:

ECTI, Thai
Hokkaido University, Graduate School of Information Science and Technology
Hokkaido University, 21st Century COE Program
IEEE Circuits and Systems Society
IEEE Sapporo Section
IEEE Circuits and Systems Society, Japan
IEEE Signal Processing Society, Japan
Sapporo City

Technical Co-Sponsored by: IEICE

ISCIT 2004

International Symposium on Communications and Information Technologies 2004 (ISCIT 2004)
Sapporo, Japan, October 26- 29, 2004

Modeling for PWM Voltage Source Converter Controlled Power Transfer

S. Douangsyla[1], P. Indarack[1], A. Kanthee[1], M. Kando[2], S. Kittiratsatcha[1] and V. Kinnares[1].
[1]Department of Electrical Engineering, King Mongkut's Institute of Technology Ladkrabang , Bangkok 10520, Thailand Phone: (662) 737-3000 Ext. 3519 Email: seumsak@hotmail.com
[2]Department of Electrical & Electronic Engineering, Tokai University, Japan. Phone:(81)463-58-1211 Ext. 4029 Email:mkkando@keyaki.cc.u-tokai.ac.jp

***Abstract*— In this paper, a model for PWM Voltage Source Converter (VSC) Controlled Power Transfer has been developed. A vector control strategy with PI controllers is proposed. This paper studied the PWM Voltage Source Converter connected to an active ac network with vector control strategy. PWM pattern generation is based on a carrier technique. The instantaneous 3-phase voltages and currents are transformed to a 2-axis (d-q) reference frame system [1] which rotates at the supply angular frequency (ω_s). Thus it is possible to have decoupled control of the active (P) and reactive (Q) power flow and it is necessary to develop a mathematical model for VSC to determine controlling variables. The design and the performance of controllers are investigated. Digital simulation shows the feasibility of the proposed control strategy.**

I. INTRODUCTION

In recent years, voltage source converter technology has made a great progress through the development of high power self-turn off type semiconductor devices. The rating for converter of this type in practical application has already reached as a high. Because of its advantage over the line commutated type in performance characteristics and compactness, various applications of the voltage source converter have been developed and researched [2].

In this paper, a model for PWM VSC Controlled Power Transfer is developed. The control variables based on mathematical model are determined and vector control strategy is proposed.

Under steady state conditions, the 3-phase quantities when expressed in the synchronously rotating frame become dc quantities. If one of the axes (usually) the d-axis arbitrarily aligned with supply voltage vector, then the d and q axis supply current components automatically represent the active (P) and the reactive (Q) power flow respectively.

Thus it is possible to have decoupled control of the active and reactive control.

The DC-link voltage controller sets the active power demand whereas the reactive power demand can be set by an outer reactive power controller or by the required displacement angle between the phase current and voltages.

Therefore, the main advantages of the vector control technique are the direct control of the active and reactive power flow in the converter during transient, steady state and the fast dynamics of the current control loops.

Additionally, the current controllers deal with dc quantities which, using PI controllers, ensures zero current error in steady state. These are the main reasons for selecting the control strategy for the implementation of the VSC. The validity of proposed model and control strategy has been verified by digital simulation using application SIMULINK MATLAB 6.5.

II. SYSTEM CONFIGURATION

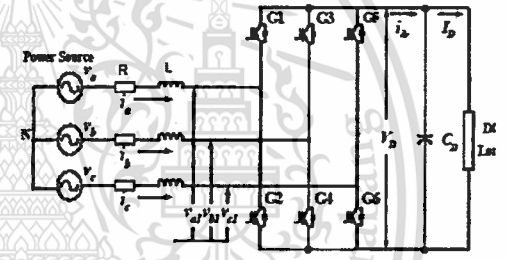

Fig. 1. Schematic diagram of a three-phase voltage source converter

The system configuration of the VSC connected to an ac network is shown in Fig. 1. The 3-phase supply voltages are v_a,v_b,v_c and the 3-phase converter voltages are v_{a1},v_{b1} and v_{c1}. The PWM control block is adopted to control IGBT, this control not only can manage the active power, but also reactive power, allowing this type of VSC to correct power factor.

III. VSC MODEL AND ITS VECTOR CONTROL STRUCTURE

According to Fig. 1, assuming ideal commutation and neglecting the effect of current harmonics, the equations that model of VSC can be derived as follows. Considering that V_{a1},V_{b1} and V_{c1} are the fundamental voltages per phase at the input of converter, the following equation can be written:

$$\begin{bmatrix} v_a \\ v_b \\ v_c \end{bmatrix} = R\begin{bmatrix} i_a \\ i_b \\ i_c \end{bmatrix} + L\frac{d}{dt}\begin{bmatrix} i_a \\ i_b \\ i_c \end{bmatrix} + \begin{bmatrix} v_{a1} \\ v_{b1} \\ v_{c1} \end{bmatrix} \quad (1)$$

From the reference frame transformations, stationary ABC reference frame to stationary reference frame for voltages are[3]:

$$v_\alpha = \sqrt{3}v_{ab} + \frac{\sqrt{3}}{2}v_{bc} \quad (2)$$

$$v_\beta = \frac{3}{2}v_{bc} \quad (3)$$

and for currents are:

$$i_\alpha = \frac{3}{2}i_a \quad (4)$$

$$i_\beta = \frac{\sqrt{3}}{2}(i_b - i_c) \quad (5)$$

And stationary αβ reference frame to rotating d-q reference frame for voltages (and currents) are :

$$v_d = \frac{1}{k}(v_\alpha \cos\theta - v_\beta \sin\theta) \quad (6)$$

$$v_q = \frac{1}{k}(v_\beta \cos\theta + v_\alpha \sin\theta) \quad (7)$$

where θ is the angle position of the *d-q* reference frame. The scaling factor k is introduced so that the *d-q* variables are scaled to have the same amplitude as the rms phase quantities as follows:

For the voltages:

$k = \frac{3}{2}\sqrt{2}$ for Delta Connection and

$k = \frac{3}{2}\sqrt{6}$ for Star Connection.

For the currents:

$k = \frac{3}{2}\sqrt{6}$ for Delta Connection and

$k = \frac{3}{2}\sqrt{2}$ for Star Connection.

Using the transformation given above, equation (1) can be transformed into a synchronously rotating (angular frequency, ω_e) *d-q* reference frame, to yield the following expressions:

$$v_d = Ri_d + L\frac{di_d}{dt} - \omega_e Li_q + v_{d1} \quad (8)$$

$$v_q = Ri_q + L\frac{di_q}{dt} + \omega_e Li_d + v_{q1} \quad (9)$$

and the following equivalent circuit is obtained as shown in Fig. 2.

Using the scaling factor for the transformations as shown above, i_{dc} is given by:

$$i_{dc} = 3\frac{i_d v_{d1} + i_q v_{q1}}{V_D} \quad (10)$$

The expressions for the active and reactive power flowing from the supply to converter are given by:

$$P = 3(v_d i_d + v_q i_q) \quad (11)$$

$$Q = 3(v_d i_q + v_q i_d) \quad (12)$$

If the d-axis of the reference frame is aligned along the supply voltage vector position, v_q is zero and since the amplitude of the supply voltage is constant, v_d is constant. Therefore the active and reactive power flow from the supply to converter will be proportional to i_d and i_q respectively.

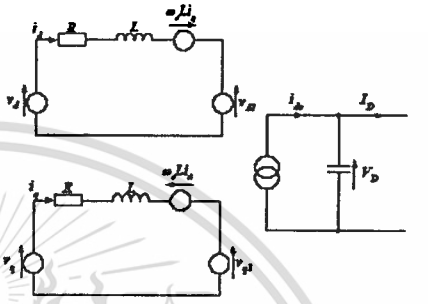

Fig.2. VSC equivalent circuit in *d-q* coordination.

To calculate the supply voltage vector position θ_e, the 3-phase voltages are transformed to a stationary 2-axis (α,β) reference frame as described above to give:

$$\theta_e = \arctan\frac{V_\beta}{V_\alpha} \quad (13)$$

$$\omega_e = \frac{d\theta_e}{dt} \quad (14)$$

where v_β , v_α are the supply voltage components. Neglecting the losses in the filter resistance and the DC-link (i.e. $v_{d1} = v_d$ and $v_{q1} = v_q = 0$) the following relations can be written:

$$V_D i_{dc} = 3v_d i_d \quad (15)$$

$$m_1 = \frac{2\sqrt{2}v_d}{V_D} \quad (16)$$

$$i_{dc} = \frac{3}{2\sqrt{2}}m_1 i_d \quad (17)$$

$$C\frac{dV_D}{dt} = i_{dc} - I_D \quad (18)$$

where m_1 is the PWM modulation index for converter. From (15)-(18) it is seen that the DC-link can be controlled by i_d.

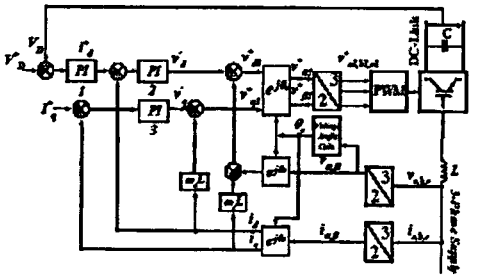

Fig. 3. Vector control structure for VSC

The control scheme thus utilizes current control loops for i_d and i_q, with the i_d demand being derived from the DC-link voltage error through a standard PI controller. The design of the vector control structure for VSC shown in Fig. 3.

IV. CONTROL LOOP DESIGN

Considering equation (8) and (9) with the d-axis of the reference frame align along the supply voltage vector position, the following relationship can be written:

$$v_d = Ri_d + L\frac{di_d}{dt} - \omega_e Li_q + v_{d1} \tag{19}$$

$$0 = Ri_q + L\frac{di_q}{dt} + \omega_e Li_d + v_{q1} \tag{20}$$

In order to decouple the d and q axis, equation compensation terms are introduced by defining:

$$v_{d1} = -v_d + (\omega_e Li_q + v_d) \tag{21}$$

$$v_{q1} = -v_q - (\omega_e Li_d) \tag{22}$$

to give

$$v'_d = Ri_d + L\frac{di_d}{dt} \tag{23}$$

$$v'_q = Ri_q + L\frac{di_q}{dt} \tag{24}$$

Or

$$F(s) = \frac{i_d(s)}{v'_d(s)} = \frac{i_q(s)}{v'_q(s)} = \frac{1}{Ls + R} \tag{25}$$

A PI current control loop is used to determine the demand values for v'_d and v'_q.

The actual values for v^*_{d1} and v^*_{q1} are given by:

$$v^*_{d1} = -v'_d + (\omega_e Li_q + v_d) \tag{26}$$

$$v^*_{q1} = -v'_q - (\omega_e Li_d) \tag{27}$$

and are then transformed to provide the 3-phase modulating waves (v^*_{a1} ,v^*_{b1} and v^*_{c1}) for the PWM generation. The PWM generator employs a 5kHz carrier frequency regular asymmetric regular sampling PWM strategy. The line inductor used in the simulation has a value of 5mH/phase.

A. DC-link voltage controller design

The design of the DC-link voltage controller follows directly from equation (15)-(18) and the transfer function of the plant is given by:

$$\frac{V_D(s)}{I_d(s)} = \frac{3m_1}{2\sqrt{2}Cs} \tag{28}$$

The closed loop block diagram for the DC-link voltage control[4] is shown in Fig. 4. In which I_D is represented as a disturbance.

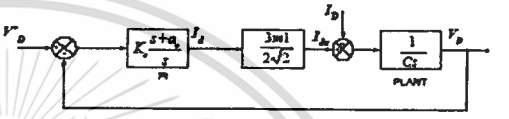

Fig. 4. Block diagram of the DC-link Voltage control loop

From Fig. 4, the characteristic equation for the DC-link voltage controller is given by:

$$s^2 + \frac{3m_1K_c}{2\sqrt{2}C}s + \frac{3K_c a_c m_1}{2\sqrt{2}C} = 0 \tag{29}$$

The controller parameters are given by:

$$K_c = \frac{4\sqrt{2}C\zeta\omega_n}{3m_1} \tag{30}$$

$$a_c = \frac{2\sqrt{2}\omega_n^2 C}{3m_1 K_c} \tag{31}$$

B. Current loop controller design.

The design of the PI current controller[5] follows directly from (24). The closed loop block diagram for the current control is shown in Fig. 5.

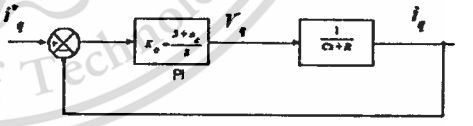

Fig. 5. Block diagram of the current control loop

From Fig. 5, the characteristic equation for the current controller is given by:

$$S^2 + \frac{R + K_c}{L} S + \frac{K_c a_c}{L} = 0 \qquad (32)$$

The controller parameters are given by:

$$K_c = 2\zeta\omega_n L - R \qquad (33)$$

$$a_c = \frac{\omega_n^2 - L}{K_c} \qquad (34)$$

A standard design procedure can be applied to the block diagram of Fig. 3.

V. SIMULATION RESULTS

The controller gains are initially calculated by equations (28)-(34). A design for a closed loop natural frequency and a damping ratio, ζ=0.707, has been chosen. To control the reactive power, I_q^* has been controlled. Fig. 8 shows the results at different load.

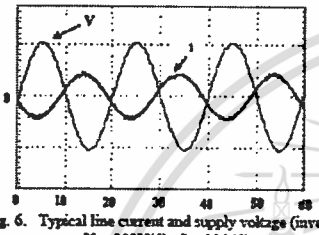

Fig. 6. Typical line current and supply voltage (inverting) Vsa:300V/div, Isa:10A/div.

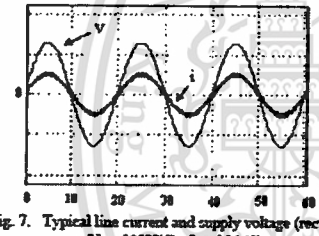

Fig. 7. Typical line current and supply voltage (rectifying) Vsa: 300V/div, Isa: 10A/div

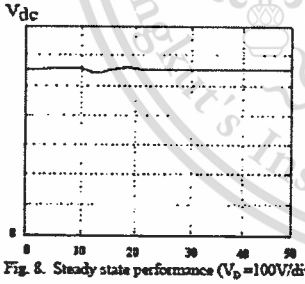

Fig. 8. Steady state performance (V_{dc}=100V/div).

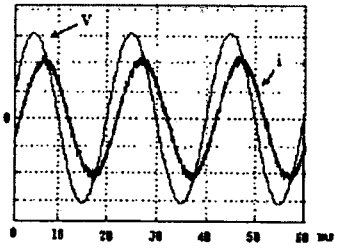

Fig. 9. Simulation result of I^*_q in the VSC. Vsa:100V/div, Isa:2.5A/div, I^*_q:3A

VI. CONCLUSIONS

A model of the PWM Voltage Source Converter Controlled Power Transfer is developed by using the *d-q* transformation. The characteristic equation of the control loops is second order. The controller gains are chosen based on the natural frequency and damping factor. The simulation results show that the line current can be calculated to be in phase or out of phase by controlling the reactive power. The DC-link voltages maintained while the load has changed.

ACKNOWLEDGEMENT

We sincerely would like to thank JICA, AUN/SEED-Net for their contribution.

REFERENCES

[1] Navid R.Zargari and Zeza Joos."Performance Investigation of a Current-Controlled Voltage-Regulated PWM Rectifier in Rotating and Stanary Frames",in IEEE Trans .on Ind.Electronics,Vol. 42, No. 42, August 1995.

[2] A. Khanthee, V. Kinnares." Analysis and Design of IGBT Converters for AC Power Transfer via DC-link", EECON-26, P 648-653, 2003

[3] Peter Vas, "Parameter Estimation, Condition Monitoring and Diagnosis of Electrical Machines" Clarendon Press, Oxford 1993.

[4] Andrzej M. Trzynadlowski, " The Field Orientation Principle in Control of Induction Motors" .

[5] Prof. J.T Boys, A.W Green,BE, " Current-forced single-phase reversible rectifier", in IEE PROCEEDINGS,Vol. 136, Pt. B,No. 5,September 1989.

Appendix B

Application Software: MATLAB 5.6.0 180913a Release 13

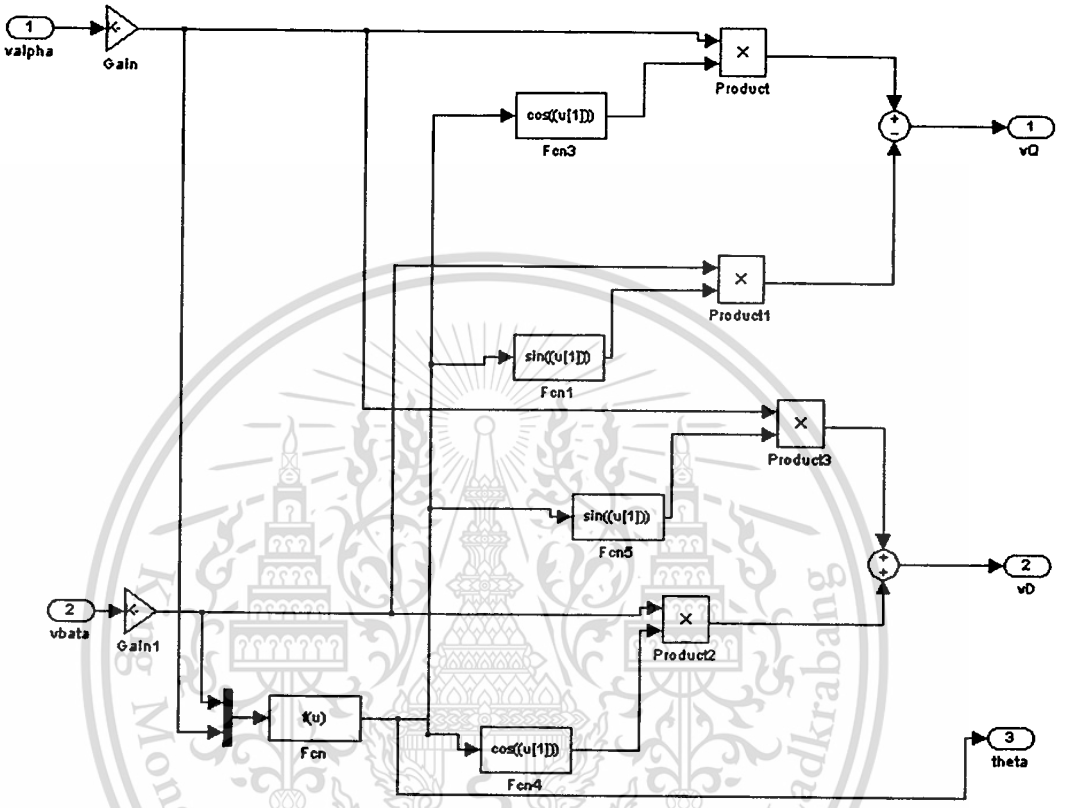

Figure 1.1 Simulation block of V_D and V_Q

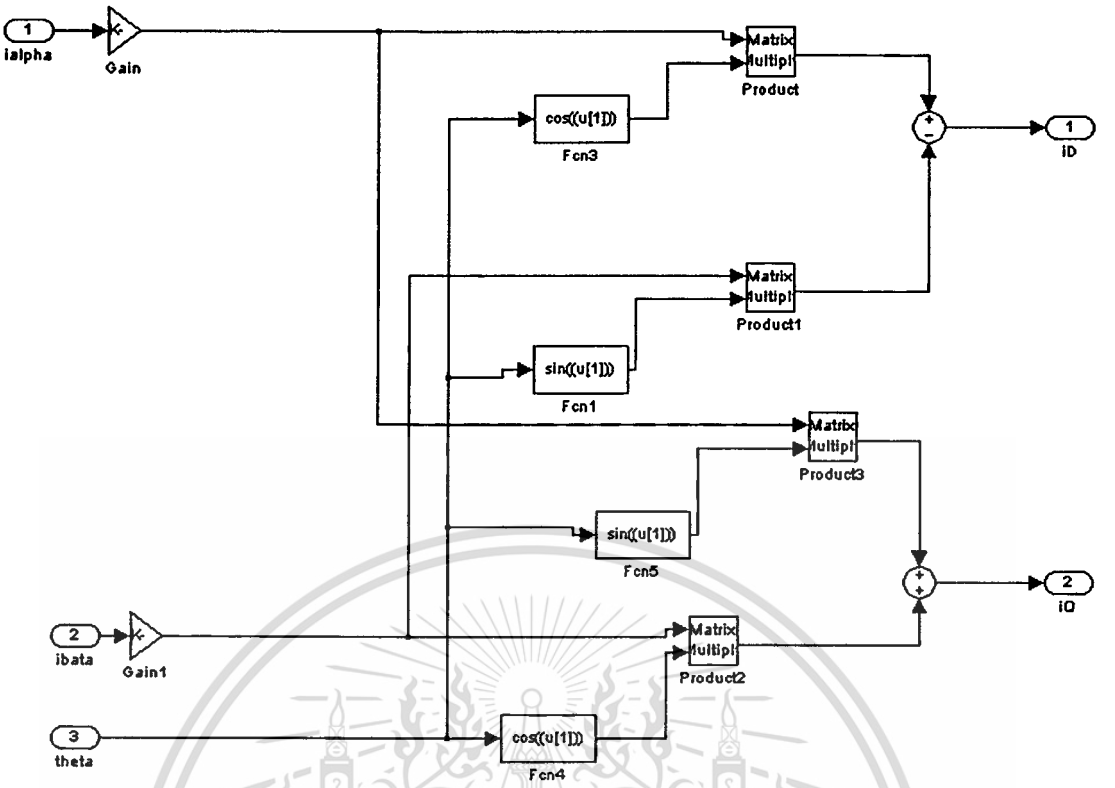

Figure 1.2 Simulation block of I_D and I_Q

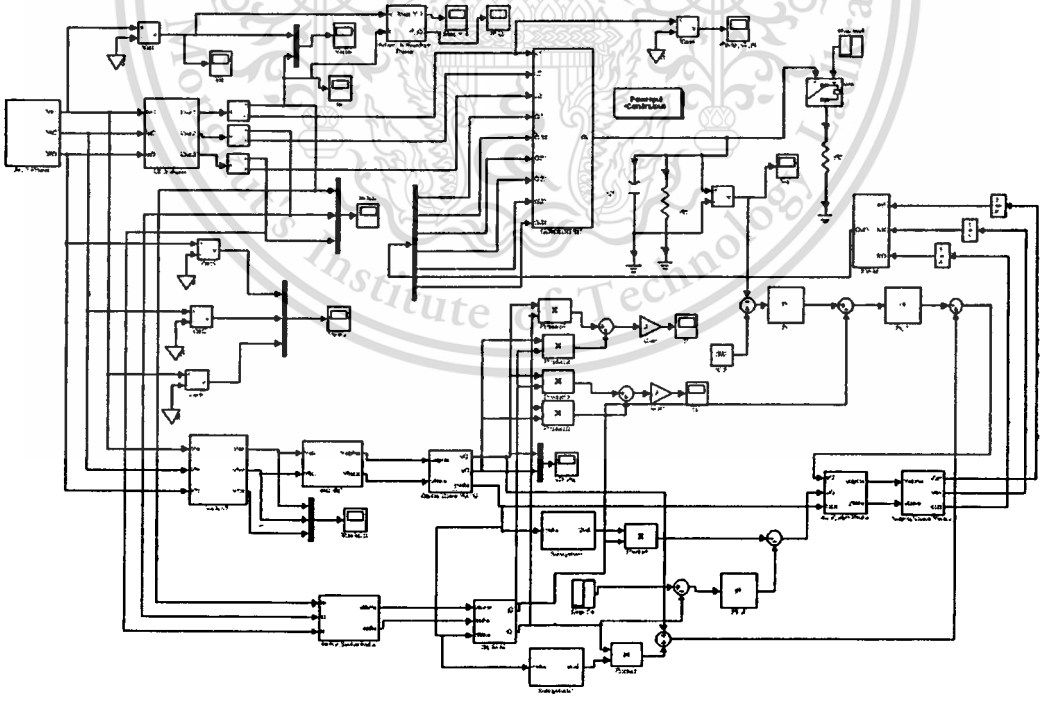

Figure 1.3 Simulation block of converter side1

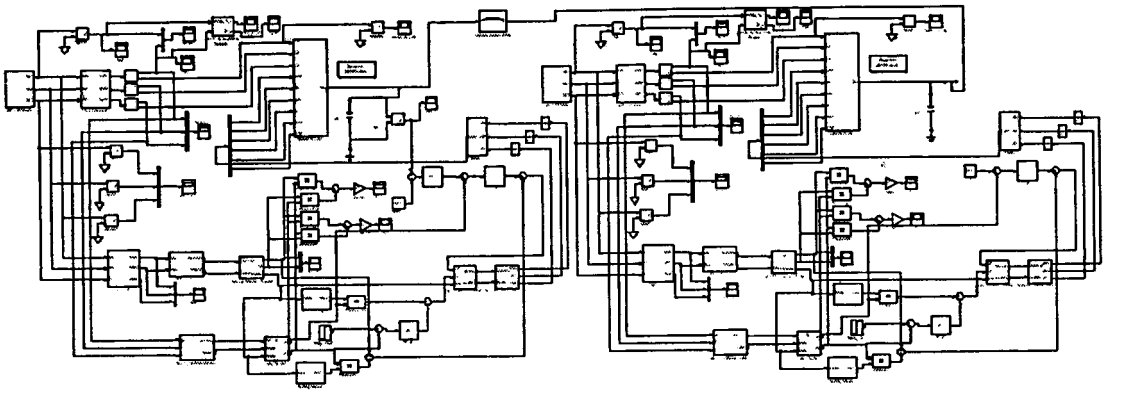

Figure 1.4 Simulation block of VSC-HVDC systems

Study case 1:

Three-phase ac source 1:

Peak amplitude (V): 220*sqrt(2)

Frequency (Hz): 60

L_s 3 Phase (H): 5e-3

Converter 1: 6 IGBT with an anti-parallel diode

Three-phase ac source 2:

Peak amplitude (V): 110*sqrt(2)

Frequency (Hz): 60

L_s 3 Phase (H): 5e-3

Converter 2: 6 IGBT with an anti-parallel diode

Study case 2:

Three-phase ac source 1:

Peak amplitude (V):110*sqrt(2)

Frequency (Hz): 60

L_s 3 Phase (H): 5e-3

Converter 1: 6 IGBT with an anti-parallel diode

Three-phase ac source 2:

Peak amplitude (V): 110*sqrt(2)

Frequency (Hz): 60

L_s 3 Phase (H): 5e-3

Converter 2: 6 IGBT with an anti-parallel diode

Denotations

G1-G6 IGBT

C_D DC-link capacitor

V_{dc} Actual dc voltage

V_{a1},V_{b1},V_{c1} AC voltage at the inverter side

V_a, V_b, V_c Three-phase supply voltages

V_D , V_{dc} DC voltage

V_{ab},V_{bc},B_{ca} Phase-to-phase ac voltages

i_a,i_b,i_c AC currents

ω_e Supply angular frequency

ω_n Natural frequency

ζ Damping ratio

V_α Stationary voltage

$V\beta$ Stationary voltage

I_α Stationary current

$I\beta$ Stationary current

D, d D-axis (rotating reference frame)

Q, q Q-axis (rotating reference frame)

V_d Voltage in rotating d-q reference frame (d-axis)

V_q Voltage in rotating d-q reference frame (q-axis)

K Scaling factor

I_d Current in rotating d-q reference frame (d-axis)

I_q Current in rotating d-q reference frame (d-axis)

V^*_{d1}, V^*_{q1} Actual values

R Load resistance

L AC line inductance

I_{dc} DC supply current of the DC-link voltage

V_{d1}, V_{q1} Compensation values

V^*_{a1},V^*_{b1},V^*_{c1} Three-phase modulating waves

θ_e Supply voltage vector position

f_c Carrier frequency

f_1 Fundamental fequency

m_1 Modulation index

P Active power

Q Reactive power

T One cycle period of the network fundamental frequency

Ts Sampling period of the control system

V_D^* Reference value of the DC-link voltage

i_d^* Reference value of the active power

i_q^* Reference value of the reactive power

Abbreviations

IGBTs Insulated Gate Bipolar Transistors

PWM Pulse Width Modulation

VSC Voltage source converter

ac or AC Alternative Current

dc or DC Direct Current

HVDC High voltage direct current

VSC-HVDC Voltage source converter based High voltage direct current